Max Planck Institut für Molekulare Pflanzenphysiologie

Arbeitsgruppe von Prof. Ralph Bock

Chloroplasts as bioreactors: High-yield production of active bacteriolytic protein antibiotics

Dissertation
zur Erlangung des akademischen Grades
“doctor rerum naturalium“
(Dr. rer. nat.)
in der Wissenschaftsdisziplin „Molekulare Pflanzenphysiologie“

eingereicht an der
Mathematisch-Naturwissenschaftlichen Fakultät
der Universität Potsdam

von
Melanie Oey

Potsdam, den 09.10.2008

Erklärung

Hiermit erkläre ich, dass diese Dissertation das Ergebnis experimenteller Arbeit ist, welche von Juli 2005 bis Oktober 2008 am Max Planck Institut für Molekulare Pflanzenphysiologie in Golm durchgeführt wurde.
Ich erkläre, dass ich die vorliegende Arbeit an keiner anderen Hochschule eingereicht sowie selbstständig und nur mit den angegebenen Mitteln angefertigt habe.

Potsdam, September 2008

_____
(Melanie Oey)

List of Publications

Oey, M., Lohse, M., Kreikemeyer, B., Bock, R.(2008)
”Exhaustion of the chloroplast protein synthesis capacity by massive expression of a highly stable protein antibiotic.” Plant J *in press*

Oey, M., Lohse, M., Kreikemeyer, B., Bock, R.(2008)
“Construction of a shuttle vector for high yield production of bacteria-toxic proteins in tobacco chloroplasts“ *in preparation*

List of Contents

Abbreviations

#	Number
°C	Degree Celsius
µE	Microeinstein
µg	Microgram
µl	Microlitre
µM	Micromolar
1x	1 time concentrated
1 U	1 unit
A	Adenine
aadA	Aminoglycoside 3''-adenylyltransferase
Amp	Ampicillin
APS	Amonium persulphate
bp	Base pairs
bromphenole blue	*3',3",5',5"-tetrabromophenolsulfonphthalein*
BSA	Bovine serum albumin
C	Cytosine
CFU	Colony forming units
cm	Centimetre
cm²	Square centimetre
cv	Cultivar
d	day
dCTP	Deoxycytosinetriphosphate
DNA	Deoxyribonucleic acid
DNase	Deoxyribunuclease
dNTP	Deoxyribonucleotide triphosphate
DTT	Dithiothreitol
E. coli	*Escherichia coli*
EDTA	Ethylenediaminetetraacetic acid
EST	Expressed sequence tag
EtBr	Ethidium bromide
Fig.	Figure
g	Gram

G	Guanine
g/l	Gram per litre
h	hour
HEPES	4-(2-hydroxyethyl)-1-piperazineethanesulfonic acid
kb	Kilo base pairs (1 kb = 1000 bp)
kDa	Kilodalton
kg	Kilogram
LC/MS/MS	Liquid Chromatography/Mass Spectrometry/Mass Spectrometry
LTQ	linear trap quadrupole
M	Molar
MCO	Molecular weight cut-off
mg	Milligram
mg/l	Milligram per litre
min	Minute
ml	Millilitre
mM	Millimolar
MOPS	3-(N-Morpholino)-propanesulfonic acid
MS/MS	Tandem mass spectrometry (Mass Spectrometry/Mass Spectrometry)
mtDNA	Mitochondrial genome
ng	Nanogram
nm	Nanometre
Nt	*Nicotiana tabacum*
OD_{600}	Optical density at 600 nm
P^{32}	radioactive phosphorus
PAGE	Polyacrylamide gel electrophoresis
PBS	Phosphate buffered saline
PCR	Polymerase chain reaction
ppm	Parts per million
ptDNA	Plastid genome
RFLP	Restriction fragment length polymorphism
RNA	Ribonucleic acid
RNase	Ribonuclease
rpr	Rounds per minute
rRNA	Ribosomal RNA

RT	Room temperature
s	Second
S. pneumoniae	*Streptococcus pneumoniae*
S. pyogenes	*Streptococcus pyogenes*
SD	Shine-Dalgarno sequence
SDS	Sodiumdodecylsulfate
Spec	Spectinomycin
Strep	Streptomycin
T	Thymine
Tab.	Table
TAE	Tris acetate EDTA
TEMED	Tetramethylethylenediamine
Tris	Tris(hydroymethyl)aminomethane
TSP	Total soluble cellular protein
UTR	Untranslated region
UV	Ultra violet
v/v	Volume per volume
w/v	Weight per volume
Wt	Wild type
x g	Acceleration of gravity

Further abbreviations are defined in the text.

Abstracts

German abstract (Deutsche Zusammenfassung)

Lytische Enzyme aus Bakteriophagen bieten Eigenschaften, die sie zu vielversprechenden Medikamenten im Einsatz gegen bakterielle Krankheiten machen. Obwohl sie speziell beim Einsatz gegen bakterielle Infektionen, welche durch Antibiotika resistente Erreger hervorgerufen werden, eine maßgebende Rolle spielen könnten, waren bisher die hohen Produktionskosten ein Hindernis für die medizinische Anwendung. Ein kostengünstiges und einfach zu handhabendes System, wie beispielsweise Chloroplasten in Pflanzen, würde diese lytischen Enzyme zu einer effizienten Alternative zu herkömmlichen Antibiotika machen.

In dieser Arbeit wird erstmals die erfolgreiche Produktion von lytischen Enzymen in Tabak-Chloroplasten vorgestellt, welche mit einem Fremdproteingehalt von mehr als 70% des gesamtlöslichen Proteins der Pflanze eine Menge beschreibt, die bisher mit diesem Verfahren noch nicht erreicht wurde.

Alle in Chloroplasten hergestellten lytischen Enzyme zeigten hohe spezifische bakteriolytische Aktivität gegen die gewählten Humanpathogene und waren innerhalb von Minuten in der Lage diese Bakterien abzutöten.

Zur Herstellung von zwei lytischen Enzymen wurde in dieser Arbeit ein spezieller Shuttle-Vektor entworfen, der die Expression von toxischen Genen innerhalb von *E. coli* Zellen im Zuge der DNA Replikation vermeidet, jedoch die Herstellung einer ungehinderten Expression der toxischen Gene in den Chloroplasten nach Beseitigung des Selektionsmarkers erlaubte.

Ein Vergleich zwischen einem herkömmlich verwendeten Transformationsvektor und dem Shuttle-Vektor mittels eines Reportergens zeigte, dass das neu entwickelte System bis zu 4-mal mehr Protein produzierte.

Diese Ergebnisse zeigen das Potential von Chloroplasten als kostengünstige und leicht zu handhabende Produktionsplattform für lytische Enzyme, welche als neue Generation von Antibiotika attraktive Alternativen zu herkömmlichen Therapien bieten.

English abstract

The features of phage lytic enzymes make them a promising tool for treatment of diseases cause by antibiotic resistant bacteria. However, the high production costs are an obstacle for their medical application. Synthesis of lysins in an inexpensive and implementable expression system such as plant chloroplasts would make lytic enzymes a cost efficient alternative to common antibiotics.

In this thesis successful production of unrivalled amounts of active phage lytic enzymes (up to more than 70% of total soluble protein) in tobacco chloroplasts is described. The products could efficiently kill their target human pathogenic bacteria with high specificity within a few minutes.

A special shuttle vector was designed that avoided expression of the toxic lytic genes in *E. coli* and allowed restoration of expression by marker gene deletion after transformation into chloroplasts.

Comparing reporter gene expression of the shuttle vector with classical chloroplast expression system, the newly developed expression system could reach up to 4 times higher protein expression rate.

These results introduce tobacco chloroplasts as new cost efficient and easily manageable production platform for phage lytic enzymes conquering a great obstacle for clinical application and making them highly attractive as next-generation antibiotics.

1 Introduction

1.1 Bacteria and antibiotics

"Throughout history, there has been a continual battle between humans and the multitude of microorganisms that cause infection and disease." Fred C. Tenover

However, in the middle of the twentieth century development of new bacterial agents and drugs, as well as increased infection controls, changed the situation for the better. With regards to bacterial infections the tide turned when the first antibiotic penicillin was found and became commercially available. Until the middle of the nineteen fifties, penicillin was suggested as a universal remedy against all kinds of diseases and was sold without prescription as an ingredient in cough drops, mouthspray, mouthwash, soaps and drinks. However, this thoughtless widespread use of antibiotics provoked new problems since the bacteria responded with a multitude of resistance mechanisms almost immediately after application of antibacterial drugs (Tenover, 2006). When the first antimicrobial agents became inefficient physicians responded with an even higher number of antibiotic prescriptions. Thus, although only three new classes of antibiotics have been discovered in the past 50 years, today antibiotics still represent a significant market with estimated worldwide sales of US$25.5 billion in 2005 (Christoffersen, 2006; Kresse et al., 2007) (Fig. 1). Around 30% of all prescriptions were issued for antibiotics, which in the USA, accounts for 160 million prescriptions per year (Stratchounski et al., 2003). In the USA annual consumption reaches up to 235 million doses of which, according to the Center for Disease Control and Prevention (CDC), 20-50% are unnecessary (Gums, 2004). Unfortunately antibiotics have not only been used for therapeutic reasons but also by stock farmers as feed additives. Out of 25 thousand tons of antibiotics produced in the USA each year, 11 thousand tons are given to animals, of which 80% (~ 9 thousand tons) are used for growth promotion. The remaining 2 thousand tons are used to control diseases such as influenza and pneumonia that emerge depending on husbandry conditions (American Medical News, "FDA Pledges to Fight Overuse of Antibiotics in Animals", 1999). Thus, in the past 50 years ~ 1 million tons of antibiotics have been released into the biosphere and commonly used antibiotics can already be detected in rivers and drinking water (Heberer, 2002).

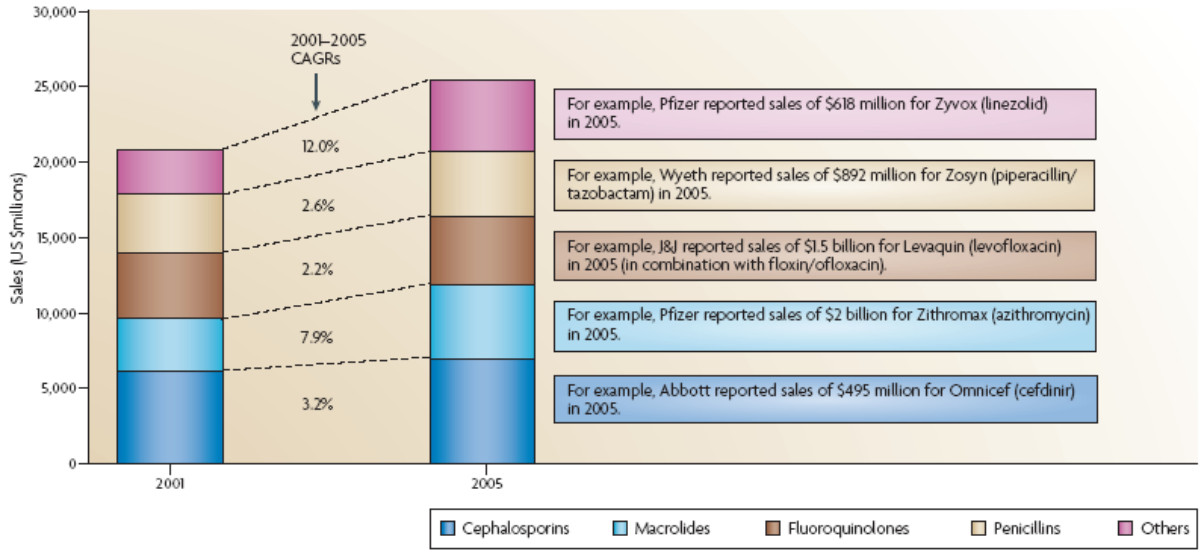

Fig. 1 Average sales of several antibacterial classes in 2001 – 2005 in US$ (from Kresse et al., 2007). Antibiotic classes are indicated in different colours, Annual sales are indicated in US$, Compound annual growth rate (CAGR) is shown as a percentage.

In view of the increasing number and complexity of bacterial resistance mechanisms due to the irresponsible use of antimicrobial drugs, the Institute of Medicine at the National Academy of Sciences has estimated the annual cost of treating infections caused by resistant bacteria to be more than US$30 billion in the USA (National Institute of Allergy and Infectious Diseases, "Antimicrobial Fact Sheet", 1999). Multiresistant bacteria are on the increase and with 93% of new drugs developed between 1980 and 2003, the development costs for new drugs will further increase as indicated by the already observed doubling between 1997 and 2001, where costs already reached US$802 million (Spellberg et al., 2004).

1.1.1 Bacterial cell wall – structure and composition

In general, eubacteria can be divided into two classes based on their different cell wall ultra structure. This different cell wall architecture can be visualized with a staining process developed by Hans Christian Joachim Gram allowing a classification into so called gram-positive and gram-negative bacteria (Gram, 1884). The cell wall forms a rigid exoskeleton, a biological shield based on the macromolecule peptidoglycan to perform its main function, which is the protection against both mechanical and osmotic cell lysis (Navarre and Schneewind, 1999). In gram-positive bacteria the peptidoglycan content accounts for up to 90% of the cell wall structural components, whereas gram-negative bacteria (with only 10% peptidoglycan) possess a relatively thin layer that is incorporated into a periplasmatic gel that is restricted by an outer lipopolysaccharide layer (Fig. 2).

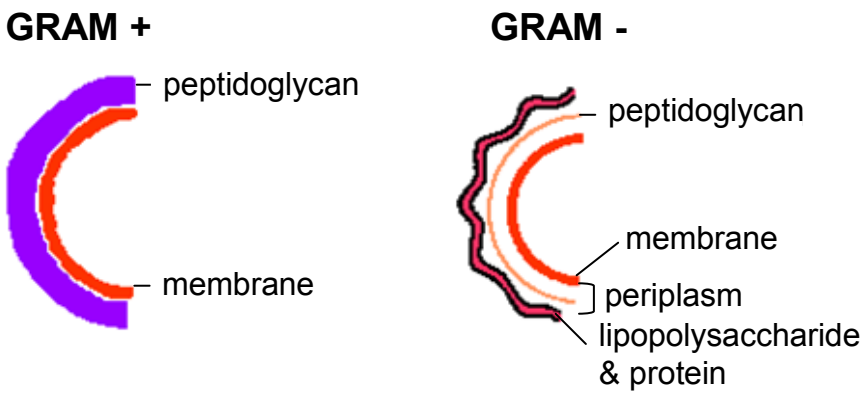

Fig. 2 Schematic diagram of cell wall construction of gram postive (gram+) and gram-negative (gram-) bacteria.

The cell wall peptidoglycan, also called murein, consists of glycan chains built by the repeating disaccharide N-acetylmuramic acid-(β1-4)-N-acetylglucosamine (MurNAc-GlcNAc). The chains with bacterial-specific lengths are covalently cross-linked via amino acids which are bound to the muramic acid residue (Navarre and Schneewind, 1999). This transpeptidase mediated crosslinking occurs to different extents in different bacteria and is the target of the antibiotic penicillin. In gram-positive bacteria the peptidoglycan chains are usually cross linked by connecting the adjacent peptides with so called peptide interbridges which often consists of five glycine residues, whereas in gram-negative bacteria cross linking occurs by direct peptide linkage of the amino group of the associated amino acid (Navarre and Schneewind, 1999).

In gram-positive bacteria several other species-specific compounds can be found in the cell wall, such as so called teichoic and lipoteichoic acids that consist of ribitol-phosphate, glucosyl-phosphate or glycerol-phosphate residues connected by phosphate esters. Teichoic and lipoteichoic acids are incorporated into the cell walls of gram-positive bacteria by covalent binding to the peptidoglycan or linkage with the glycerol-phosphate polymer to a lipid anchor such as the glycolipids of the plasma membrane (Navarre and Schneewind, 1999). An overview of cell wall construction of gram-positive bacteria is outlined in Fig. 3. Some bacteria modify their teichoic and lipoteichoic acid structure with other sugars and unusual amino acids like D-alanine or even use entirely different compounds, subunit repeats and/or lipid anchors for assembly.

The composition of teichoic and lipoteichoic acids is highly species-specific (Borysowski et al., 2006).

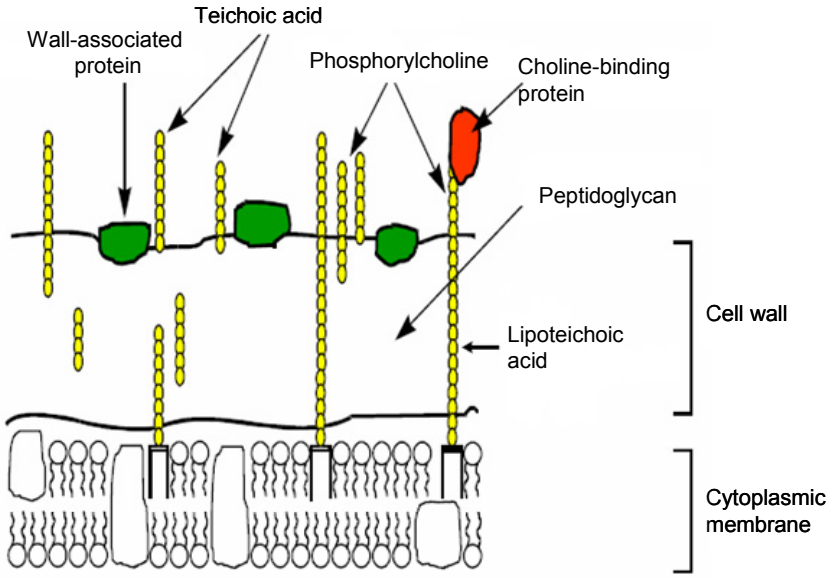

Fig. 3 Simplified illustration of the cell wall of gram-positive bacteria (modified from Prieß, 2002).

For example, teichoic and lipoteichoic acids of pneumococcal cell walls contain phosphorylcholin, where two choline residues are covalently bound to each carbohydrate repeat (Loeffler et al., 2001; Borysowski et al., 2006; Tuomanen, 2006). Choline residues are necessary for pneumococci to attach and enter their host cell, and thus, are essential for bacteria viability but also serve as attachment sites for pneumococcal lytic enzymes (Cundell et al., 1995; Cundell et al., 1995; Ring et al., 1998; Loeffler et al., 2001; McCullers and Tuomanen, 2001; Borysowski et al., 2006).

1.2 Bacteriophage lytic enzymes as next generation antibiotics

Sir Alexander Fleming already prophesied in his Nobel lecture in 1945 that bacteria will develop resistances against antibiotics. Today, decades later, bacteria have indeed responded with an enormous diversity of antibiotic resistance mechanisms while also displaying accelerating rates of emergence and distribution of resistant varieties.

The development of resistance, the overuse of commonly used antibiotics for infection treatment combined with the low discovery rate of novel drugs over the past years emphasizes the need to find alternative therapies.

In 1917 Felix d'Herell first published the discovery of invisible microbes that were able to clarify a bacterial suspension (d'Herell, 1917). He called these microbes bacteriophages, a name they still carry today. It is known that bacteriophages or phages are viruses that attack

eubacteria (Fischetti, 2006; Fischetti et al., 2006). Given the huge numbers of bacterial species, it can be assumed that phages are the most abundant entities on earth. Furthermore, as the relationship between bacteria and phages has been a dynamic process through evolution, phages provide a powerful and exhaustless tool to fight bacterial infections (Fischetti, 2006; Fischetti et al., 2006). Phages were first successfully used by Felix d'Herell for so called phage therapy in 1919. However, to understand the potential of phages for medical use the knowledge of the phage replication cycle is important.

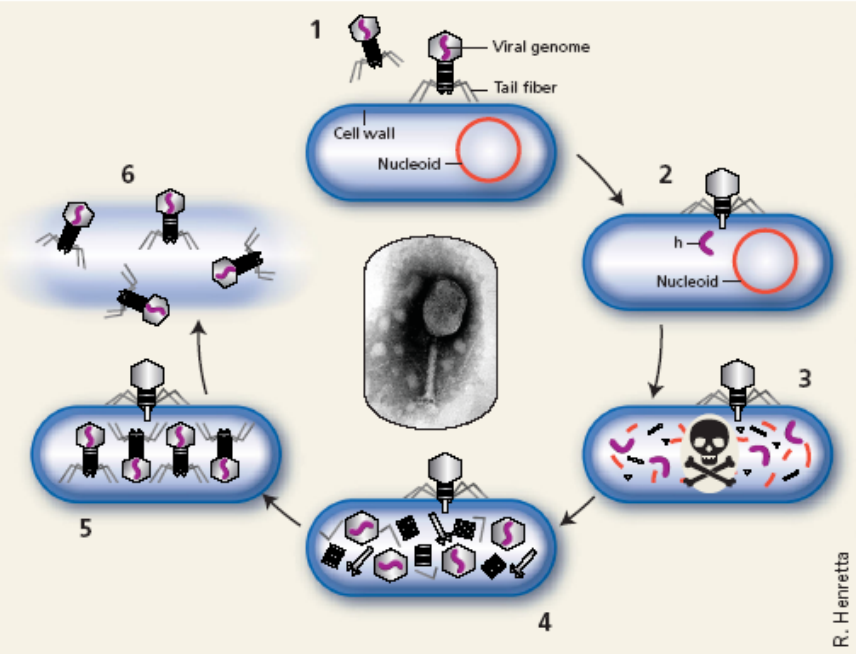

Fig. 4 Life cycle of a lytic phage (from Thiel, 2004). (1) Attachment of the phage to the host bacterium and (2) DNA injection. (3) Host killing and disruption of the bacterial genome. (4) Takeover of the bacterial DNA and protein synthesis machinery to express new phage parts. (5) Assembly of new phage particles, and (6) lysin mediated cell lysis to release new phages into the environment.

A phage that infects a bacterium immediately kills its host and takes over the complete replication machinery to produce copies of itself (Fig. 4) (Thiel, 2004). At the end of the replication cycle the completely assembled phages have to be released from the host cell into the environment, which is mediated by a lytic system degrading the bacterial cell wall (Fischetti, 2006; Fischetti et al., 2006).

The lytic system consists of a holin that forms pores in the cell membrane enabling the lytic enzymes (lysins) to attach and specifically cleave the cell wall peptidoglycan layer (Fig. 5a). Once the cell wall is degraded, the bacteria burst due to osmotic pressure.

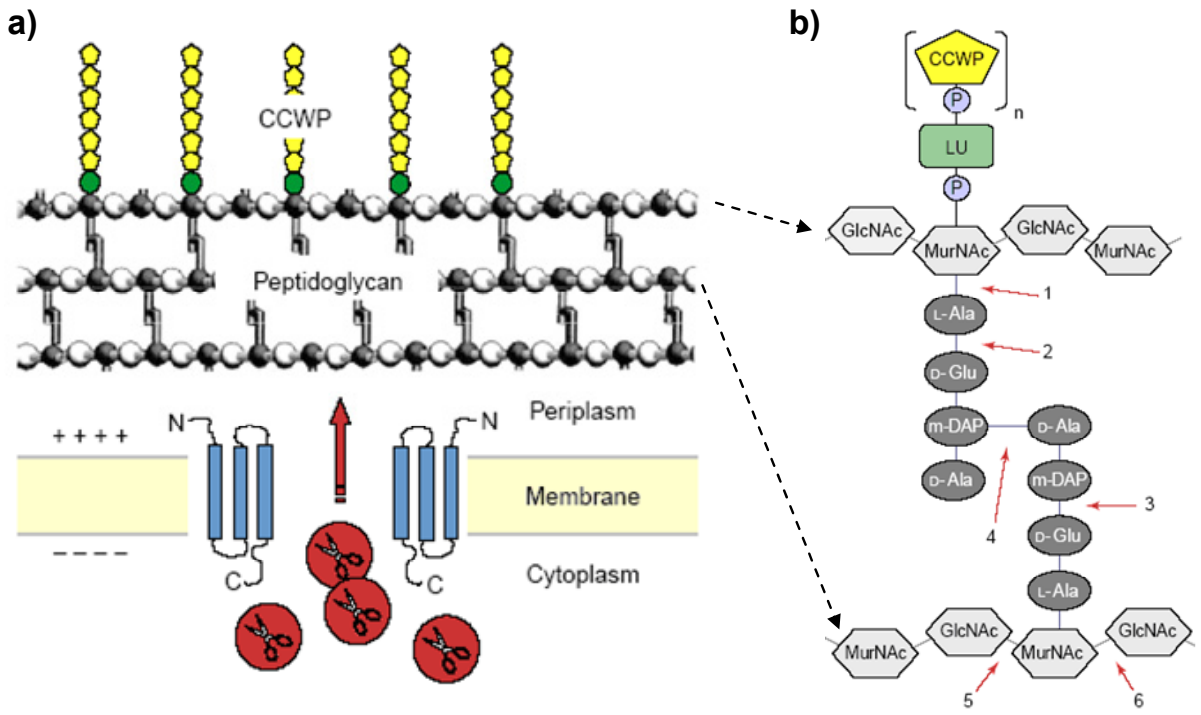

Fig. 5 Bacterial cell wall structure and endolysin targets (modified from Loessner, 2005). (a) Schematic illustration of the gram-positive bacterial cell wall and the interaction of the components of the lytic system. Expressed holin proteins (blue) insert themselves and by oligomerization form pores into the cytoplasmic membrane where the endolysins (red) pass through to gain access to the peptidoglycan. (b) Displays the fine structure of peptidoglycan with its disaccharide backbone and the interpeptide bridge consisting of a meso-diaminopimelic acid (m-DAP) that is directly cross-linked to the terminal D-Ala of the opposite peptide chain. The bonds potentially attacked by endolysins of different enzymatic specificities are indicated by numbers: 1, N-acetylmuramoyl-L-alanine amidase; 2, L-alanoyl-D-glutamate endopeptidase; 3, D-glutamyl-m-DAP endopeptidase (note that this activity has not yet been identified in a phage endolysin); 4, interpeptide bridge-specific endopeptidases (see text); 5, N-acetyl-β-D-glucosaminidase; and 6, N-acetyl-β-D-muramidase (also known as muramoylhydrolase and 'lysozyme'). Abbreviations: CCWP, carbohydrate cell wall polymer; GlcNAc, N-acetyl glucosamine; LU, linkage unit; m-DAP, meso-diaminopimelic acid; MurNAc, N-acetyl muramic acid; P, phosphate group.

Although originally incorporated into a lytic system, when applied exogenously as recombinant proteins nanograms of lysins per millilitre are capable of efficiently lysing a 10^7 bacteria cell culture suspension within seconds, regardless of their antibiotic sensitivity (Borysowski et al., 2006; Fischetti, 2006). Regarding their cleavage targets, lysins can be classified as lysozymes that cleave the peptidoglycan chains, endopeptidases that act on the peptide cross bridge at different positions or, more commonly, amidases that hydrolyze the peptide bond between the peptidoglycan and peptide intercross bridge (Loessner, 2005; Fischetti, 2006) (Fig. 5b).

Additionally, based on their mode of action, lysozymes and amidases can act synergistically (Loeffler and Fischetti, 2003; Fischetti, 2005). Phage lytic enzymes have been shown to be

highly specific to their host bacteria with such specificity conferred by such factors as substrate composition and enzyme structure (Navarre and Schneewind, 1999; Monterroso et al., 2002; Hermoso et al., 2003; Fischetti, 2006). A typical lysin obtains an N-terminal catalytic domain responsible for substrate cleavage and a C-terminal domain mediating the binding of the enzyme to the bacterial cell wall (Fig. 6) (Fischetti, 2005). Sequence alignments between several lytic enzymes revealed high similarity within the N-terminal domain and relatively low similarity within the C-terminal domain leading to the conclusion that the high specificity of the lytic enzymes is due to a stringent substrate binding reaction (Lopez et al., 1992; Fischetti, 2005).

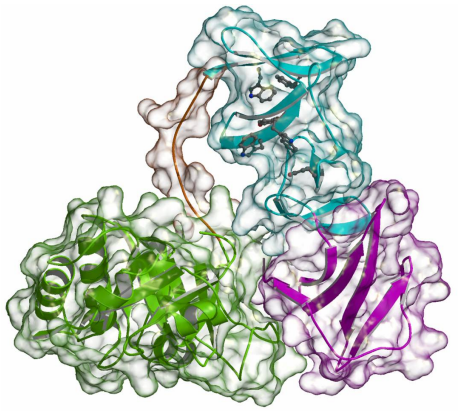

Fig. 6 Crystal structure of phage lytic enzyme Cpl-1 (from Buey et al., 2007). Cpl-1 possesses a catalytic module (green) and a choline binding module arranged in two different structural regions: CI (blue) displays two functional choline binding sites, whereas the structural domain CII (pink) with a hydrophobic surface functions as hinge, responsible for interactions of the catalytic and the CI binding domains. Both modules are connected by a negatively charged linker (orange) whose tightness in cooperation with the structural domain defines orientation, distance and position of catalytic and binding domain.

Once specific binding occurs, the catalytic domain, which is locked into a specific orientation, is activated and cleavage of the cell wall structure only occurs once the cleavage substrate is in a proper position (Monterroso et al., 2002; Hermoso et al., 2003).

Due to their domain structure, another advantage of lytic enzymes for biotechnological use is possible domain swapping resulting in new lytic enzymes with different specificities (Garcia et al., 1990). Although lytic enzymes might be problematic for medical application due to immune response *in vivo*, tests with mice and rabbits revealed that lytic enzymes are able to clarify pathogenic bacteria from mucosal membranes, as well as blood, and neither harmed the animal nor showed significant decreases in enzyme activity (Jado et al., 2003; Fischetti, 2005; Borysowski et al., 2006; Fischetti, 2006). Thus, lytic enzymes offer potential for long term therapy of bacterial infections.

Importantly, when considering lytic enzymes as novel anti-infectives, the development of resistance against phage lysins is highly unlikely because lysin targets appear to be unique and essential molecules in the cell wall, such as the choline residues in the pneumococcal cell wall which are necessary for bacterial viability (Fischetti, 2005; Borysowski et al., 2006). In addition, repeated exposure of bacteria to low concentrations of lysins in solid as well as liquid media did not lead to the generation of resistant bacteria (Loeffler et al., 2001; Schuch et al., 2002; Fischetti, 2005; Borysowski et al., 2006; Fischetti, 2006). Furthermore, as lysins are highly specific to their bacterial targets, undesired effects on the normal human bacterial flora are likely to be prevented. Thus, the reduced likelihood of resistance development, their apparent safety and relatively easy genetic modification makes lytic enzymes a desirable antibiotic alternative. Taken together, phage lytic enzymes, with their potent antibacterial activity *in vivo* and *in vitro* as well as their novel mode of action (enzymatic cleavage of peptidoglycan), show great potential to become a novel class of antibacterial agents also suitable against antibiotic resistant bacteria.

1.3 Efficiency and cost-effectiveness of protein expression systems

Since recombinant proteins can be produced in several different systems, it is important to find the most suitable system offering the most advantages regarding production costs, safety and product outcome. Depending on the protein, using mammalian cells as a production platform for recombinant proteins offers the advantage of products that are highly similar to those originating in nature but have the disadvantages of cost intensive cell culturing and scale limitations. In comparison, production in microorganisms such as bacteria allows large-scale production but can result in undesired product differences such as unnatural conformation due to incorrect folding or lack of disulfide bridges. Thus, often the largest proportion of the operating costs are associated with further processing of the derived protein required, for example, for formation of disulfide bridges or cleavage of methionine (Petrides et al., 1995).

With these issues in mind, the production of recombinant proteins in plants shows the most advantages since all plant production systems show higher economic efficiency than industrial facilities using fermenter or bioreactor systems.

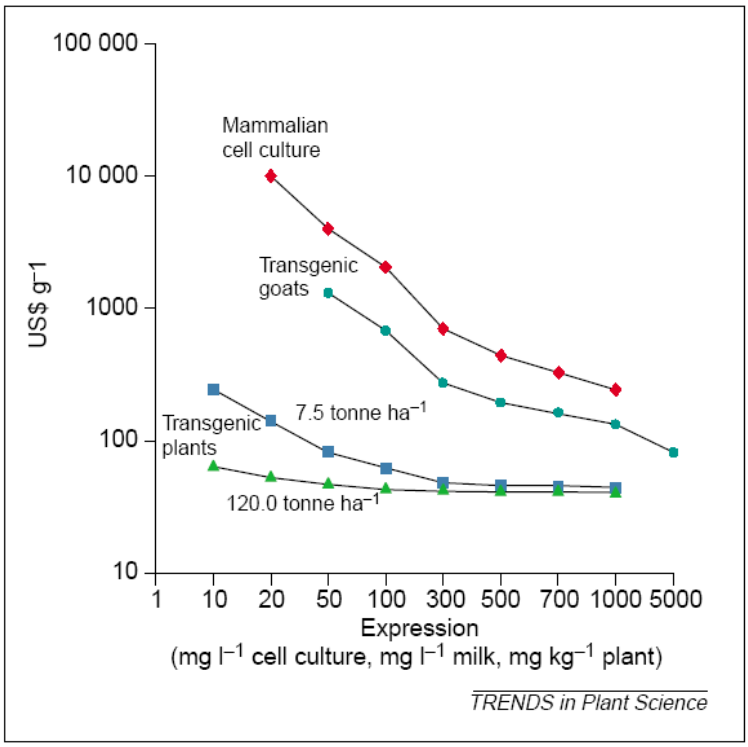

Fig. 7 Comparison of estimated costs per gram of purified immunoglobulin A derived from different expression systems (from Daniell et al., 2001). Expression levels of different expression systems are indicated whereas transgenic plants as expression system compare green biomass (12.0 tonne ha-1) and seed production (7.5 tonne ha-1).

However, cost estimations are difficult since not many plant-derived pharmaceuticals, such as antibodies are yet commercially produced. Nevertheless, according to Planet Biotechnology (Mountain View, California, USA) estimated final production costs of, for example, IgA, produced in plants should significantly undercut the costs needed for cell culture or transgenic animal production systems (Fig. 7) (Daniell et al., 2001). In addition to the economic reasons for protein production in plants, which is mainly based on the high productivity of some species (tobacco annual biomass yield of > 100 tonne ha^{-1}), plant based systems offer further advantages such as the elimination of purification steps since the expressed product can be produced in edible plant tissue. Another safety aspect is the possible enclosure of proteins into cellular compartments (e.g. chloroplasts) (Bock, 2001).

Other advantages of using plants as a production platform includes reduced health risks potentially arising from product contamination with potential human pathogens or toxins (as seen when production occurs in other systems) and easy storage opportunities (e.g. seeds or tubers). Finally, the protein amount achievable by plant production can reach industrial-scale

levels since technologies are already available to harvest and process plants and their products (Daniell et al., 2001).

1.4 Chloroplasts and their transformation

Plants as a production platform for pharmaceuticals are obtaining an increasing status in biotechnology due to their advantages such as high productivity and economic efficiency as well as product containment, easy handling and storage, which could not be provided by any other system (Gomord et al., 2005; Ma et al., 2005; Streatfield, 2006). The first proteins produced in plants are now commercially available, 18 years after the first plant-derived recombinant protein, human serum albumin, was produced in 1990 (Sijmons et al., 1990; Ma et al., 2005).

Tab. 1 Overview of chloroplast produced foreign proteins and their accumulation rate as well as expression cassette and chloroplast genome target site (from Daniell et al., 2005).

Proteins	Transgene	Promoter	5′/3′ UTRs	Tsp expression (%)[d]	Homologous recombination site	Laboratory
Elastin-derived polymer	*EG*121	Prrn	T7 gene10/ T*psb*A	ND[e]	*trn*I/*trn*A	Daniell
Human somatotropin	*hST*	Prrn[a], P*psb*A[b]	T7 gene10[a], *psb*A[b]/T*rps*16	7.0%[a], 1.0%[b]	*trn*V/*rps*12/7	Staub
Cholera toxin	*Ctx*B	Prrn	Ggagg/T*psb*A	4%	*trn*I/*trn*A	Daniell
Antimicrobial peptide	*MSI*-99	Prrn	Ggagg/T*psb*A	21%	*trn*I/*trn*A	Daniell
Interferon α2b	*INFa*2B	Prrn	P*psb*A/T*psb*A	19%	*trn*I/*trn*A	Daniell
Human serum albumin	*hsa*	Prrn[a], P*psb*A[b]	ggagg[a], *psb*A[b]/ T*psb*A	0.02%[a], 11.1%[b]	*trn*I/*trn*A	Daniell
Interferon γ	*IFN-g*	P*psb*A	P*psb*A/T*psb*A	6%	*rbc*L/*acc*D	Reddy
Monoclonal antibodies	*Guy's 13; HSBV-Isc*	Prrn; atpA/rbcL	Ggagg/T*psb*A AtpA/rbcL	ND	*trn*I/*trn*A; psbA/5S/23S	Daniell Mayfield
Anthrax protective antigen	*Pag*	Prrn	P*psb*A/T*psb*A	18.1%	*trn*I/*trn*A	Daniell
Plague vaccine	*Ca*F1 ~ *Lcr*V	Prrn	P*psb*A/T*psb*A	4.6%	*trn*I/*trn*A	Daniell
CPV VP2	*CTB-2L21*[a]; *GFP-2L21*[b]	Prrn	*psb*A/T*psb*A	31.1%[a], 22.6%[b]	*Trn*I/*trn*A	Daniell/ Veramendi
Rotavirus VP6	*Vp6*	Prrn[a], P*psb*A[b], P*trc*[c]	*rbc*L/T*rrn*B[a] *psb*A/T*rrn*B[b] lacZ/ T*rrn*B[c]	3%[a], 0.6%[b], 0%[c]	*rbc*L/*accD*	Gray
Tetanus toxin	*Tet C*	Prrn	T7 gene10[a], atpB[b]/Trbc L	25%[a], 10%[b]	*Trnv/rps12/7*	Maliga

[a–c]Refer to genes and their respective regulatory sequences and % tsp.
[d]Tsp: total soluble protein.
[e]ND: Not determined.
[f]Falconer, R. (2002) Expression of interferon α2b in transgenic chloroplasts of a low-nicotine tobacco. M.S. Thesis, University of Central Florida, Orlando, FL, USA.
[g]Singleton, M.L. (2003) Expression of CaF1 and LcrV as a fusion protein for a vaccine against *Yersinia pestis* via chloroplast genetic engineering. M.S. Thesis, University of Central Florida, Orlando, FL, USA.

When considering plants as an optimal platform for protein production, two transformation techniques, nuclear and chloroplast transformation, must be distinguished. In comparison to nuclear transformation, which often has the major drawback of very low expression levels (often less than 1% of total soluble protein - the level needed for commercial viability if the

protein must be purified), chloroplast transformation has decisive advantages, such as maternal inheritance in most crop plants, which allows higher transgene containment due to the avoided undesired distribution of the transgene via pollen (Kusnadi et al., 1997; Koya et al., 2005). In addition, chloroplasts show high transgene expression rates (so far > 40% total soluble protein has been reported by De Cosa et al. (2001)), absence of variations due to position effects or epigenetic gene silencing and the option to express polycistronic information from a single promoter. The transgene is inserted via homologous recombination which allows precise integration and positioning in the chloroplast genome and thus, if desired, an exact elimination of a target gene. Furthermore, the enclosure of the foreign protein into an organellar compartment avoids potentially negative interactions with the cytoplasmic environment. Tab. 1 gives an overview of successfully expressed vaccines and biopharmaceuticals derived via chloroplast transformation.

1.4.1 Chloroplast genomes

A huge difference between plants and animals is their ability to convert solar energy into energy rich molecules that were used by all organisms in the entire biosphere for life. The cellular compartments which are responsible for this feature are called chloroplasts. Based on the endosymbiotic theory, chloroplasts are derived from the engulfment of cyanobacteria. A process which occurred approximately 450 million years ago, and resulted in the compartmentalization of the reactions of photosynthesis and starch, amino acid, lipid and pigment biosynthesis in higher plants (Bock and Khan, 2004; Maliga, 2004; Lopez-Juez and Pyke, 2005).

Plastids as a general organellar category include several different types such as the progenitors of all plastid types, proplastids, plastids that carry pigments, chloroplasts and chromoplasts, as well as different types of white plastids such as amyloplasts and elaioplasts (Maliga, 2004; Lopez-Juez and Pyke, 2005).

As was the case for the mitochondria, which originate from engulfed α-proteobacteria (Fig. 8), the endosymbiotic uptake of the chloroplast cyanobacterial ancestor was accompanied by a gradually increasing division of labor between host cell and acquired organelle as well as by an elimination of redundant and dispensable genes (Bock, 2006).

In comparison to a cyanobacterial genome encoding 3200 genes, a contemporary higher plant chloroplast genome encoding around 130 genes is much smaller indicating that a drastic reduction as well as a reorganization of information storage has taken place during evolution.

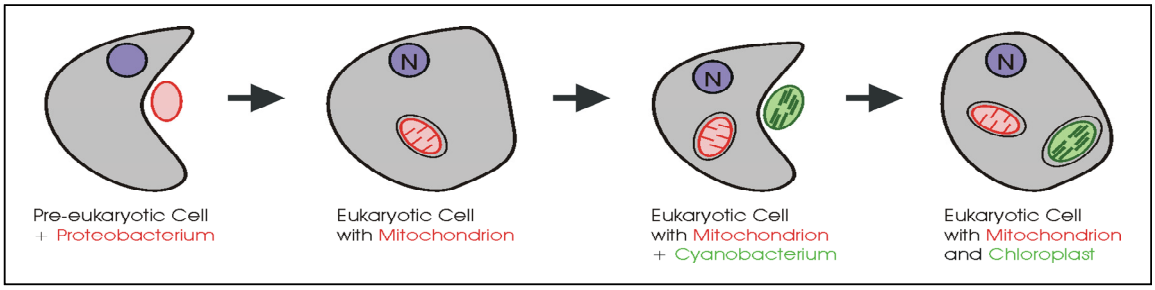

Fig. 8 Schematic development of cell organelles within a eukaryotic cell via endosymbiosis (modified from Bock, 2007). A eukaryotic cell is formed via uptake of a proteobacterium which is comparable to contemporary animal cells containing mitochondria. A second uptake of a photosynthetically active cyanobacterium forms the currently known eukaryotic plant cell containing chloroplasts.

This genetic information distribution among the three compartments required new organization strategies regarding coordination of gene expression and metabolism within the new eukaryotic cell (Bock, 2006).

The chloroplast genome, ranging from 120 to 180 kb in size, is also called the plastome or ptDNA. Due to its bacterial origin, the chloroplast genome has retained several prokaryotic features such as the prokaryotic gene expression machinery. Thus, many genes are organized in an operon like structure where polycistronic mRNAs are expressed and posttranscriptionally processed (Lopez-Juez and Pyke, 2005; Bollenbach et al., 2007). Posttranscriptional modification, in some cases, also includes splicing since some chloroplast genes contain introns (Schmitz-Linneweber and Barkan, 2007).

The chloroplast genome is highly polyploidy. The plastid DNA is organized into membrane attached clusters, so called nucleoids which harbor 5-10 plastome copies (Kuroiwa, 1989, 1991). Up to 100 chloroplasts with 10-14 nucleoids each and thus approximately ~10 000 identical ptDNA copies can be found in a single leaf cell (Tewari and Wildman, 1966; Bendich, 1987). With this high plastome copy number, plastid DNA can comprise up to ~ 10-20% of total cellular DNA (Bock, 2001, 2007). The number of plastome copies only changes during plastid differentiation, and once complete, the copy number remains constant with leaf age and plant developmental stages (Li et al., 2006; Zoschke et al., 2007). In comparison to the two other plant cell genomes, the plastome with approximately 100 genes encoded by 120 to 160 kb is the most gene dense (Sugiura, 1989, 1992; Wakasugi et al., 2001; Bock, 2007).

When comparing the approximately 120 plastomes for which full sequence data is now available (NCBI, (http://www.ncbi.nlm.nih.gov/genomes/static/euk_o.html) and Université de

Montréal, (http://megasun.bch.umontreal.ca/ogmp/projects/other/cp_list.html)) there is striking conservation observed within the plastomes of land plants. Generally the coding regions are relatively AT-rich, which is manifested in a strong codon usage preferring synonymous codons displaying A or T at the third position. The non coding intergenic regions, which are relatively GC-rich, contribute most to the relatively low GC content of plastomes (typically around 30-40%) (Shimda and Sugiura, 1991; Bock, 2007).

The striking tetrapartite organization of the plastomes of most land plants showing a large and small single copy region (LSC and SSC) separated by two inverted repeat regions (IR_A and IR_B) is shown in Fig. 9 with the tobacco plastome as an example. It is believed that an increase in the number of highly expressed genes or genome stabilization might be a reason for the presence of the inverted repeat regions although the function is not fully clear so far (Palmer and Thompson, 1982).

Homologous recombination within the inverted repeats can result in two isoforms of the plastome which then differ in the relative orientation of LSC and SSC (Palmer, 1983; Stein et al., 1986). Generally three classes of genes are encoded by the plastome. The genetic system genes represent the largest group responsible for transcription, RNA processing, translation and protein degradation. Additionally, genes encoding components relevant for photosynthesis as well as genetic information for other functions are stored on the chloroplast genome (Bock, 2007).

As mentioned previously, all functions of contemporary plastids strictly depend on collaboration with the nucleus and nuclear products which are synthesized in the cytosol and subsequently imported into the chloroplast (Bock, 2007). In fact it is estimated that more than 95% of the proteins present in the chloroplast are imported from the cytosol (Abdallah et al., 2000; Rujan and Martin, 2001; Martin et al., 2002).

For example, division of labour between the cellular compartments occurs with regards to the chloroplast gene expression machinery, where the RNA components are expressed exclusively in the chloroplast, whereas additional essential components are encoded in the nucleus. The import of proteins into the chloroplast is mediated by transit peptides located at the N-terminus of the imported proteins and protein complexes located in the inner and outer envelope of the chloroplast (translocon of the outer envelope of the chloroplast (TOC) and translocon of the inner envelope of the chloroplast (TIC), (Hormann et al., 2007)).

Transit peptides have a high content of hydroxylated, positively charged and small amino acids but a low abundance or absence of acidic or large amino acids (Lopez-Juez and Pyke, 2005).

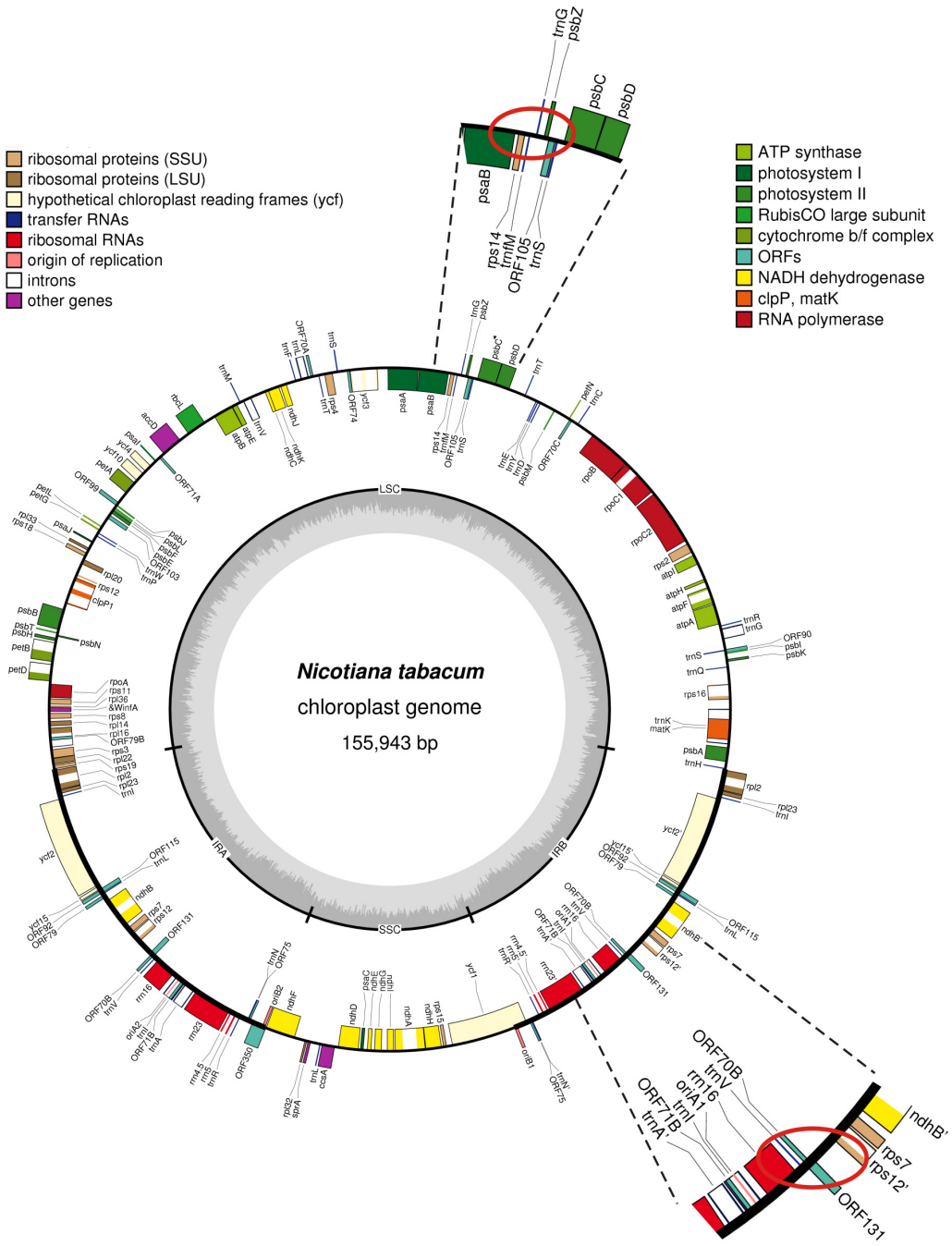

Fig. 9 Plastome map from *Nicotiana tabacum*. Genes on the outside of the circle are transcribed counter clockwise whereas those on the inside of the circle are transcribed clockwise. Genes for transfer RNAs are represented by the one-letter code of amino acids. Open reading frames are shown by orf plus codon number (≥70 codons). Gene classification is explained in the legend above. Plastome map was created using OGDRAW (Lohse et al., 2007) with the updated plastome sequence from Yukawa et al. (2005).

Another striking example of the coordination between the nuclear and plastid compartments is the transcriptional apparatus, since chloroplasts utilise RNA polymerases encoded by both the plastid and the nuclear genome (Lopez-Juez and Pyke, 2005; Bock, 2007).

1.4.2 Chloroplast gene expression and posttranscriptional steps

Posttranscriptional regulation plays a major role in controlling gene expression in chloroplasts, whereas transcriptional regulation is less important. Although one would anticipate that chloroplasts with their bacterial ancestors would exclusively possess a bacterial-like plastid encoded RNA polymerase (PEP), PEP mutants confirmed the presence of a second nuclear encoded single subunit bacteriophage-like RNA polymerase (NEP). However, the plants showed an albino phenotype indicating that NEP alone is not sufficient for gene expression necessary for photosynthetically active chloroplasts (Allison and Maliga, 1995; Hajdukiewicz et al., 1997; Krause and Krupinska, 2000; Legen et al., 2002). Thus, the presence of two different RNA polymerases in the chloroplast does indicate a certain control at the transcriptional level. Genes with housekeeping functions such as genes involved in transcription and translation carry a NEP as well as an *E. coli*-like PEP promoter. In contrast, there are only few genes that are exclusively transcribed from a NEP promoter, including the plastid encoded RNA polymerase. Genes encoding core subunits of the PEP can be found in plastomes of nearly all land plants, whereas the sigma factors necessary for a functional bacterial type polymerase are nuclear encoded, indicating again division of labour between the compartments (Liere and Börner, 2007). Once PEP is expressed it is thought to be more important for the synthesis of photosynthesis related genes of which, according to their bacterial origin, many show conserved boxes within their promoter region at position -35 and -10 upstream of the transcriptional start site (Lopez-Juez and Pyke, 2005; Liere and Börner, 2007). Thus, it is not surprising that plastidial genes driven by a bacterial type promoter can be efficiently recognized and transcribed by an *E. coli* RNA polymerase (Gatenby et al., 1981; Bradley and Gatenby, 1985; Boyer and Mullet, 1988; Eisermann et al., 1990).

Whereas three nuclear encoded polymerases (*RpoT* for RNA polymerase of the phage T3/T7 type) have been identified for eudicots, in cereals, the only analyzed representatives for monocots so far, possess only two nuclear encoded polymerases (Hedtke et al., 1997; Chang et al., 1999; Ikeda and Gray, 1999; Hedtke et al., 2000; Kobayashi et al., 2001; Kobayashi et al., 2001; Emanuel et al., 2004; Kusumi et al., 2004).

The information for subsequent subcellular localization of the polymerases are stored in their N-terminus. Whereas *RpoTp* encodes a plastid targeted polymerase, *RpoTm* encodes a polymerase that is transported to the mitochondria. Interestingly, the third gene, *RpoTmp* encodes a polymerase that, depending on its 5' end, can be transported either into the plastids or into the mitochondria (Hedtke et al., 1997; Hedtke et al., 1999; Hedtke et al., 2000;

Kobayashi et al., 2001; Kobayashi et al., 2001; Kobayashi et al., 2002). This different localization is translationally regulated since the mRNA for the NEP carries two translation initiation sites resulting in two different N-termini.

It was mentioned previously that chloroplast gene expression is mainly regulated posttranscriptionally, and thus, accumulation rates of different transcripts are not controlled by transcription rates, but rather by mRNA stability (Gruissem, 1989; Monde et al., 2000; Bollenbach et al., 2004). The stability of chloroplast mRNA is mainly regulated by polyadenylation of the 3' end which targets the RNA for degradation (Hayes et al., 1999). The mRNA degradation pathway in chloroplasts was shown to be similar to the process in bacteria including the steps of endonucleolytic cleavage, polyadenylation and exonucleolytic degradation (Bollenbach et al., 2007). Furthermore, RNA maturation plays a role regarding translation efficiency. Chloroplast mRNA maturation includes 5' and 3' end processing as well as intercistronic processing that is mediated by nuclear encoded ribonucleases (Stern and Kindle, 1993; Barkan et al., 1994; Hayes et al., 1996). Major endo- and exonucleases involved in maturation and degradation pathways are further described in Bollenbach et al. (2007).

Two other mechanisms highlight chloroplast diversity compared to their bacterial ancestors. First, chloroplasts possess mechanisms resulting in RNA editing, where single nucleotides are modified resulting in C to U, or less frequently, U to C conversions. These reactions may generate a translation initiation codon which is not encoded within the DNA sequence or restore evolutionary conserved amino acids (Wakasugi et al., 1994; Hirose et al., 1996; Bock, 2000; Shikanai et al., 2001; Inada et al., 2004; Tillich et al., 2005). The process of RNA editing involves *cis*-acting elements as well as *trans*-acting factors. The editing mechanism is not yet fully understood although two models for the editing reaction and machinery have been established so far (Schmitz-Linneweber and Barkan, 2007). RNA editing is common in land plants and has been shown to be crucial for the efficient translation of certain genes as well as for protein functionality (Bock et al., 1994; Hirose and Sugiura, 1997).

In addition to RNA editing, chloroplast genes require splicing reactions since they often contain introns, intervening sequences, which are relatively rare in bacteria. RNA splicing is essential for chloroplast development since genes encoding components of the expression machinery and the photosynthetic apparatus contain introns, and thus, represents an excellent regulatory mechanism for gene expression within the chloroplast by controlling the level of spliced vs. unspliced mRNA (Schmitz-Linneweber and Barkan, 2007). Interestingly, components of the splicing machinery are nuclear encoded which again suggests nuclear

control over chloroplast gene expression. Chloroplast introns are divided into three different groups (I, II and III), whose splicing reactions likely occur in a canonical process known from other group I and group II introns (Qin and Pyle, 1998; Bonen and Vogel, 2001; Lambowitz and Zimmerly, 2004). Since both of these mechanisms, RNA editing and splicing, were not present in the chloroplast ancestors, accomplishment of these processes necessitates engaging new proteins and shows further evidence for collaboration between the nuclear and plastid compartments (Schmitz-Linneweber and Barkan, 2007).

As previously described, the predominant transcriptional regulation, as observed in their prokaryotic ancestors, has shifted to mostly posttranscriptional and translational regulation in chloroplasts. Although the translation machinery in chloroplasts is bacteria-like and possesses 70S ribosomes inherited from their cyanobacterial ancestors, translation is separated from transcription, enabling protein synthesis to be regulated (Martin and Herrmann, 1998; Yamaguchi and Subramanian, 2000; Yamaguchi et al., 2000). Shift to translational regulation was concomitant with the drastic reduction of the engulfed cyanobacteria genome and led to a multitude of different regulation strategies including: the importance of Shine-Dalgarno sequences (SD), nuclear encoded factors, translation elongation, subcompartmental translation localization as well as *cis*-elements located in the untranslated regions of the mRNA. For example, the SD appear to have different regulatory effects depending on their positioning within the 5' UTR and the mRNA identity while for some genes an SD is absent and proper translation relies on other sequences (Peled-Zehavi and Danon, 2007). Secondary structures within the untranslated regions are also important regarding translation control, but compared to bacteria, who tend to negatively regulate translation by the formation of hairpin structures that hide the ribosome binding site, chloroplasts rely on positive regulation by the implementation of translation promoting *cis*-elements and secondary structures (Gold, 1988; Rochaix et al., 1989; Mayfield et al., 1994; Zerges et al., 1997; Kozak, 2005). A further regulation mechanism is displayed in the distribution of components of the translation machinery between the nucleus and chloroplast, highlighted by nuclear mutations resulting in chloroplast translation defectives (Barkan et al., 1994; McCormac and Barkan, 1999).

A last important regulatory step in protein synthesis is of course the balance between synthesis and degradation and thus protein stability within the chloroplast. In the chloroplast seven different protease families could be identified including Clp, FtsH, Lon and Deg proteases (Adam, 2007). The huge diversity of posttranscriptional modifications, such as maturation or activation by 5' N-formyl group and methionine cleavage (Giglione and Meinnel, 2001; Giglione et al., 2003), cleavage of transit peptides, turnover of proteins in

response to changing light quality (Lindahl et al., 1995) as well as protein quality control, point to the great importance of proteolytic processes involved in expression regulation. Although the peptide bond cleavage does not require energy, some proteases, as known from bacteria, depend on the presence of ATP for proper substrate unfolding (Baumeister et al., 1998). Interestingly, certain proteases such as the ClpP protease are crucial for plant development since deletion of several *clpP* genes resulted in more or less severe phenotypes including loss of shoot development (Shikanai et al., 2001; Kuroda and Maliga, 2003).

1.4.3 Chloroplast transformation and selection strategy

Although stable transformation of chloroplasts is now possible, initially, it was first thought to be impossible due to the double membrane which acts as physical barrier for the DNA delivery and the lack of a proper delivery system like viruses or bacteria that could be utilized as transformation vehicles (Bock, 2001).

Presently, three successful strategies for foreign gene delivery into plastids, the first critical step regarding chloroplast transformation, have been established: biolistic bombardment with a particle gun, polyethyleneglycol (PEG) treatment of protoplasts and the use of glass beads for unicellular algae (Hager and Bock, 2000; Bock, 2001; Maliga, 2004). Since later treatment of leaf explants is easier and requires less experience compared to protoplast treatment, biolistic bombardment is the most often used technique for plant transformation. The first biolistic chloroplast transformation was performed in 1988 where Boynton and Gillham succeeded to transform the unicellular alga, *Chlamydomonas reinhardtii,* with its single large chloroplast that accounts for approximately 60% of the total cellular volume (Boynton et al., 1988). Only two years later, successful chloroplast transformation was achieved using the higher plant *Nicotiana tabacum* (Svab et al., 1990). For biolistic gene delivery a particle gun was used to shoot small metal particles (tungsten or gold, 0.4-1.7µm diameter) which were coated with plasmid DNA into the cell (Hager and Bock, 2000) (Fig. 10A, B). The selection of an appropriate DNA transformation vector is critical for successful subsequent gene integration into the chloroplast genome. Generally chloroplast transformation vectors are *E. coli* plasmid derivatives carrying the gene of interest flanked by DNA sequences (> 400bp each) that are homologous to the plastid DNA representing the target area for integration into the plastome via homologous recombination (Hager and Bock, 2000; Bock, 2001). The transformed plastid subsequently disappears during cell propagation due to the absence of a plastid replication origin (Maliga, 2004).

As mentioned previously the integration of the desired DNA fragments into the chloroplast genome occurs via homologous recombination that is mediated by an efficient *RecA* type system inherited from their cyanobacterial ancestors (Cerutti et al., 1992; Cerutti et al., 1995; Kavanagh et al., 1999) (Fig. 10C). So far 14 suitable intergenic regions for foreign DNA integration were identified, whereof two, *trnG/trnfM* and *3'rps12/trnV*, are highlighted as an example in Fig. 9 (Maliga, 2004). Due to the high ploidy of the plastid genome and the fact that usually only a single plastome copy is transformed, it is important to establish an efficient and suitable selection system or strategy to identify and enrich cells containing transformed ptDNA copies (Hager and Bock, 2000). Today introduction of antibiotic-resistance genes or antibiotic-insensitive alleles of ribosomal RNA genes as well as markers that restore photoautotrophic growth by complementing non-photosynthetic mutants represent the three common techniques for chloroplast transformation (Boynton et al., 1988; Newman et al., 1990; Svab et al., 1990; Goldschmidt-Clermont, 1991; Carrer et al., 1993; Svab and Maliga, 1993; Bateman and Purton, 2000; Huang et al., 2002).

A commonly used strong antibiotic resistance gene is the *aadA* gene encoding a bacterial aminoglycoside 3''-adenylyltransferase that confers resistance against spectinomycin and streptomycin that effectively inhibit translation on 70S ribosomes present in the chloroplast (Bock, 2001; Maliga, 2004). To generate an actively transcribed and translated selectable marker system it is necessary to fuse the marker gene to a plastid expression system containing a plastid promoter as well as a 5' untranslated region (UTR) that provides a Shine-Dalgarno sequence for ribosome binding and a 3' UTR containing *cis*-acting elements known to confer transcript stability and control efficient translation (Goldschmidt-Clermont, 1991; Staub and Maliga, 1993; Bock, 2001). Once a selectable marker is chosen, the transformed chloroplast confers resistance against the chosen selection pressure. At this stage the plastid genome population is termed "heteroplasmic", since a single chloroplast with its hundreds of plastome copies carries both recombinant and wild type plastomes. For stable transformation it is important that the chloroplasts and respective cell lines that carries the transformed plastomes contains exclusively transformed plastome copies, thus termed "homoplasmic".

Constantly applied selection pressure that force the plants to obtain high amount of recombinant plastid DNA together with cell propagation actively promote homoplasmy (Hager and Bock, 2000; Maliga, 2004) (Fig. 10A; Fig. 11).

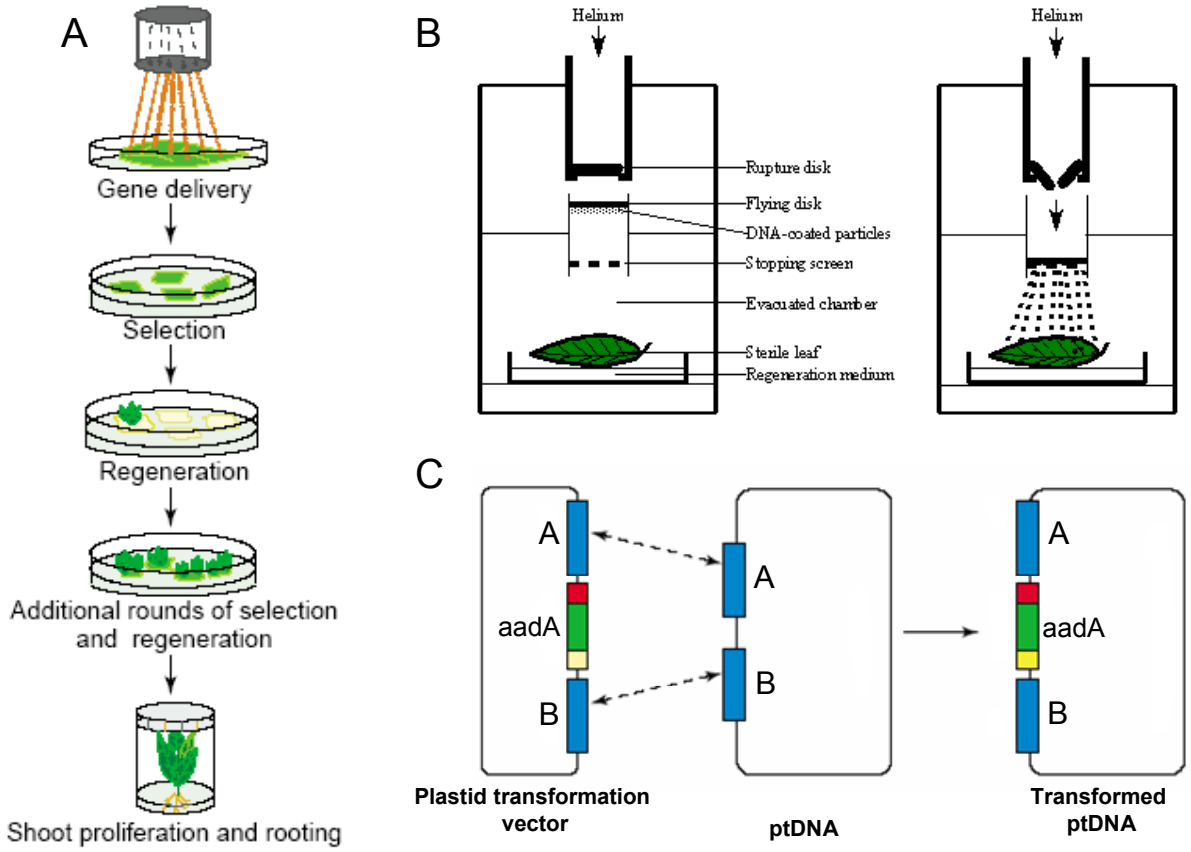

Fig. 10 Simplified scheme for biolistic chloroplast transformation and transgene integration into the plastid genome via homologous recombination (modified from Hager and Bock, 2000 and Bock and Khan, 2004). (A) The DNA construct is immobilized to the surface of microscopic gold particles and introduced into living leaf cells via biolistic transformation. Subsequently the leaf sample is cut into pieces which are exposed to regeneration medium containing the plastid translation inhibitor spectinomycin. Since the transformation vector carries the selection marker gene *aadA*, which confers spectinomycin resistance, transplastomic cells can regenerate on antibiotic containing medium and form resistant calli and shoots, whereas untransformed antibiotic sensitive cells bleach and turn yellow. Homoplasmy and thus stable transformation is obtained from heteroplasmic material through several additional regeneration rounds under selection pressure. Finally, root proliferation of homoplasmic shoots is obtained in MS medium supplemented with sucrose. (B) Schematic overview of a helium-driven particle gun. A plastic rupture disk seals the gas tube and allows for building up a defined gas pressure inside the tube (left). At a certain pressure the rapture disk bursts and the flying disk, to which gold particles carrying the transforming DNA are immobilized to the lower side, is accelerated. The flying disk is stopped by a metal grid, the stopping screen, and the gold particles that pass the screen penetrate the cells of the sterile leaf (right). (C) Integration of a transgene (in this case the selection marker *aadA*) into a non-coding intergenic region of the plastome (ptDNA) via homologous recombination (dashed lines) between two flanking plastidal regions (blue) within the vector and the plastid DNA. The selection marker *aadA*, marked in green, is framed by an expression cassette consisting of a promoter with a 5' untranslated region containing a Shine-Dalgarno sequence (yellow) and a 3'untranslated region (red) to confirm stability.

Once homoplasmy is obtained, transformation is stable and the formerly needed selection marker genes become undesired since transmission to wild relatives or microorganisms cannot be excluded when plants are grown in the field (Daniell, 2002; Kay et al., 2002).

For this reason, elimination of the selectable marker gene is desirable but also to allow the reuse of the few available markers for further transformations as well as release the plant from the burden to express the selection marker gene (Khan and Maliga, 1999; Corneille et al., 2001).

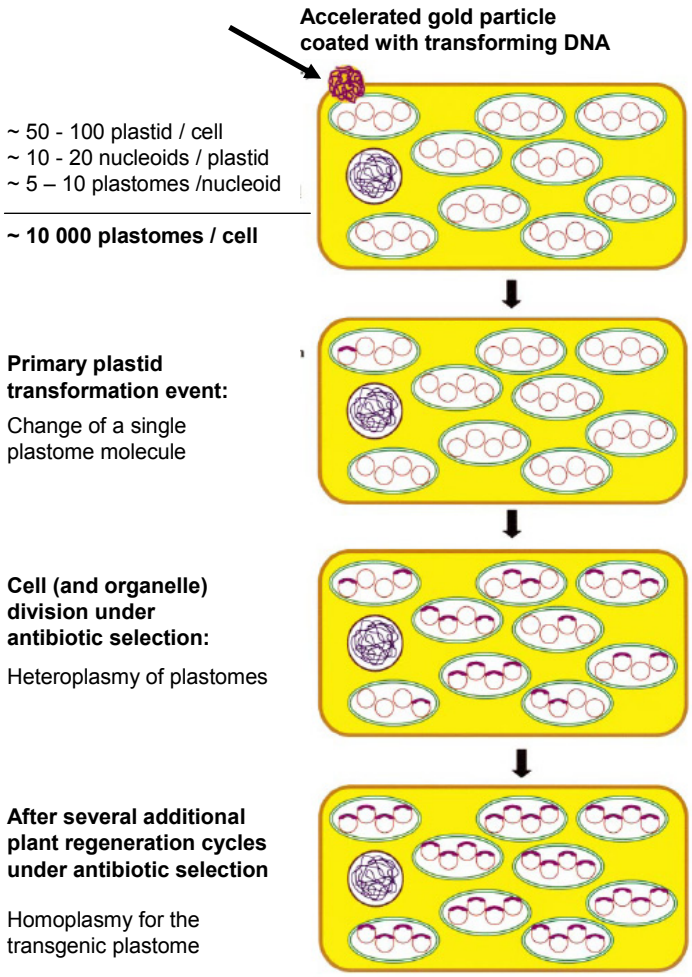

Fig. 11. Schematic description of plastid genome sorting and obtainment of homoplasmic transplastomic cell lines during cell and organelle division (from Bock, 2001). Chloroplast transformation usually involves the change of only a single or at most a few plastid genome copies within the highly polyploid plastome of a leaf cell. Cell and organelle division under selection pressure promote an enrichment of chloroplasts containing transformed genomes, whereas chloroplasts harbouring only wild type genomes are effectively eliminated. Cells with chloroplasts that still contain a mixed population of wild type and transformed plastid genome molecules are termed "heteroplasmic". Through additional regeneration rounds under selection pressure gradual loss of residual wild type plastome copies leads to cells with a homogenously transformed plastid population commonly termed "homoplasmic".

So far four strategies have been established for successful removal of the selectable marker gene, so called "marker recycling" (Fischer et al., 1996; Hager and Bock, 2000; Iamtham and Day, 2000).

The first strategy is based on homologous recombination. The marker gene is flanked by two direct repeats which lead to a loss of the marker due to recombination between those repeats (Fischer et al., 1996). The second strategy uses the co-transformation of two independent transformation vectors. While the gene of interest is inserted as usual into the chloroplast genome, the co-transformed selection marker is inserted into an essential gene, thus preventing homoplasmy. The selectable marker gene is segregated out while homoplasmy is obtained via regeneration without selection pressure (Fischer et al., 1996). A third approach was presented by Klaus et al. (2004) using "visually aided" complementation of knock out mutants combined with transiently co-integrated marker genes. Although marker-free plants can be obtained already in the first T_0 generation a disadvantage might be the dependence upon a mutant donor plant for plastid transformation rather than wild type plants (Klaus et al., 2004).

The fourth efficient approach uses marker genes that are flanked with recombination sites recognized by a site-specific recombinase. With this feature the marker gene can be recombined out using *loxP* sites (locus of X-over P1), recognized by the P1 phage CRE site-specific recombinase (cre: cyclization recombination), or between *attB* and *attP* bacterial attachment sites recognized by the phiC31 phage site-specific recombinase (Corneille et al., 2001; Hajdukiewicz et al., 2001; Ghosh and Van Duyne, 2002; Kühn and M. Torres, 2002; Corneille et al., 2003; Kuroda and Maliga, 2003; Maliga, 2003; Maliga, 2004; Kittiwongwattana et al., 2007).

1.5 CRE-lox recombination system

The well characterized CRE-lox recombination system is based on the site-specific recombination between two *loxP* sites mediated by the CRE recombinase derived from phage P1 (Adams et al., 1992; Guo et al., 1997; Corneille et al., 2001; Hajdukiewicz et al., 2001; Maliga, 2003). CRE (approximately 38 kDa) can mediate recombination between linear, circular or supercoiled DNA both *in vivo* and *in vitro* (Abremski et al., 1983). Depending on the orientation of the *loxP* sites either an inversion resulting from inverted *loxP* sites or an excision resulting from directly orientated *loxP* sites of the *loxP*-flanked ("floxed") DNA is mediated by CRE. An integration caused by intermolecular recombination occurs when the *loxP* sites are located on two different DNA molecules (Saraf-Levy et al., 2006). To date successful Cre-mediated deletion in plants is reported for nuclear as well as chloroplast genes and is also used in mammalian systems (Dale and Ow, 1991; Bayley et al., 1992; Russell et

al., 1992; Odell et al., 1994; Kuhn et al., 1995; Corneille et al., 2001; Jia et al., 2006; Lutz et al., 2006).

To obtain successful marker deletion a marker gene flanked by two directly orientated *loxP* sites was introduced into the chloroplast genome of a CRE-free plant (Corneille et al., 2001). *loxP* sites are 34 bp sequences consisting of 13 bp inverted repeats and an 8 bp asymmetrical linker indicating the orientation (Guo et al., 1997; Corneille et al., 2001).

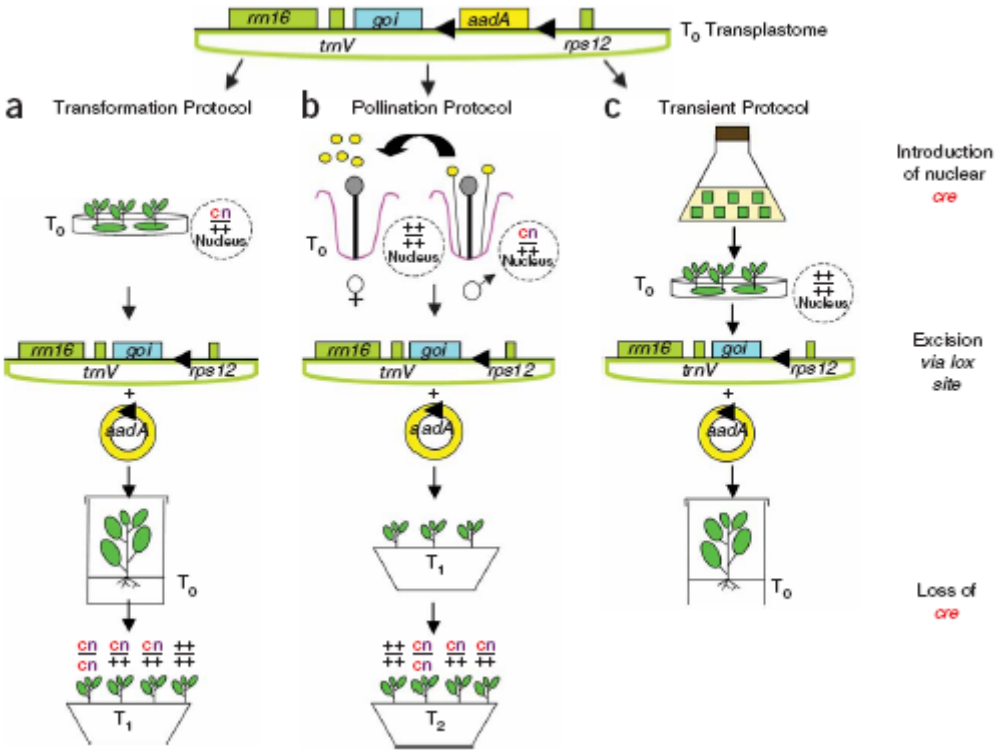

Fig. 12 Overview of approaches for CRE-mediated plastid marker gene excision (Lutz et al., 2006). The transformed ptDNA map containing a floxed *aadA* and the gene of interest as well as the plastidial homologous sequences of the *rrn16*, *trnV* and *3'rps12* genes is shown on top. Triangles indicate presence and orientation of *loxP* sites through which CRE-mediated circular *aadA* excision occurs. Single protocols for *Cre* integration via (a) transformation, (b) pollination and (c) transient expression are shown. Presence of *Cre* and the linked kanamycin resistance (*Neo*) gene in the nuclear genome are indicated by c and n, respectively; their absence by a "+". T_0 refers to transgenic plants regenerated from tissue culture; T_1 and T_2 are the first and second generation progeny of T_0 produced by self pollination.

In terms of chloroplast targeted marker gene elimination, the CRE recombinase is nuclear encoded and translationally fused to a transit peptide derived from the nuclear encoded small subunit of Rubisco to mediate subsequent import into the chloroplast (Corneille et al., 2001). There are at least three ways to introduce the CRE recombinase into the nucleus with the possibility to segregate it out again once all marker genes are excised (Fig. 12). The first approach is based on *Agrobacterium* mediated transformation of the transplastomic plant. The

advantage is a very fast introduction of the recombinase and thus a fast expression of the recombinase activity and the loss of the CRE recombinase in the T_1 seed progeny (Lutz et al., 2006). A major disadvantage in using this technique are the commonly observed CRE-mediated recombination events between direct repeats within the chloroplast genome, so called non-*loxP* recombination events (Corneille et al., 2001; Corneille et al., 2003; Lutz et al., 2006). The second and most laborious approach is the transient expression of CRE recombinase using non-integrating T-DNA delivered by *Agrobacterium* mediated transformation (Lutz et al., 2006).

The third approach to obtain marker-free transplastomic plants is based on the introduction of the CRE recombinase via pollination where a CRE expressing plant is used to pollinate a transplastomic plant. Although this technique is the most time consuming, since marker and CRE-free plants are first recovered in the T_2 seed generation, undesired CRE activity regarding recombination between plastome sequences is not observed (Lutz et al., 2006). Several detailed protocols to obtain marker-free transplastomic plants are described in Lutz et al. (2006).

1.6 Target bacteria and their specific lysins

The target bacteria used in this thesis belong to the ten pathogens causing the highest mortality worldwide (Fig. 13).

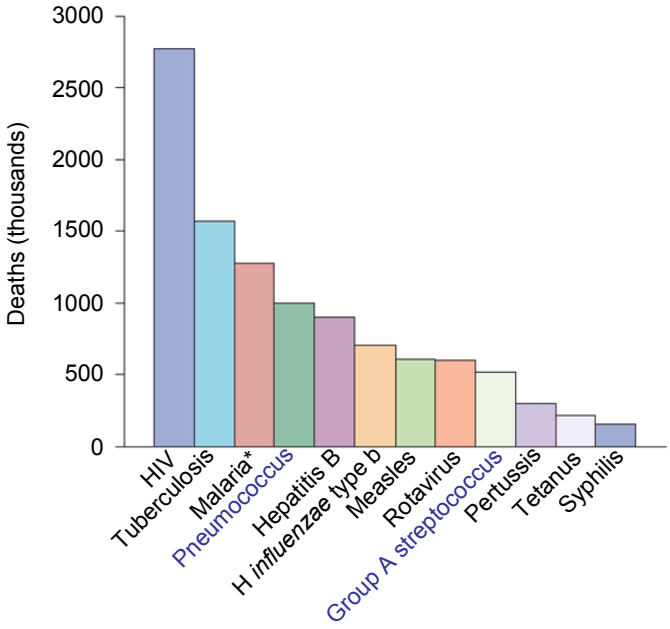

Fig. 13 Estimated number of global deaths caused by individual pathogens in 2002 (modified from Carapetis et al., 2005). Bacterial pathogens used in this work are indicated in blue.

Detailed information regarding annual costs caused by the target bacteria can be found at Institute of Medicine, "Vaccines for the 21st century: a tool for decision-making", National Academy Press, 2000.

1.6.1 Streptococcus pyogenes and PlyGBS

PlyGBS, the lytic enzyme of the streptococci phage NCTC 11261 attacks Group A (*Streptococcus pyogenes,* GAS) and Group B (*Streptococcus agalactiae,* GBS) streptococci (Cheng et al., 2005). Due to a specific antigen, a C-polysaccharide in their cell wall, streptococci were classified according to Rebecca Lancefield into different streptococci groups labelled with a capital letter (Lancefield, 1933).

S. pyogenes is specialised to live in human hosts which often harbour the bacterium in their respiratory tract without signs of diseases. Symptomatic colonization by the bacterium that has already developed several resistance mechanisms against commonly used antibiotics causes a broad range of infections that attack skin and mucosal membranes and can cause life threatening diseases (Kim and Kaplan, 1985; Köller et al., 2008). Generally the infections caused by *S. pyogenes* can be divided into (a) non invasive diseases such as strep throat, sinusitis, otitis, cellulitis and impetigo, (b) invasive disease such as joint or bone infections, necrotizing fasciitis (so called flesh eating disease), streptococcal toxic shock syndrome, myositis, bacteremia, scarlet fever, meningitis, endocarditis and pneumonia and (c) nonsupprative sequelae such as rheumatic fever and post-streptococcal glomerulonephritis (CDC, (http://www.cdc.gov/ncidod/dbmd/diseaseinfo/groupastreptococcal_g.htm); RKI (http://www.rki.de/cln_048/nn_504496/DE/Content/Infekt/EpidBull/Merkblaetter/Rat__Scharlach.html#doc200740bodyText1)). The prevalence of severe group A diseases is at least 18.1 million cases with 1.78 million new cases and at least 517 000 estimated deaths per year. Thereof, the greatest burden is caused by rheumatic heart disease with at least 15.6 million cases with 282 000 new cases and nearly the same amount of deaths per year (Carapetis et al., 2005). In addition to these severe diseases there are more than 111 million cases of pyoderma and more than 616 million cases of pharyngitis per year.

Streptococcus agalactiae or group B streptococci are the major cause of neonatal meningitis and sepsis worldwide. GBS were found to colonize the human genital and lower intestinal tract from which the bacteria can be transmitted perinatally to the fetus. Beside the newborn infections, GBS can also cause substantial morbidity and mortality in adults (Farley et al., 1993; Cheng et al., 2005). As is the case with other bacteria, significant numbers of antibiotic resistant GBS isolates have been identified so far (Fernandez et al., 1998; Cheng et al., 2005).

Taken together *S. pyogenes* and *S. agalactiae* are important causes of morbidity and mortality worldwide forcing the need to develop new prevention strategies (Carapetis et al., 2005; Cheng et al., 2005).

As discussed previously phage lytic enzymes display a promising tool to control and prevent GAS and GBS diseases. A suitable phage lytic enzyme, PlyGBS was recently identified and was shown to successfully remove GBS colonizing the vagina and oropharynx of mice when expressed recombinantly. *In vitro* experiments showed its narrow host spectrum as well as its pH optimum (pH 5) within the range normally found in the human vaginal tract (Nelson et al., 2001; Cheng et al., 2005).

1.6.2 Streptococcus pneumoniae and Pal and Cpl-1

Cpl-1, a lysozyme and Pal, an amidase, are lytic enzymes of the pneumococcal phages Cp-1 and Dp-1, respectively, whose host bacteria *Streptococcus pneumoniae* claims around 1.6 million deaths per year (Lopez, 2004; López and García, 2004; Fernandez-Tornero et al., 2005; Witte et al., 2008). It has been a bacterium of clinical relevance since Louis Pasteur (1822-1895) and George Miller Sternberg (1838-1915) discovered it independently in 1881. *S. pneumoniae* frequently colonizes the nasopharyngeal tract of healthy subjects without any symptoms but also represents the 6th most frequent cause of death, pneumonia (Montagnani et al., 2008). Currently around 100 million people are infected every year with around 10% of infections resulting in fatalities (Lopez, 2004). In Germany 800 000 cases of pneumonia are reported annually (Welte et al., 2003). Since it causes a huge variety of diseases ranging from otis media, sinusitis and exacerbations of chronic bronchitis, to severe infections such as pneumonia, bacteraemia, arthritis, endocarditis, meningitis and sepsis it is an important cause of invasive infections in humans and a leading cause of concern for public health (Montagnani et al., 2008). So far around 12 000 deaths per year are reported for Germany due to pneumococci infections (Randerath et al., 2000). Regarding the broad range of infections caused by pneumococci, bacterial resistance displays an increasing problem worldwide. 10 to 90% of *S. pneumoniae* are resistant to commonly used antibiotics (depending on the geographical area) and 56% are already multidrug resistant (Syrogiannopoulos et al., 1997; Schrag et al., 2004).

Pal and Cpl-1 were identified to be lytic enzymes that efficiently kill their target bacteria *S. pneumoniae in vitro* (e.g. from aortic vegetation cultures) and *in vivo* regardless of its antibiotic sensitivity (Loeffler et al., 2001). Cpl-1 was used to eliminate pneumococci *in vivo* from the blood of rats with experimental endocarditis and from mice (Loeffler et al., 2001;

Loeffler et al., 2003; Entenza et al., 2005). Based on the assumption that development of neutralizing antibodies against lysins should not be an obstacle because phages are common entities in the environment and are consumed in food, it was demonstrated that *in vivo* activity of Cpl-1 was equal in both previously exposed and unexposed animals (Loeffler et al., 2003). A possible explanation may be the kinetics of phage or lysin action in that it is much faster than the host's production of antibodies, and thus, since no signs of anaphylaxis or adverse side effects could be observed, repeated administration is feasible (Sulakvelidze et al., 2001; Jado et al., 2003). Both endolysins display modular organization consisting of two domains, an N-terminal catalytic domain and a C-terminal binding domain that facilitates the anchoring of the enzyme to choline residues of teichoic and lipoteichoic acids incorporated into the cell wall and thus helps to orientate the substrate in a proper way (Garcia et al., 1988; Sheehan et al., 1997; Hermoso et al., 2003; Varea et al., 2004). Due to their mode of action the amidase Pal and the lysozyme Cpl-1 have been shown to act synergistically as well as together with antibiotics (López and García, 2004; Djurkovic et al., 2005).

1.7 Aim and focus of this work

Due to the increasing resistances of bacteria against common antibiotics it is important to produce effective and cost efficient alternatives. Phage lytic enzymes offer the property of high efficient killing of target bacteria combined with high target specificity. Additionally no resistances against these proteins are known so far.

Utilisation of a chloroplast transformation system has numerous advantages. Beside high containment due to the maternal inheritance of chloroplasts, it offers the possibility to produce high amounts of foreign proteins and thus, provides the perfect expression system for the aforementioned phage lytic enzymes.

Thus, the aim of this project was the evaluation of the potential of tobacco chloroplasts as a production platform for phage lytic enzymes. The biological functionality of the proteins, their stability within the plant and possible effects of the expressed proteins were analyzed.

2 Material and methods

All solutions and buffers were made with high-purity, filtered (water filter equipment Purelab plus, USF Deutschland GmbH, Ransbach-Baumbach, Germany) and autoclaved water (here after termed as water or H_2O). All items used for work with RNA were autoclaved immediately before using.

2.1 Chemicals and enzymes

The basic sets of chemicals used for preparing solutions and media were ordered from the following companies:

- Merck (Darmstadt, Germany)
- Sigma (St. Louis, USA)
- Serva (Heidelberg, Germany)
- Difco Laboratories (Detroit, USA)
- Qbiogene (Heidelberg, Germany)
- Sigma Chemie (Deisenhofen, Germany)
- Duchefa (Haarlem, Netherlands)
- GibcoBRL (Karlsruhe, Germany)
- Applichem (Darmstadt, Germany)
- Invitrogen (Karlsruhe, Germany)
- Biozym (Hessisch Oldendorf, Germany)
- Roche (Mannheim, Germany)
- Sigma-Aldrich Chemie GmbH (Munich, Germany)

Enzymes and chemicals for the modification of DNA, such as restriction enzymes and dNTPs, were obtained from Roche (Mannheim, Germany), Bioline GmbH (Luckenwalde, Germany), Promega GmbH (Mannheim, Germany) and New England Biolabs GmbH (Frankfurt, Germany). Enzymes were used according to manufacturer's description.

2.2 Synthetic oligonucleotides

The following synthetic oligonucleotides were synthesized by Metabion (Martinsried, Germany) and used for PCR.

Restriction site modification (insertion of *Nco*I site)

Pal:

Pal-F	(5'-AACCATGGCTAGCGGAGTAGATATTGA -3')	forward
M13-rev	(5'-GGAAACAGCTATGACCATGA-3')	reverse

Cpl-1:

Cpl-1-NcoI	(5'-CCATGGCTAGCGTAAAAAAAAATG -3')	forward
M13-rev	(5'- GGAAACAGCTATGACCATGA -3')	reverse

pTox promoter fragment amplification

Tox-pro-fwd	(5'-AAAGAGCTCGCTCCCCCGCCGTCGTTCAA-3')	forward
Tox-pro-rev	(5'TTCTGCCATGAATCCCTCCCTAATAACTTCGTATAG CATACATTATACGAAGTTATCAACTGTATCCAA-3')	reverse

Plasmid sequencing

pHK20-fwd	(5'-GGG AGG GAG ACC ACA ACG G-3')	forward
pHK20-rev	(5'TTG GGC CCA GTT TAA TTG CA-3')	reverse

2.3 Plasmids and vectors

For cloning and heterologous expression via transformation, the following plasmids and vectors were used:

- pHK20 (Kuroda and Maliga, 2001)
- pKP6 (Katrin Piepenburg, Max Planck Institute of Molecular Plant Physiology, Golm, Germany; see appendix)
- pKP9 (Katrin Piepenburg, Max Planck Institute of Molecular Plant Physiology, Golm, Germany; see appendix)
- pOD1 (Oliver Drechsel, Max Planck Institute of Molecular Plant Physiology, Golm, Germany; see appendix)
- pMO16 (see appendix)
- pToxGFP (see appendix)
- pToxPal (see appendix)
- pToxCpl-1 (see appendix)
- pTox (see appendix)
- pMO24 (see appendix)

2.4 Markers

The following markers were used for DNA (Gene Ruler™), RNA (RNA Ladder (0.5-10 kb) and protein (SeeBlue® Plus2) gels:

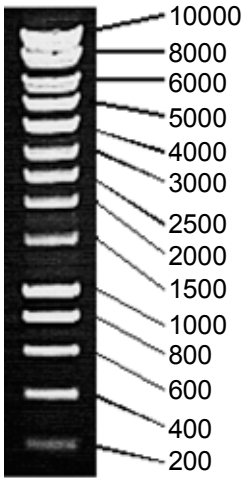	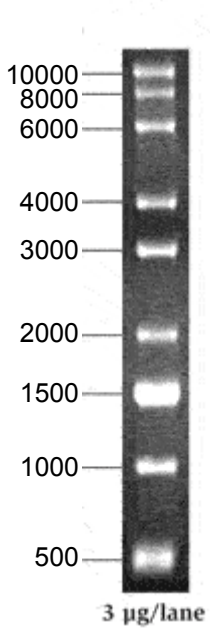	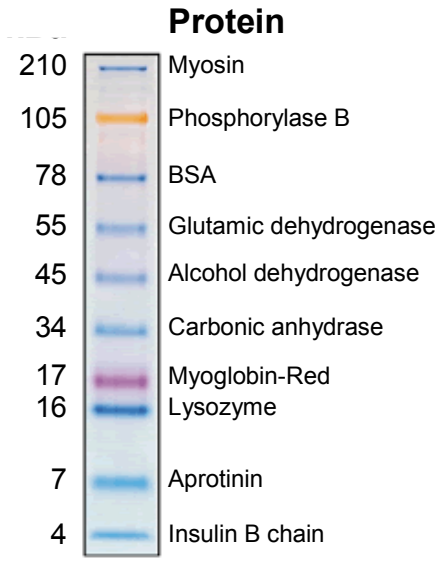
Gene Ruler™, fragment length in base pairs (bp) (Fermentas GmbH, St.Leon-Rot, Germany)	**RNA ladder (0.5-10 kb)**, fragment length in base pairs (bp) (Invitrogen, Karlsruhe, Germany)	**SeeBlue® Plus2 protein marker** Protein size in kilo Dalton (kDa) (Invitrogen, Karlsruhe, Germany)

2.5 Appliance

- Centrifuge 5415R and mini-spin plus (Eppendorf AG, Hamburg, Germany): used for all experiments using small reaction tubes (≤ 2.0 ml)
- Centrifuge Sorvall RC-6 (Thermo scientific, Karlsruhe, Germany): used for sample volumes larger than 2 ml
- UV/Visible spectrophotometer (Ultrospec 3100 pro, GE Healthcare Europe GmbH, Munich, Germany)
- Thermomixer (comfort 5355, Eppendorf AG, Hamburg, Germany)

- PCR-cycler (Mastercycler ep gradient thermal cycler, Eppendorf Ag, Hamburg, Germany)
- UV-crosslinker (Vilbert Lourmat, Marne la Vallee, France)
- PerfectBlue™ Double Gel System (Peqlab Biotechnology GmbH, Erlangen, Germany)
- PerfectBlue™ Gel system (Mini S-L) (Peqlab Biotechnology GmbH, Erlangen, Germany)
- Infinity™ Video System (Peqlab Biotechnology GmbH, Erlangen, Germany)
- PowerPac™ basic power supply and HC (Bio-Rad Laboratories GmbH, Munich, Germany)
- Analytical balance (XS802S, Mettler-Toledo GmbH, Gießen, Germany)
- Digital sonifier (W-250D, Heinemann, Schwäbisch Gmünd, Germany)
- Storage phosphor screens (GE Healthcare Europe GmbH, Munich, Germany)
- Typhoon™ Trio Variable Mode Imager (GE Healthcare Europe GmbH, Munich, Germany)
- Water bath (FBC 620, Fisher Scientific GmbH, Schwerte, Germany)
- Platform shaker (Heidolph®Polymax 1040, Heidolph Instruments GmbH & Co KG, Schwabach, Germany)
- Magnetic stirrer (IKA RH basic KT/C IKAMAG, AL-Labortechnik, Amstetten, Germany)
- Stereomicroscope (MZ 16FA, Leica, Wetzlar, Germany)
- Fluorescence microscope (BX60, Olympus GmbH, Hamburg, Germany)
- Camera (RT spot, Visitron Systems, Munich, Germany)
- Vortex-Genie 2 (Roth, Karlsruhe, Germany)
- pH-meter (pHI® 340, Beckman Coulter GmbH, Krefeld, Germany)

2.6 Biomaterial and strains

2.6.1 Bacterial strains

Within this work the following bacteria strains were used to carry out cloning, transformation and bacterial assays:

***Escherichia coli* (*E. coli*) strains.**

strain	genotype	reference/derivation
One shot® Top10F' *E. coli*	F#{*lac*^{q}Tn10 (Tet^R) *mcr*A Δ(*mrr-hsd*RMS-*mcr*BC) Φ80*lac*ZΔM15 Δ*lac*X74 *rec*A1 *ara*D139 Δ(*ara-leu*)7697 *gal*U *gal*K *rps*L *end*A1 *nup*G	(Invitrogen, Karlsruhe, Germany)

***Streptococcus pyogenes* (*S. pyogenes*) strains.**

strain	reference/derivation
M49 (591)	(B. Kreikemeyer, Rostock, Germany)

***Streptococcus pneumoniae* (*S. pneumoniae*) strains.**

strain	reference/derivation
RKI 720 capsule type 6B	(S. Hammerschmidt, Munich, Germany)

2.6.2 Higher plants / plant lines

All procedures with plants were done using the following higher plant species and accessions as well as transgenic plants:

Existing plants:

- *Nicotiana tabacum c.v. petit havana* (wild type, Wt)
- *Nicotiana tabacum Nt-Cre-2-200,* transgenic *N. tabacum* line expressing CRE recombinase

Constructed transgenic plants:

- *Nicotiana tabacum Nt-pMO16,* transplastomic *N. tabacum* line expressing PlyGBS, T_0 generation
- *Nicotiana tabacum Nt-pMO24,* transplastomic *N. tabacum* line expressing GFP, T_0 generation
- *Nicotiana tabacum Nt-pToxGFP,* transplastomic *N. tabacum* line expressing GFP, T_0 generation
- *Nicotiana tabacum Nt-pToxCpl-1,* transplastomic *N. tabacum* line expressing Cpl-1, T_0 generation
- *Nicotiana tabacum Nt-pToxPal,* transplastomic *N. tabacum* line expressing Pal, T_0 generation

- *Nicotiana tabacum Nt-pToxGFP-Cre,* T_1 generation obtained from transplastomic *N. tabacum* line expressing GFP by pollination with *Nt-Cre-2-200*
- *Nicotiana tabacum Nt-pToxCpl-1-Cre,* T_1 generation obtained from transplastomic *N. tabacum* line expressing Cpl-1 by pollination with *Nt-Cre-2-200*
- *Nicotiana tabacum Nt-pToxPal-Cre,* T_1 generation obtained from transplastomic *N. tabacum* line expressing Pal by pollination with *Nt-Cre-2-200*
- *Nicotiana tabacum Nt-pMO24-selfed,* T_1 generation obtained from *Nt-pMO24* by self-pollination
- *Nicotiana tabacum Nt-pToxGFP-Cre-selfed,* T_2 generation obtained from *Nt-pToxGFP-Cre* by self-pollination, homoplasmic, *aadA* cassette recombined out
- *Nicotiana tabacum Nt-pToxCpl-1-Cre-selfed,* T_2 generation obtained from *Nt-pToxCpl-1-Cre* by self-pollination, homoplasmic*, aadA* cassette recombined out
- *Nicotiana tabacum Nt-pToxPal-Cre-selfed,* T_2 generation obtained from *Nt-pToxPal-Cre* by self-pollination, homoplasmic, *aadA* cassette recombined out

Homoplasmic plants lines of T_0 generation (*Nt-pMO16*, *Nt-pMO24*, *Nt-pToxGFP*, *Nt-pToxPal*, *Nt-pToxCpl-1*) were obtained through several regeneration rounds on spectinomycin containing media.
Recombined plants of T_1 generation (*Nt-pToxGFP-Cre*, *Nt-pToxPal-Cre*, *Nt-pToxCpl-1-Cre*) were identified by selection on spectinomycin containing media. Corresponding homoplasmic plants were either identified by Southern blot and seed assay or were obtained from the T_2 generation (*Nt-pToxGFP-Cre-selfed*, *Nt-pToxPal-Cre-selfed*, *Nt-pToxCpl-1-Cre-selfed*).
CRE recombinase expressing plant (*Nt-Cre-2-200*) was kindly provided by Dr. Pal Maliga.

2.7 Growth conditions

2.7.1 Bacteria growth conditions

2.7.1.1 Growth conditions

Escherichia coli cells were cultured in LB medium at 37 °C (Sambrook et al., 1989). Transformed *E. coli* cells were selected by its antibiotic resistance (2.7.1.2), which was obtained through the transformation with the antibiotic resistant marker gene. Only cells containing these plasmids were able to grow on selection media.

2.7.1.2 Antibiotics

antibiotic	final concentration
Ampicillin	100 mg/l
Spectinomycin	100 mg/l

2.7.1.3 Media

LB (Luria-Bertani) liquid media (Bertani, 1951):

10 g/l NaCl
10 g/l select peptone 140
5 g/l yeast extract
pH 7.0 with NaOH

THY liquid media (Köller et al., 2008):

30 g/l Todd-Hewitt Broth
5 g/l yeast extract

Media were autoclaved. For solid media 1.5% (w/v) agar were added to the appropriate liquid media. If required, appropriate antibiotics were added to the sterile media at a temperature of less than 50 °C and at final concentrations given above (2.7.1.2). All work was done under sterile conditions (clean bench).

2.7.2 Plant growth conditions

2.7.2.1 Plant growth in sterile culture

For shoot regeneration and obtainment of homoplasmic plants, bombarded leaf tissue or heteroplasmic tissue was placed on RMOP medium containing 500 mg/l spectinomycin. To confirm resistance, leaf material was in parallel set on RMOP medium containing 500 mg/l spectinomycin and 500 mg/l streptomycin. Regenerated shoots were put on RM medium containing 500 mg/l spectinomycin. All sterile cultures were grown under following phytochamber conditions (light/ dark period: 16 h/ 8 h; 25 °C/ 20 °C; 55 µE).

2.7.2.2 Grafting

For grafting 4 weeks old transplastomic plants derived from regeneration were cut at an ankle of 45°. A 4 weeks old wild type rootstock derived from cuttings was cut in the same way and

the transplastomic plant was transferred onto the wild type rootstock and fixed with a plastic tube used as cuff until plants merged.

2.7.2.3 Homoplasmy (seed) tests

To verify the homo- respectively heteroplasmic stage of the plant plastome, seeds of the transformed plants were sterilized and germinated using the following protocol. After initial washing with 70% Ethanol, 3 min sterilization via shaking in a bleaching solution (NaOCl (13% (v/v)) and water [2:1], 0.02% (v/v) Triton X-100) and at least two washing steps in sterile water the sterilized seeds were swollen in water over night at 4 °C and placed on MS plates for germination under phytochamber conditions (2.7.2.1).

2.7.2.4 Antibiotics

antibiotic	final concentration
Streptomycin	500 mg/l
Spectinomycin	500 mg/l
Kanamycin	200 mg/l

2.7.2.5 Media

RMOP medium for shoot regeneration (Svab et al., 1990):

100 ml/l	10x RM Macro
10 ml/l	100x RM Micro
5 ml/l	1% FeEDTA
30 g/l	Sucrose
100 mg/l	Myo-Inositol
1 ml/l	ThiaminexHCl
100 µg/l	1- Naphthaleneacetic acid (NAA)
1 mg/l	6- Beznylaminopurine (BAP)
	pH 5.8 with KOH

RM medium for plant maintenance in steril environment (Svab and Maliga, 2007):

100 ml/l	10x RM Macro
10 ml/l	100x RM Micro
5 ml/l	1% EDTA
30 g/l	Sucrose
	pH 5.8 with KOH

RM Macro:

4.4 g/l	$CaCl_2 \times 2\ H_2O$
1.7 g/l	KH_2PO_4
19 g/l	KNO_3
3.7 g/l	$MgSO_4 \times 7\ H_2O$
16.5 g/l	NH_4NO_3

RM Micro:

1.69 g/l	$MnSO_4 \times H_2O$
860 mg/l	$ZnSO_4 \times 7\ H_2O$
620 mg/l	H_3BO_4
83 mg/l	KI
25 mg/l	$Na_2MoO_4 \times 2\ H_2O$
2.5 mg/l	$CuSO_4 \times 5\ H_2O$
2.5 mg/l	$CoCl_2 \times 6\ H_2O$

2.8 Nucleic acid methods

2.8.1 Preparation of DNA

2.8.1.1 Plasmid-DNA preparation (Miniprep)

The *E. coli* plasmid preparation was done according to a modified method of Bimboim and Doly (1979) and Sambrook et al. (1989).

For isolation of plasmid DNA 2 ml of an *E. coli* over night culture was transferred into a reaction tube and centrifuged (1 min, 12000 x g, RT). The supernatant was discarded and the pellet was resuspended by vortexing in 100 µl Buffer I. For lysis of bacteria, 200 µl Buffer II were added and mixed by inverting. 150 µl Buffer III were added and the tube inverted. The solution was centrifuged (15 min, 12000 x g, 4 °C) to spin down the precipitate. The upper phase (approximately 400 µl) was transferred into a new tube and 280 µl isopropanol were added and mixed. After centrifugation (15 min, 12000 x g, 4 °C), the supernatant was carefully removed and the pellet was washed with 70% ethanol. To remove the ethanol the tube was placed upside down to dry the pellet. The pellet was resuspended in 50 µl water containing 150 µg RNAse (10 mg/ml in 10 mM Tris, pH 7.6) by vortexing and stored at -20 °C.

Buffer I:	Tris/HCl, pH 8.0	25 mM
	EDTA	10 mM
	Glucose	50 mM
Buffer II	NaOH	0.2 M
	SDS	1% (w/v)
Buffer III:	KAc, pH 4.8	3 M

2.8.1.2 Plasmid-DNA preparation (NucleoBond® Xtra Midi kit)

For biolistic transformation, plasmid DNA was isolated by using the NucleoBond® Xtra Midi kit (Machery-Nagel, Düren, Germany). This method allows a rapid preparation of up to 500 µg highly pure plasmid DNA per preparation. The principle of this plasmid DNA purification kit is based on alkaline/SDS lysis procedure. Both chromosomal and plasmid DNA are denatured under these alkaline conditions. After addition of potassium acetate (KAc) to the denatured lysate, plasmid DNA, which remains in solution, can revert to its native supercoiled structure. After equilibrating the appropriate NucleoBond® column, plasmid DNA is bound to the anion-exchange resin and finally eluted under low ionic strength conditions with a slightly alkaline buffer (buffers supplied by manufacturer) after several washing steps. The eluted DNA is precipitated with isopropanol and dissolved in pure water for further use.

2.8.1.3 Isolation of genomic DNA from plant tissue

Isolation of genomic DNA from plant tissue was performed according to Thomson and Henry (1995). Approximately 1 cm^2 of ground, frozen leaf material was mixed with 1 ml extraction buffer and incubated for 10 min at 75 °C. After cooling down to room temperature, 500 µl phenol-chloroform-isoamylalcohol (PCI) (25:24:1) were added and vortexed. The mixture was briefly centrifuged to spin down the precipitate as well as the cell debris (2 min, 12000 x g, RT). This step was repeated using the supernatant and 500 µl chloroform-isoamlyalcohol (24:1). After centrifugation the supernatant was transferred into a new tube and 650 µl isopropanol were added. After inverting the tube three to four times, genomic DNA was pelleted by centrifugation (10 min, 12000 g, 4 °C). The pellet was washed in 70% ethanol (v/v), the supernatant was discarded and the reaction tube was placed upside down to dry the

pellet. The genomic DNA was then resuspended in 50 µl water containing RNase (see 2.8.1.1) and stored at -20 °C for further use.

Extraction buffer	Tris-HCl, pH 9.5	0.1 M
	KCl	1 M
	EDTA	0.01 M

2.8.2 Preparation of RNA

RNA is less stable than DNA. Since RNA is subjected to higher self-hydrolysis and is easily degraded by ubiquitous RNases, all methods have to be done on ice, with gloves, ethanol washed and autoclaved equipment and RNase-free water. The isolated RNA was either directly used or stored at -80 °C.

2.8.2.1 Isolation of RNA from plant tissue

For extraction of total RNA from plant tissue peqGOLD TriFast™ reagent was used. TriFast includes phenol and guanidinium thiocyanate in a monophasic solution and is used to isolate RNA by a single-step method (Chomczynski and Sacchi, 2006). Briefly, homogenized frozen leaf material (approximately 1 cm²) was mixed with 1 ml TriFast solution. After addition of 200 µl chloroform, samples were mixed and kept at room temperature for 3-10 min. The incubation procedure is for dissociation of the nucleoprotein complexes. After centrifugation (10 min, 12000 x g, 4 °C) the mixture shows a separation into a lower red phenol-chloroform phase, an interphase, and a colorless upper aqueous phase. The upper phase containing the RNA was transferred into a new reaction tube and the RNA was precipitated by 500 µl isopropanol and subsequent centrifugation (10 min, 12000 x g, 4 °C). The RNA pellet was washed with 70% ethanol (v/v), air dried and re-dissolved in RNase-free water.

2.8.3 Extraction, precipitation and quantification of nucleic acids

2.8.3.1 Extraction by phenol-chloroform-isoamyl alcohol (PCI)

Phenol-Chloroform-Isoamylalcohol (PCI; 25:24:1) solution is used to precipitate protein contaminations out of nucleic acid solutions. To extract proteins 1 volume PCI was added to the nucleic acid solution and vortexed to homogenicity. Proteins were denatured under the influence of phenol and were found in the interphase after centrifugation (1 min, 12000 x g,

4 °C). Isoamylalcohol supports the separation of the organic and hydrophilic phase. The upper phase contained the purified nucleic acids and was transferred into a fresh reaction tube.

2.8.3.2 Ethanol-sodium acetate precipitation

To concentrate nucleic acid solutions, nucleic acids were precipitated by 0.1 volume 3 M KAc (pH 4.8) and 2 volume 100% ethanol for 20 min at 4 °C. After centrifugation (15 min, 12000 x g, 4 °C) and discarding the supernatant the pellet was washed twice with 70% ethanol to remove salt contaminations. The washed and dried pellet was dissolved in an appropriate volume of water.

2.8.3.3 Determination of nucleic acid concentration

For UV absorption based determination of a nucleic acid concentration in a solution the absorption maximum of purin/ pyrimidine at 260 nm is used (Sambrook et al., 1989). The determination of concentration (c) was done spectrophotometrically by absorption (A) measurement at 260 nm in silica cuvettes using H_2O as blank. The concentration was calculated according to the Lambert-Beer law:

$c = A_{260} / (E*d)$

[E = specific absorption coefficient; d = cuvette thickness in cm]

An absorption value of 1.0 at 260 nm equals approximately:

50 µg/ml double-stranded DNA (dsDNA) → factor 50 for dsDNA

40 µg/ml single-stranded DNA (ssDNA or RNA) → factor 40 for ssDNA or RNA

For the measurement 2 µl nucleic acid solution were added to 58 µl water (dilution factor 30). The nucleic acid concentration in µg/µl was calculated as follows:

$c = (A_{260} * [\text{factor for nucleic acid}] * [\text{dilution factor}]) / 1000$

2.8.3.4 DNA digestion with restriction enzymes

Digestion of appropriate amounts of plasmid DNA with restriction endonucleases (reaction volume 30 µl) was performed in buffer systems provided by the manufacturers at the recommended temperature.

2.8.4 Cloning and E. coli transformation

2.8.4.1 Dephosphorylation of linearized vectors

In order to prevent linearized vectors from religation, the 5'-phosphate groups were hydrolyzed with Antartic Phosphatase for 15 min at 37 °C according to manufacturer's protocol, followed by heat inactivation of the enzyme at 65 °C for 5 min.

2.8.4.2 Ligation of vector and DNA fragments

T4-DNA-ligase catalyzes the formation of a phosphodiester bond between the 5'-phosphate and 3'-hydroxy termini in duplex DNA. To ligate DNA fragments, the following reaction mixture was prepared in a reaction tube and incubated at 16 °C over night.

Linear vector DNA	~ 50 ng
Insert DNA	3:1 molar ratio of insert to vector DNA
10x ligation buffer for T4 DNA ligase	1.5 µl
T4-ligase	1.0 µl
H_2O	add to 15.0 µl

2.8.4.3 Transformation of E. coli competent cells

For heat-shock transformation, plasmid DNA (10 to 50 ng for retransformation) or half of a ligation reaction (7.5 µl) was added to *E. coli* competent cells (2.6.1). The cells were incubated on ice for 30 min and then subjected to 42 °C for 30 s. The cells were then incubated on ice for 1 min. After adding 1 ml LB medium (2.7.1.3), the sample was slowly shaken at 37 °C for 1 h. 20 to 200 µl of transformed bacterial cells were plated on LB agar, containing the appropriate antibiotics and incubated at 37 °C over night.

2.8.5 Vector construction

Detailed vector maps are displayed in the appendix (7.3).

2.8.5.1 Codon optimization

Codon usage plays an important role regarding the protein biosynthesis. While often used codons are able to enhance translation efficiency, seldom used codons tend to slow down translation. Thus, for successful expression of the genes of interest *plyGBS*, *pal* and *cpl-1* genes were optimized with respect to the usage of AT-rich codons in tobacco chloroplasts.

This was kindly done by Dr. Marc Lohse (Max Planck Institute of Molecular Plant Physiology, Golm, Germany) employing *CodonWorkbench* a taylor-made software (http://www.buba-basis.de/software/cwb/cwb.html).

2.8.5.2 pMO16

A synthetic gene for PlyGBS was generated by DNA synthesis (GENEART GmbH, Regensburg, Germany) using the codon usage from *Nicotiana tabacum* chloroplasts. A 5' *Nde*I and *Nhe*I restriction site and a 3' *Xba*I site were introduced for subsequent cloning steps. The synthetic gene was subsequently cloned as *Nde*I/ *Xba*I fragment into the strong expression cassette of plasmid pHK20 (7.3.1) (Kuroda and Maliga, 2001) which contains the strongest known plastidial promoter, the constitutive ribosomal RNA operon promoter followed by the 5'UTR of gene 10 from the *E. coli* phage T7 (P*rrnT7g10*) and a 3'UTR derived from the tobacco chloroplast gene *rbcL* (T*rbcL*). This cloning procedure resulted in Plasmid pMO4. The actual transformation vector, pMO16, was constructed using *Sac*I and *Hind*III sites to insert the complete *plyGBS* containing expression cassette into the transformation vector pKP9 (7.3.2) to target the transgene to the plastid intergenic region between *trnfM* and *trnG* via homologous recombination. To confirm successful cloning and to rule out possible mutations the derived plasmid pMO16 was sequenced using the primer pHK20-fwd and pHK20-rev (2.2).

2.8.5.3 pTox derivatives

To construct the toxin shuttle (pTox) a *loxP* site was inserted downstream the promoter of plasmid pZS195 (Svab and Maliga, 1993). The *loxP* site was placed 3 base pairs upstream of the Shine-Dalgarno sequence using PCR with the primers Tox-pro-fwd and Tox-pro-rev (2.2). The amplified fragment containing the promoter and the *loxP* site, was sequenced and cloned as *Sac*I/*Fat*I fragment into pZS195, which was cut with *Sac*I and *Nco*I, resulting in pMO22. A synthetic terminator fragment (7.1.3) was synthesized by GENEART GmbH (Regensburg, Germany) and cloned as *Spe*I/*Xba*I fragment into pMO22, linearized with *Xba*I, and dephosphorylated with Antarctic Phosphatase resulting in pMO23. The complete expression cassette was cloned as *Sac*I/*Dra*I fragment into pKP6 (7.3.6) previously digested with *Sac*I and *Sma*I resulting in transformation vector pTox (7.3.7). Genes of interest (*gfp*, *pal* and *cpl-1*) were cloned as *Nco*I/*Xba*I fragment into the transformation vector pTox resulting in pToxGPF, pToxPal and pToxCpl-1, respectively.

2.8.5.4 pMO24

The terminator *Trps16* in pOD1 (7.3.4) was replaced by the terminator *TpsbA* as *Xba*I/*Hind*III fragment resulting in pMO24 (7.3.5).

2.8.6 Electrophoretic separation of nucleic acids

Separation of nucleic acids under electrophoretic conditions was performed in a in a gel matrix (Sambrook et al., 1989). The results were documented in a Gel Doc™ 2000 system (Biorad, California, USA).

2.8.6.1 Non-denaturing agarose gel electrophoresis of DNA

1% (w/v) agarose was added to 1x TAE-buffer (40 mM Tris, 15 mM NaAc, 1.25 mM EDTA), (1% w/v, mesh aperture: 150 nm) and boiled to dissolve the agarose. After cooling down to ~ 60 °C ethidium bromide (Pharmacia Biotech AB, Uppsala, Sweden) was added to a final concentration of 0.175 µg/ml. The solution was poured into gel-brackets with a comb forming the slots for sample application. After solidification the comb was removed, and the gel was placed in a horizontal gel-chamber containing 1x TAE-buffer used for electrophoresis. 6 µl of the size standard (Gene Ruler™, see 2.4) and DNA samples together with appropriate amounts of 6x loading buffer were applied into separate slots.

Loading buffer:	Glycerol	50% (v/v)
	Xylenecyanol	0.1% (w/v)
	Bromphenol blue	0.1% (w/v)
	in 1x TAE	

2.8.6.2 Agarose gel electrophoresis of RNA

RNA was analyzed on a 1% (v/v) formaldehyde gel prepared as follows: 1x MOPS buffer was boiled with 1% (w/v) agarose. After cooling to 50-60 °C, appropriate amounts of formaldehyde (37%) were added. RNA samples were mixed with adequate volumes of loading buffer, denatured by incubation at 95 °C for 5-10 min and loaded on the gel. The agarose gels should be made under RNase-free conditions. The separation of RNA was performed in 1 x MOPS buffer.

10x MOPS buffer:	MOPS, pH 7.0	200 mM
	NaAc	20 mM
	EDTA, pH 8.0	10 mM
1.6x RNA loading buffer:	Formamide	60% (v/v)
	Formaldehyde	18% (v/v)
	Bromophenol blue	0.25% (w/v)
	10x MOPS	15% (v/v)
	EtBr	0.1 µg/µl

2.8.7 Southern and Northern blotting

Southern blotting is the transfer of DNA fragments from an electrophoresis gel to a membrane by capillary force. After immobilization, the DNA is subjected to hybridization with a sequence-specific radioactively labelled probe to visualize the sequence of interest.

2-5 µg DNA were digested with appropriate restriction enzymes and separated by gel electrophoresis in a 1% agarose gel. The gel was then incubated in Southern I, which contains HCl for depuriniation for 15 min. Afterwards, the gel was transferred to NaOH containing solutions (Southern II and III, 30 min each) for DNA denaturation. Finally the gel was neutralized by incubation in Southern IV for 15 min. After transferring the DNA onto a Hybond^{TM}-N+ nylon membrane (GE Healthcare, Munich, Germany) by capillary blotting over night, the DNA was crosslinked to the membrane with UV light at 0.120 Joules/cm^2 (UV-Crosslinker; Peqlab, Erlangen, Germany). For Northern blotting 2-5 µg of total cellular RNA samples were denatured (10 min, 95 °C) before loading onto the gel and then separated by electrophoresis in formaldehyde-containing 1% agarose gels (2.8.6.2) and directly transferred onto Hybond^{TM}-N+ nylon membranes (GE Healthcare, Munich, Germany) by capillary blotting. The immobilized RNA was covalently bond to the membrane by UV irradiation, as described above.

After immobilization Southern and Northern blots, respectively, were hybridized with appropriate probes (7.1.1; purified PCR products or restriction fragments) which had previously been labelled with α-^{32}P-dCTP using the Megaprime DNA labelling kit (GE Healthcare, Munich, Germany) according to the manufacturer's protocol. Briefly, the membranes were prehybridized in Church buffer for 1 hour at 65 °C. Hybridization was performed by incubating the membrane with the previously denatured radio labelled probe

(95 °C, 5 min) in the Church buffer over night at 65 °C. Afterwards membranes were washed with wash buffer (Wash I: 20 min, RT; Wash II: 10-15 min, 65 °C) in order to increase hybridization stringency and thereby eliminating the non-specific background. Finally, the blot was displayed in a suitable manner with the help of a phosphorimager screen and Typhoon TM TRIO+ scanner (GE, Healthcare, UK).

Southern I:	HCl	0.25 M	Southern II:	NaOH	0.50 M
Southern III:	NaCl	1.50 M	Southern IV:	NaCl	3.00 M
	NaOH	0.50 M		Tris	1.00M
				pH 6.5 with HCl	

Church buffer	Na_3PO_4, pH 7.15	500 mM
	SDS	7% (w/v)
	EDTA	1 mM
	BSA	1% (w/v)

20x SSC	NaCl	175.3 g/l
	$Na_3C_6H_5O_7$	88.2 g/l

Wash I	2x SSC		Wash II	0.5x SSC	
	SDS	0.1% (w/v)		SDS	0.1% (w/v)

For blot stripping 0.5% SDS solution was heated up to 80 °C and the blot was shaken in the solution for 30-45 min. Stripped blots were hybridized as described above.

2.8.8 Polymerase chain reaction (PCR)

PCR is a powerful method to rapidly and efficiently amplify DNA fragments (Saiki et al., 1985). In general, amplification of DNA fragments was performed in a 50 µl reaction mixture using thin-walled PCR tubes in a PCR cycler (Thermocycler, Eppendorf, Hamburg, Germany).

Reaction mixture:

Template	2-10 ng
Primer (20 µM)	0.5 µl (each)
dNTPs (10 mM)	3.0 µl
$MgSO_4$ (100 mM)	0.8 µl
PCR buffer (10 x)	5.0 µl
DeepVent$_R^{TM}$ DNA polymerase	2.5 U
H_2O	add to 50µl

2.9 Transformation techniques

2.9.1 Plastid transformation and selection of transplastomic lines

Plastid transformation was done by biolistic transformation (Hager and Bock, 2000). Young leaves were harvested from sterile tobacco plants and bombarded with gold particles (Ø 0.6 µm) coated with plasmid DNA by using the biolistic gun (DuPont PDS1000He, BioRad, Salt Lake City, USA). Spectinomycin-resistant shoots were selected on regeneration medium containing 500 mg/l spectinomycin (2.7.2.5). In order to obtain homoplasmic plants transplastomic lines were subjected to 2-4 additional rounds of regeneration on RMOP selection medium. To prevent selection for spontaneous mutants, resistant shoots were also tested on streptomycin/spectinomycin double selection RMOP medium (2.7.2.5) (Svab and Maliga, 1993; Bock, 2001; Bock and Khan, 2004).

2.10 Biochemical methods and light microscopy

2.10.1 Protein analysis

2.10.1.1 Extraction of total soluble protein from plant tissue

For the characterization and identification of proteins, 200 mg frozen homogenized plant material were mixed with 1 ml extraction buffer and incubated for 5-10 min on ice. After centrifugation (10 min, 12000 x g, 4 °C) the supernatant was taken as total soluble protein. The total protein concentration was determined by Bradford assay (Bradford, 1976) (Roth, Karlsruhe, Germany; 2.10.1.2) using known concentrations of bovine serum albumin (BSA; Roth, Karlsruhe, Germany) as protein standard. Afterwards the samples were treated and processed as described below.

HEPES extraction buffer:

	HEPES-KOH, pH 7.5	50 mM
	KAc	10 mM
	MgAc	5 mM
	EDTA	1 mM
(freshly added)	DTT	1 mM
	1x Complete™ Protease Inhibitor	

2.10.1.2 Bradford assay

The Bradford assay is based on the property of Coomassie brilliant blue to change its colour when binding to aromatic amino acids (Bradford, 1976). This assay allows detecting the amount of proteins in a given sample by photometric measurement. For the measurement of the protein amount, 1 ml Bradford reagent (1:5 diluted with water) and 5 µl protein rich solution were mixed. After 5 min, the extinction was measured at 595 nm. To interpolate the protein concentration in a given sample, a protein calibration curve was made using a dilution series of BSA with known concentration. The curve turned linear between 5 and 40 µg/ml protein. The protein concentration can be interpolated by linear regression.

2.10.1.3 SDS-polyacrylamide gel electrophoresis (SDS-PAGE) and Coomassie staining

Protein separation was done by 1-dimensional SDS-polyacrylamide gel electrophoresis (1DSDS-PAGE), according to Schagger and von Jagow (1987), using a 15% (v/v) polyacrylamide gel. The added anionic detergent SDS effectively clamps the surface charge of the protein. This results in the formation of anionic micelles with constant charge to mass ratio, in average 1.4 g SDS per g protein. Low molecular thiols like ß-mercaptoethanol and dithiothreitol (DTT) were used in the loading buffer to reduce the disulfide-bonds of the polypeptide chains.

For gel preparation the following components were mixed and carefully poured into a PerfectBlue™ Double gel system Twin L (PeqLab Biotechnology GmbH, Erlangen, Germany) for solidification.

Resolving gel:	Acrylamide Gel 40 (29:1) (Roth, Karlsruhe, Germany)	2.5 ml
	Glycerol	0.5 ml
	Gelbuffer	3.3 ml
	H_2O	5.5 ml
	APS (10% (w/v))	20 µl
	TEMED	5 µl

Stacking gel:	Acrylamide Gel 40 (29:1) (Roth, Karlsruhe, Germany)	1.0 ml
	Gelbuffer	3.3 ml
	H_2O	5.6 ml
	APS (10% (w/v))	100.0 µl
	TEMED	10.0 µl

Gelbuffer:	SDS	0.1% (w/v)
	Tris-HCl pH 8.9	3 M

To prevent drying and to straighten the gel, the resolving gel was overlaid with isopropanol which was removed after solidification. The stacking gel was poured after solidification of the resolving gel. To determine the molecular weight, 15 µl SeeBlue® Plus2 protein marker (Invitrogen, Karlsruhe, Germany) were used as a size standard.

For visualization the protein gels were stained using Imperial™ Protein Stain (Pierce, Rockford, Illinois, USA) which is based on a Coomassie R-250 dye according to manufacturer's protocol.

2.10.1.4 Quantification of Proteins

To quantify the proteins, commercial available Rubisco (Sigma-Aldrich Chemie GmbH, Munich, Germany) was loaded in dilution series as reference. The Rubisco samples including the small Rubisco subunit were assumed to be only 90% pure (e.g. 15 µg Rubisco were accounted to be only 13.5 µg protein). After Coomassie staining, the gel was scanned and the band intensities of the large Rubisco subunit were compared to the band intensities of the foreign protein. Foreign protein content was calculated using the band intensities and corresponding amounts of large Rubisco subunit as reference.

2.10.1.5 Electrophoretic transfer of proteins to nitrocellulose membrane (Western blot)

To determine proteins via immunodetection, separated proteins were electrophoretically transferred to a Hybond™-P membrane (GE Healthcare, Munich, Germany) using a tank blot system (Trans-Blot® Electrophoretic Transfer Cell, Bio-Rad, Munich, Germany), and a standard transfer buffer (25 mM Tris, 192 mM Glycine, pH 8.3) (Kyhse-Andersen, 1984). The membrane was activated by methanol. The gel and the membrane were arranged in a pad of Whatman papers as blotting sandwich. The blotting process was set up for 3.5 h at 1 A.

Transfer buffer:	Tris	25 mM
	Glycin	192 mM
	pH~ 8.3	

2.10.1.6 Detection of immobilized protein via antibodies

After protein transfer, the membranes (Western blot), with their protein-binding side up, were blocked with 0.5% BSA (w/v) in TBS-T (1x TBS, 0.1% (v/v) Tween 20) for 1 hour. Blots were then incubated for one hour with primary antibodies. Before incubation (1 h) with the secondary peroxidase-conjugated antibody, the membrane was washed in TBS-T for 15 min and twice for 5 min. Unspecific bound antibodies were removed by washing in TBS-T for 15 min and four times 5 min. Immunolabelling was visualized by using ECL Plus™ (Amersham, Buckinghamshire, UK) detection system according to the manufacturers instructions. This reaction was detected exposing the blots to an X-ray film (Sigma-Aldrich, Munich, Germany) for 1-10 sec.

10x TBS	NaCl	1.4 M
	Tris/ HCl	0.2 M
	pH 7.6	

2.10.2 Activity tests of lytic enzymes

2.10.2.1 Preparation of target human pathogenic bacteria

Target bacteria (*Streptococcus pyogenes* and *Streptococcus pneumoniae*) were cultured at 37 °C either with or without preculture in liquid THY media (2.7.1.3) to OD_{600} ~ 0.5

(exponential phase). After harvesting cells by centrifugation (5 min, 4000 x g, RT), the pellet was washed using PBS buffer (pH 5 for *S. pyogenes* and pH 7 for *S. pneumoniae*). Cells were resuspended in appropriate PBS buffer and adjusted to $OD_{600} = 1$.

2.10.2.2 Protein preparation

To support protein stability total soluble protein from Nt-pToxPal and Nt-pToxCpl-1 plants was dialyzed against 25 mM Tris-HCl pH 7 over night at 4 °C using a dialyze tube (MCO 10 kDa) and afterwards mixed with glycerol to a final concentration of 10%.

2.10.2.3 OD_{600} measurements

To determine the bacterial cell death as monitored by clearing of bacterial cultures in a time-dependent manner, cuvettes were prepared with appropriate µg total soluble protein derived from the wild type, Nt-pToxPal, Nt-pToxCpl-1 or Nt-pMO16 plants, respectively (2.6.2). To determine the synergistic effect of Pal and Cpl-1, 150, 100 or 50 µg each derived from Nt-pToxPal and Nt-pToxCpl-1 were mixed and used for activity tests. Protein samples were filled up to 200 µl with extraction buffer (or 25 mM Tris-HCl pH 7 containing 10% glycerine for Pal and Cpl-1 samples) and 800 µl of the bacteria suspension (*S. pyogenes* for PlyGBS and *S. pneumoniae* for Pal and Cpl-1, 2.10.2.1) were added. OD_{600} was measured starting with the highest protein concentration in descending order. Proteins diluted in the appropriate buffer were used as blank. For each measurement 3 replicates per protein concentration were measured at the time points 0, 15, 30 and 60 min. During measurement cuvettes were kept at 37 °C.

2.10.2.4 Colony forming units

To determine the viability of the bacterial cell culture, their capability to form colonies was verified. Therefore, after each OD_{600} measurement, 10 µl cell suspension were removed immediately for CFU (colony forming units) quantification. Dilution series were prepared, whereof 100 µl were plated on THY plates (end dilutions 10^{-4} to 10^{-7}). Plates were incubated at 37 °C over night and the colonies were counted the next day. To make the comparison of the colony numbers easier, the results were normalized to the number of colonies at time point zero.

2.10.2.5 Live/dead staining and light microscopy

In order to improve the monitoring of cell viability or the membrane integrity a live/dead staining of the bacterial cell culture was performed using LIVE/DEAD® *Bac*Light™ Bacterial Viability Kit, (Invitrogen, Karlsruhe, Germany).

This kit contains two nucleic acid stains, the green fluorescent SYTO®9 and the red fluorescent propidium iodide stain. The stains differ in their ability to penetrate healthy bacterial cells. SYTO®9 is able to stain both live and dead bacteria whereas propidium iodide is only able to penetrate bacteria with damaged membranes, reducing SYTO®9 fluorescence when both dyes are present. Thus, living bacteria fluoresce green, while dead bacteria with damaged membranes fluoresce red. The experiment was done according to the manufacturer's protocol. 50 µl of one replicate were directly taken after cell removal for CFU quantification (2.10.2.4) at the time points 3, 15, 30 and 60 min and stained for microscopic analysis. Pictures were taken with the use of the microscope BX60 (Olympus, Hamburg, Germany) and the digital camera from Visitron Systems. The microscope was set-up according to manufacturer's manual.

2.11 Mass spectrometry

2.11.1 Sample preparation and trypsin digestion

PlyGBS, Pal and Cpl-1 were identified using mass spectrometry (MS). Hence colloidal Coomassie-stained protein bands were prepared according to Shevchenko et al. (1996). Bands were cut out of the SDS acrylamide gel and gel fragments were washed with 200 µl water by vortexing for 10 min. After removing the liquid the gel pieces were washed with 200 µl 100 mM NH_4HCO_3 by vortexing 10 min. 200 µl acetonitrile were added directly to the sample and mixed another 10 min. The washing step with acetonitrile and NH_4HCO_3 was repeated. The liquid was discarded and the gel piece was dried for 5 min in a vacuum centrifuge. 100 µl of 100 mM NH_4HCO_3 and 1 µl of 1 M DTT were added to the gel piece and incubated for 45 min at 56 °C. After cooling to room temperature the solution was replaced by 100 µl 55 mM iodacetamide in 100 mM NH_4HCO_3. The sample was incubated for 30 min at room temperature in the dark by vortexing occasionally. After removing all the liquid the gel piece was washed with 200 µl 100 mM NH_4HCO_3 by vortexing for 10 min. 200 µl acetonitrile were directly added to sample and mixed for another 10 min. The gel piece was washed twice for 5 min with 200 µl 50% acetonitrile with 50 mM NH_4HCO_3. After removal of all liquid gel piece was again dried in vacuum centrifuge for 15 min.

The trypsin digestion was done according to preparation instructions (Trypsin Proteomics Grade, Sigma-Aldrich, Saint Louis, Missouri, USA) for in-gel digestion. 20 µl of trypsin solution (0.4 µg of trypsin) prepared according to manufacturer's manual were added for in-gel digestion and incubated over night at 37 °C. The liquid including the peptides was removed and used for MS-analyses.

2.11.2 Mass spectrometrical analysis

For protein identification tryptically digested peptide mixtures were analyzed by LC/MS/MS using nanoflow HPLC (Proxeon Biosystems, Denmark) and a linear ion trap instrument (LTQ, Thermo Electron, USA) as mass analyzer. The procedure was kindly done by Dr. Stefanie Wienkoop (identification of PlyGBS) and Dr. Waltraud Schulze (identification of Pal and Cpl-1). Briefly, peptides were eluted from a 75 µm analytical column (Reprosil C18, Dr. Maisch GmbH, Germany) using a linear gradient running from 10% to 30% acetonitrile in 50 min and sprayed directly into the LTQ-Orbitrap mass spectrometer. Proteins were identified by tandem mass spectrometry (MS/MS) by information-dependent acquisition of fragmentation spectra of multiple-charged peptides. Fragment MS/MS spectra from raw files were extracted as DTA-files and then merged to peak lists using default settings of DTASuperCharge version 1.18 (msquant.sourcforge.net) with a tolerance for the precursor ion detection of 50 ppm.

Fragmentation spectra were searched against a non-redundant Arabidopsis protein database (TAIR7, version 2007-04; 31921 entries; www.arabidopsis.org) and HITRGEN database (in-house tobacco chloroplast EST database) where the sequence of the target proteins was added. Analyses were done using the Mascot algorithm (version 2.2.0; Matrix Science, UK) or SEQUEST (Tabb et al., 2002).

3 Results

3.1 PlyGBS

Chloroplast expression systems offer great advantages over nuclear systems due to their simpler prokaryotic structure. Advantages such as prokaryotic-like degradation machinery and a large genome copy number are useful for foreign protein expression. Regarding the expression of phage lytic enzymes, chloroplasts show an additional advantage over bacterial expression systems, since they lack bacterial-like cell wall structures, which may become undesired targets of phage lysins. The gene, *plyGBS*, that encodes a lysin from a phage infecting group B streptococci, was selected to determine whether plants, and in particular chloroplasts, could be used as a cheap and effective production platform to produce phage lytic enzymes.

3.1.1 Vector construction and plasmid maps

Since it is known that chloroplast genes are relatively AT-rich the sequence coding for *plyGBS* was adjusted to the codon usage preferred by the tobacco chloroplasts and re-synthesized to maximize gene expression (GenBank accession number EU433376). The synthetic gene was subsequently cloned into the strong expression cassette of plasmid pHK20 (Kuroda and Maliga, 2001) (7.3.1) which contains the strongest known plastid promoter, the constitutive ribosomal RNA operon promoter followed by the 5'UTR of gene 10 from the *E. coli* phage T7 (P*rrnT7g10*) and a 3'UTR derived from the tobacco chloroplast *rbcL* gene (T*rbcL*). The transformation vector pMO16 was obtained by insertion of the complete *plyGBS*-containing expression cassette into the transformation vector pKP9 (7.3.2) to target the transgene to the plastid intergenic region between *trnfM* and *trnG*.

The plasmid pMO16 was used for chloroplast transformation of *Nicotiana tabacum cv. petit havana* leaves according to the established protocol for biolistic bombardment (2.9.1). After several regeneration rounds, 3 independent transplastomic lines (Nt-pMO16-3, Nt-pMO16-16 and Nt-pMO16-14) were obtained and characterized in detail. Detailed physical maps of the target region of wild type and transgenic plastomes as well as relevant restriction sites used for cloning and later RFLP analysis are shown in Fig. 14.

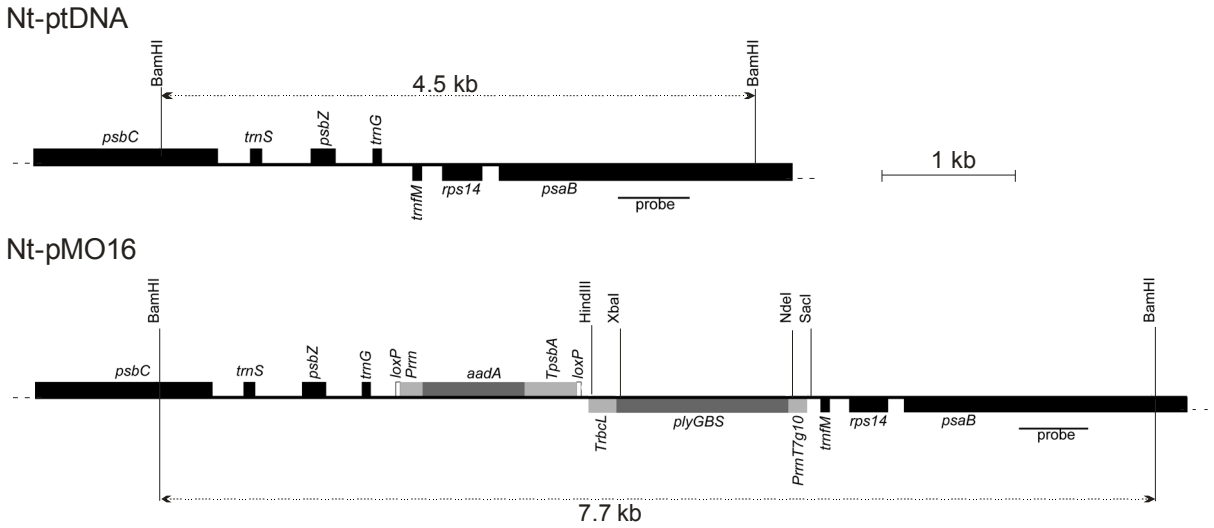

Fig. 14 Physical map of the plastid genome target region for the introduction of the optimized transgene *plyGBS*. The target region in the wild type plastid genome (Nt-ptDNA) and the transgenic genome (Nt-pMO16) after chloroplast transformation with the vector pMO16. Relevant restriction sites used for cloning and RFLP analysis as well as fragment sizes are indicated. The transgene *plyGBS* is flanked by the plastid rRNA operon promoter fused to the 5' UTR from the T7 phage gene 10 (P*rrnT7g10*) and a 3' UTR from the plastid *rbcL* gene (T*rbcL*). The *aadA* marker gene expression cassette is driven by the P*rrn* promoter and includes the 3' UTR from the plastid gene *psbA* (T*psbA*). To facilitate later excision of the marker gene by site-specific CRE recombinase, the chimeric *aadA* is flanked by directly orientated *loxP* sites. The probe used for subsequent RFLP analysis is shown as a black bar.

3.1.2 Molecular and genetic analyses

3.1.2.1 Southern blotting

To confirm successful integration of the transgene cassettes into the plastid genome, total DNA was isolated from the transgenic lines, digested overnight with the restriction enzyme *Bam*HI and used for Southern blotting. To this end, the DNA was membrane-immobilized and hybridized to a radiolabelled *psaB* probe (7.1.1) that binds to a region of the plastid genome next to the insertion site (Fig. 14).

The Southern blot, displayed in Fig. 15, shows two bands corresponding to the expected sizes for the wild type and transformed plastomes. The strong upper band at 7.7 kb in the transplastomic plants shows successful integration of the two inserted cassettes (*plyGBS* and *aadA*). The band in the wild type sample corresponds to the size (4.5 kb) expected from wild type plastome, lacking both expression cassettes. The faint but visible wild type band within the transplastomic lines is presumably caused by evolutionarily obtained nuclear copies of the target plastome sequence (Ayliffe and Timmis, 1992). Comparable intensities of the 7.7 kb fragment within the transplastomic lines and the 4.5 kb fragment in the wild type band

tentatively indicate that the transplastomic lines may have already reached homoplasmy. However, it cannot be fully excluded that residual wild type plastome copies are present, since it is not possible to distinguish between the wild type plastome signal and the evolutionarily transferred nuclear copies.

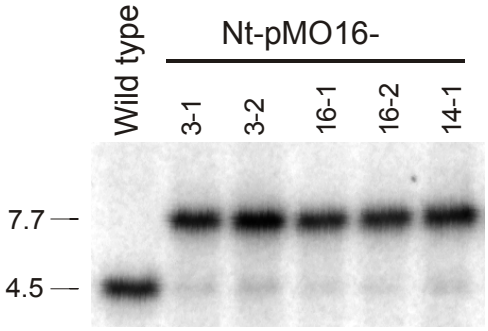

Fig. 15 RFLP analysis of transplastomic Nt-pMO16 plants. 2.5 µg of total cellular DNA was extracted, digested with *Bam*HI, electrophoretically separated, blotted and hybridized with a radiolabelled probe binding to the *psaB* gene (see Fig. 14). Numbers of independent lines and individual plants are indicated above. Obtained fragment sizes are indicated in kilo base pairs (kb).

3.1.2.2 Confirmation of homoplasmy via seed assay

Since Southern blotting just gives indications about the homoplasmic status of a transplastomic plant, a seed assay was performed to confirm homoplasmy.

Seeds obtained from the transformed T_0 plants were germinated on selection media (see 2.7.2.3) and the greening of the plants was monitored. Since only a few chloroplasts are inherited from the mother plant to a single seedling, this test is useful to determine if the mother plant is homoplasmic. More precisely, it shows whether all inherited chloroplasts contain the transgene cassettes, as inherited residual wild type chloroplasts leads to bleaching and inhibited growth of the seedlings, whereas transplastomic, *aadA*-containing seedlings show antibiotic resistance and are indistinguishable from seedlings grown on antibiotic-free medium. Fig. 16 shows wild type and transplastomic seedlings on antibiotic-free medium (-Spec) compared to spectinomycin containing medium (+Spec). Wild type seedlings on antibiotic-free medium appeared green whereas growth on spectinomycin containing medium led to bleached white seedlings that cease to grow. The light green phenotype of the Nt-pMO16 seedlings was clearly visible on spectinomycin-free as well as antibiotic containing medium indicating the presence of the resistance maker gene *aadA*. Since all seedlings displayed this phenotype, this confirmed that the mother plant was homoplasmic.

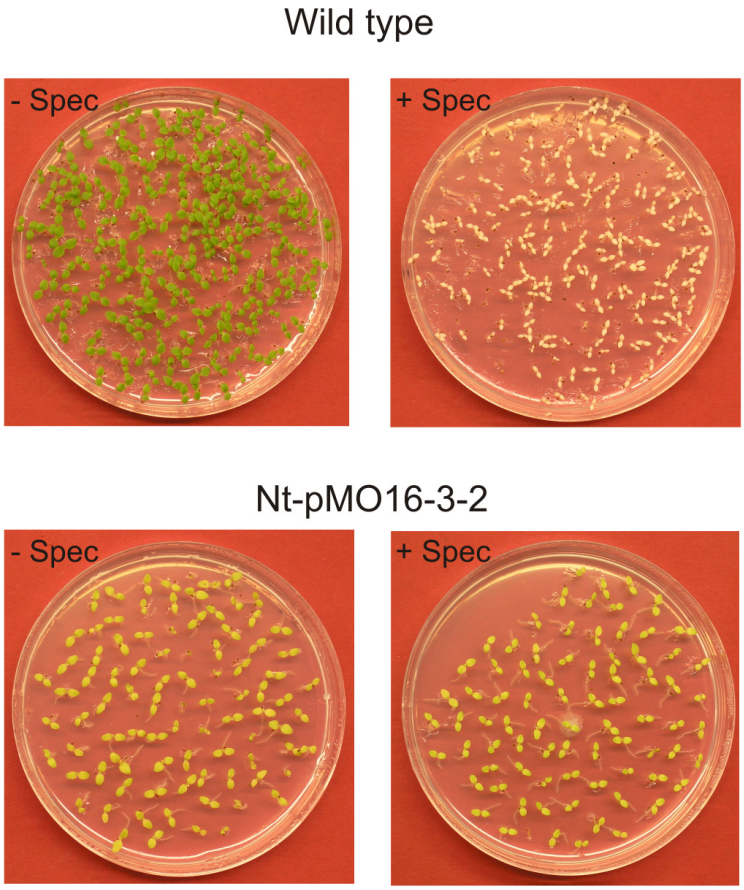

Fig. 16 Seed assay to confirm homoplasmy. –Spec and +Spec indicate presence or absence of spectinomycin in the germination medium. Wild type seedlings were compared to seedlings derived from the transplastomic plant Nt-pMO16-3-2. Green seedlings in +Spec medium show resistance whereas white seedlings indicate sensitivity to antibiotic selection.

3.1.2.3 Northern blotting

To confirm successful transcription driven by the P*rrn* promoter, *plyGBS* mRNA accumulation was visualized via Northern blotting (Fig. 17). Total RNA was isolated from the transplastomic plants, separated by gel electrophoresis, blotted and hybridized with a *plyGBS*-specific probe (full coding region of *plyGBS*). The resulting Northern blot showed no signal in the wild type plants, as expected. In the transplastomic plants, two major transcripts, the small monocistronic *plyGBS* mRNA (1.6 kb) and a longer transcript (2.5 kb) resulting from read-through transcription, could be detected indicating that stable transcript was produced. Read-through transcript is commonly observed in chloroplasts since it has been shown that 3' UTRs are incapable of efficient transcription termination (Stern and Gruissem 1987), but rather have stabilizing function. Using the gel image as a reference to normalise for equal

RNA loading, the band intensity of the Northern blot showed that in all transplastomic lines, equal amounts of the *plyGBS* transcript were produced.

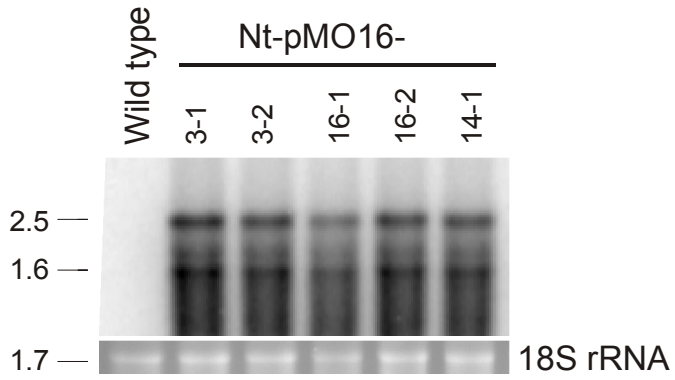

Fig. 17 RNA gel blot analysis of *plyGBS* mRNA accumulation. 3 µg of total RNA were separated in a formaldehyde containing 1% agarose gel and blotted. Major transcripts were detected by the *plyGBS*-specific hybridization probe at the sizes of 2.5 kb and 1.6 kb. The gel image beneath the Northern blot displays 18S rRNA bands (1.7 kb) from the gel used for blotting and serves as a reference for RNA loading.

To verify the content of *rbcL* transcript the blot was stripped and hybridized with a radiolabelled probe binding to the endogenous *rbcL* gene (6.1). Slightly different loading was assumed to be responsible for the slightly lower mRNA accumulation in the wild type sample (compare RNA gel loading). With this difference taken into consideration, no significant differences in *rbcL* transcript accumulation between wild type and Nt-pMO16 plants could be observed (Fig. 18).

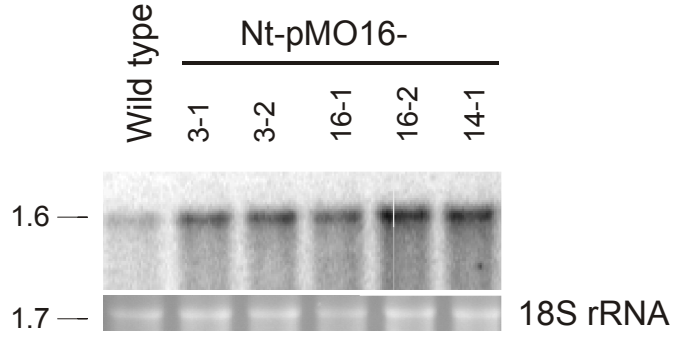

Fig. 18 RNA gel blot analysis of *rbcL* mRNA accumulation. Major transcripts were detected at the expected size of 1.6 kb corresponding to the monocistronic mRNA expected from *rbcL*. The gel image beneath the blot serves as an RNA loading control and displays 18S rRNA bands (1.7 kb).

3.1.3 PlyGBS identification and quantification

3.1.3.1 Identification via Coomassie staining

To test whether the accumulated *plyGBS* mRNA was efficiently translated in the chloroplast, total soluble protein was extracted and electrophoretically separated. Protein accumulation of 1-2% of total soluble protein (TSP) in plants can usually be visualized on Coomassie-stained polyacrylamide gels. Thus, a colloidal Coomassie stain was used to identify the separated protein bands and a protein marker was used to estimate protein band sizes. In addition, Rubisco, which accumulates in general up to 50-60% of TSP in wild type plants served as size indicator since the large and small subunit are 55 kDa and 13 kDa, respectively (Fig. 19, labelled 'L' and 'S' respectively). However, in all transplastomic lines, the level of both subunits of Rubisco was far below the typical intensity level and instead, a strong band, slightly smaller than Rubisco could be detected indicating that a novel protein, consistent with the size of PlyGBS (53 kDa), accumulated at levels comparable to the Rubisco large subunit in wild type plants.

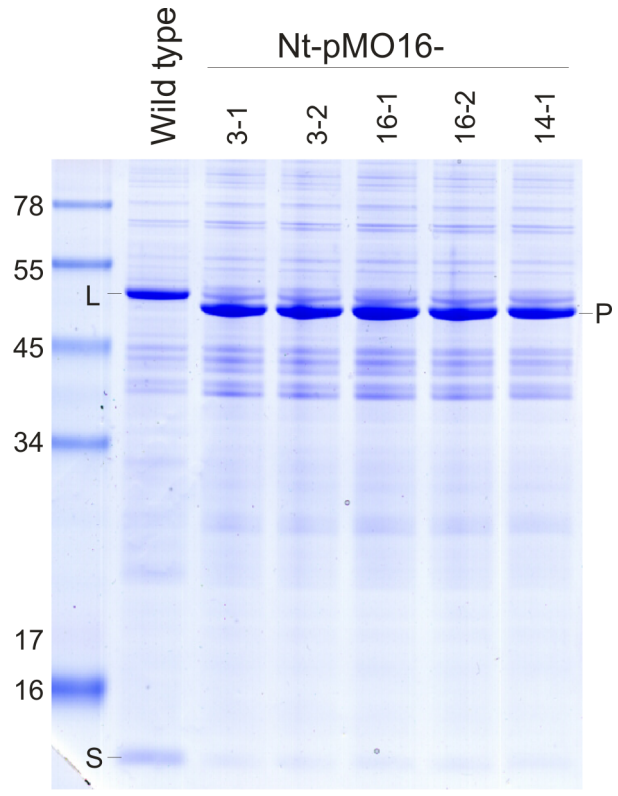

Fig. 19 PlyGBS accumulation monitored by Coomassie staining. 15 µg of total soluble protein was electrophoretically separated and stained with colloidal Coomassie. Protein bands derived from the marker are indicated in kDa. The large and small subunit of Rubisco are indicated with L and S, respectively; PlyGBS with P.

3.1.3.2 Identification via mass spectrometry (MS)

To verify that the 53 kDa protein showing massive accumulation in the transplastomic lines was indeed PlyGBS, bands were excised from the Coomassie-stained gel, tryptically digested and analyzed via mass spectrometry. For identification, an in-house tobacco chloroplast database (HITRGEN, AG Lein), to which the PlyGBS protein sequence was added, together with SEQUEST was used. These analyses were kindly done by Dr. Stefanie Wienkoop (Max Planck Institute of Molecular Plant Physiology, Golm, Germany). The peptide coverage for the target protein was 52.5% and thus, the 53 kDa protein could be confidently identified as PlyGBS. Single fragments of RbcL (large subunit of Rubisco) were also identified in the PlyGBS samples, indicating a low level of contamination from this similarly sized protein.

3.1.3.3 Quantification of PlyGBS

It was of great interest to determine how much foreign protein was accumulating in the transplastomic lines.

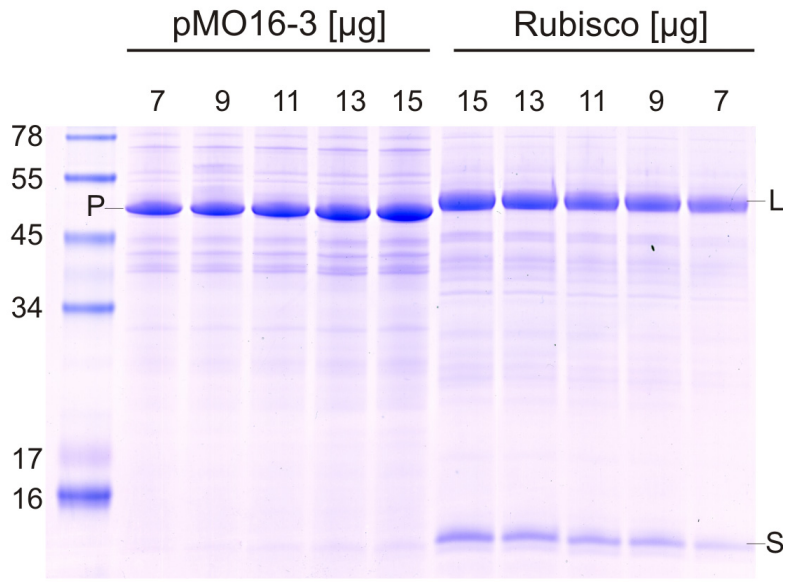

Fig. 20 Quantification of PlyGBS accumulation in transplastomic plants. Dilution series of 15, 13, 11, 9 and 7 µg of TSP from Nt-pMO16-3-2 and commercially available Rubisco respectively were loaded, electrophoretically separated and stained using a colloidal Coomassie stain. The large subunit of Rubisco is marked with L, small subunit with S, PlyGBS with P. Bandsizes of the marker are indicated in kDa.

Thus, to quantify the protein content, total soluble proteins extracted from a transplastomic line were compared with commercially available Rubisco by loading both as a dilution series (15, 13, 11, 9 and 7 µg) on an SDS gel. Since it was shown previously that all lines express

comparable amounts of PlyGBS, TSP from Nt-pMO16-3-2 was used as a representative sample. After electrophoretic separation and colloidal Coomassie staining, the gel was scanned and the Scion Image for Windows software was used to quantify the band intensities of PlyGBS and RbcL (Fig. 20).

The commercially available Rubisco was found not to be completely pure, as indicated by the presence of protein bands in addition to the small and large subunits. Thus, to avoid an overestimation, the Rubisco (including the small subunit) was assumed to be only 90% pure (i.e. 15, 13, 11, 9 and 7 µg of total protein was assumed to be represent 13.5, 11.7, 9.9, 8.1 and 6.3 µg of Rubisco). Comparison of the band intensities revealed that PlyGBS levels were estimated to be more than 70% of total soluble protein. However, this protein amount was likely to be an underestimate since Rubisco, compared to PlyGBS, has a much higher isoelectric point (PlyGBS: 4.9; RbcL: 6.4) as well as contains more basic amino acid residues (PlyGBS: 38; RbcL: 55) (6.2.1 and 6.2.2). These two properties make the large Rubisco subunit more easily stained with Coomassie compared to PlyGBS.

Tab. 2 Amino acid composition of PlyGBS and the Rubisco large subunit. Amino acids are indicated by the one-letter code and grouped according to their properties. The sum of amino acids belonging to each group are indicated.

Amino Acids	PlyGBS	Rubisco (RbcL)
Charged (RKHYCDE)	135	155
Acidic (DE)	52	59
Basic (KR)	38	55
Polar (NCQSTY)	145	101
Hydrophobic (AILFWV)	148	173

3.1.4 Phenotype of Nt-pMO16 plants

From the above data it can be assumed that Rubisco and probably other endogenous chloroplast proteins were reduced by the excessively high expression level of PlyGBS. The reduction of essential proteins, such as Rubisco, within the chloroplast should affect photosynthesis and as a result, affect growth. Thus, the high level of foreign protein accumulation should place a significant metabolic burden on the transplastomic plant. Indeed, PlyGBS expressing plants that were grown on synthetic medium showed a pale green phenotype (Fig. 21A) and, when transferred or grown directly in soil, transplastomic Nt-

pMO16 plants additionally showed growth retardation but normal development, flowering and seed production (Fig. 21B,C).

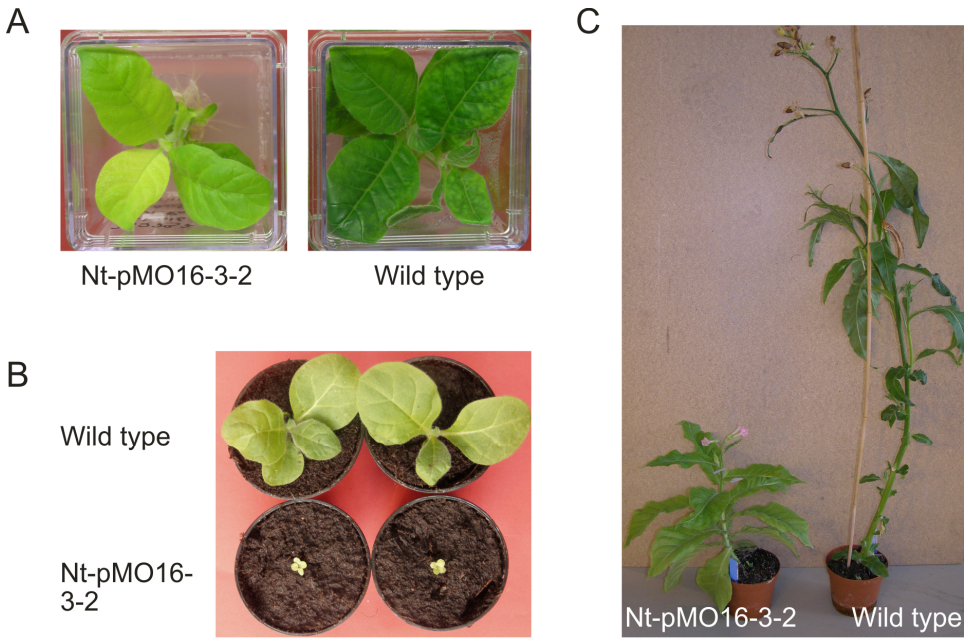

Fig. 21 Phenotype of PlyGBS expressing plants. (A) Nt-pMO16-3-2 and wild type plant grown on synthetic medium. (B) Seedlings of the same age from transplastomic and wild type plants grown on soil. (C) Retarded growth and development of a transplastomic plant compared to a wild type plant of the same age.

To obtain normalized growth and development and decrease the time required for seed production, a PlyGBS expressing plant was grafted onto a wild type rootstock.

Fig. 22 Growth normalization of a PlyGBS expressing plant by grafting onto a wild type rootstock. Differences in leaf colour are clearly visible and indicate transplastomic plant (pale green) and wild type rootstock (dark green).

Subsequent cultivation under greenhouse conditions revealed faster growth and seed development although a slightly pale green colouring of the transplastomic plant was still visible (Fig. 22).

3.1.5 Protein stability in vivo

For production of therapeutic proteins in plants it is important to verify the stability of the protein over leaf age since it is known that protein biosynthesis decreases in older leaves (Daniell et al., 2001). Thus, any decrease in foreign protein content over leaf aging serves as an indicator of protein stability. To test this, total soluble protein was extracted from 12 different leaves counted from the top to the bottom (Fig. 23) and loaded on an SDS gel followed by colloidal Coomassie staining.

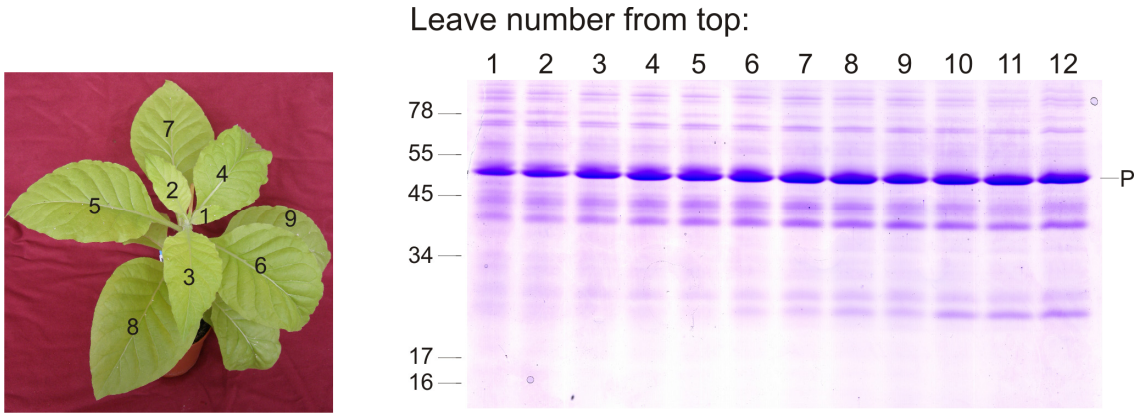

Fig. 23 PlyGBS protein accumulation is independent of leaf age. Sampling of leaves from a mature Nt-pMO16 plant and leaf numbering (left). Coomassie-stained polyacrylamide gel shows comparison of PlyGBS protein (P) levels in 12 leaves of different ages (right). Equal amounts (10 µg) of total soluble protein were loaded. No significant difference in foreign protein accumulation can be seen.

By comparing the total soluble protein samples in a developmental series of 12 leaves from top to bottom, no significant difference or decline in PlyGBS accumulation could be seen indicating that PlyGBS appeared to be stable under physiological conditions when expressed in the chloroplast.

3.1.6 Activity tests of PlyGBS

It was of great importance to show that the chloroplast produced PlyGBS did not only accumulate to high levels, but also showed bactericidal activity when applied to its target bacteria. Therefore the protein was assayed for its potential to kill *Streptococcus pyogenes*.

3.1.6.1 Cell density decrease

In a first approach, the clearance of bacterial suspension cultures after addition of total soluble protein derived from PlyGBS expressing plants was used to monitor cell death. Since the protein accumulated to such enormously high levels, no further purification of PlyGBS was performed. Different amounts of total soluble protein from wild type plants (control) as well as PlyGBS expressing plants were added to cultures of known optical density (OD) at the time point 0. The decrease in optical density was followed at 600 nm (OD_{600}) for 60 min (Fig. 24). While wild type protein did not lead to significant changes in cell density, PlyGBS-containing samples showed a dose-dependent decrease in cell number as monitored by optical density. It was assumed that, at the final time point, lysis of the bacterial culture incubated with 10 and 50 µg of PlyGBS-containing TSP was not complete, since the OD did not plateau as see in the samples with the highest amount of PlyGBS-containing protein extract (150 µg). Stabilization of the OD_{600} in these samples could be attributed to the remaining bacterial cell debris in the culture.

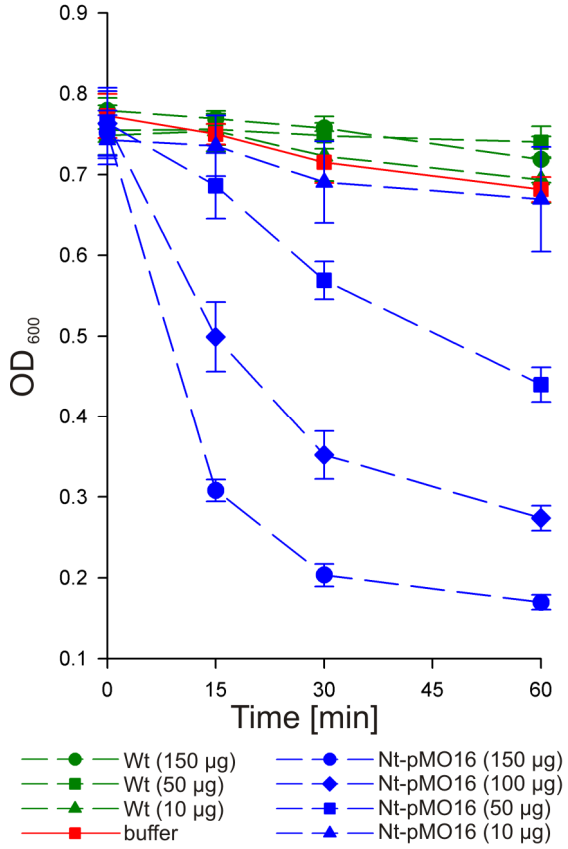

Fig. 24 Time course of bactericidal activity of PlyGBS monitored by clearing of *S. pyogenes* bacterial cell cultures. Wt and Nt-pMO16 indicate plants from which total protein was isolated. Amounts of total soluble protein added to the bacterial cell culture at time point 0 are indicated. Optical density was measured at 600 nm (OD_{600}). The graph shows the average of two sets of experiments with three replicates each as well as standard deviation for every time point.

3.1.6.2 Viability tests

In addition to the OD decrease, the viability of the bacteria was determined by its ability to form colonies after exposure to PlyGBS-containing protein extract (Fig. 25). Bacteria whose cell wall is degraded should no longer be able to grow and form colonies. Thus, *S. pyogenes* cells exposed to different amounts of total soluble protein derived from Nt-pMO16 plants were grown over night and their colony forming units were determined the next day. Not all samples grew over night and only two replicates could be obtained for each time point. While this results in a high standard deviation for the data derived from samples containing 150 µg PlyGBS extract at 30 min, where the upper point was assumed to by an outlier due to comparison with the OD measurements (Fig. 24), this result is encouraging given that the purpose of the PlyGBS is to have an anti-bacterial effect. These data showing a remaining viability of only 10% after 1 to 2 h, give strong indications that PlyGBS is indeed effective at killing *S. pyogenes*.

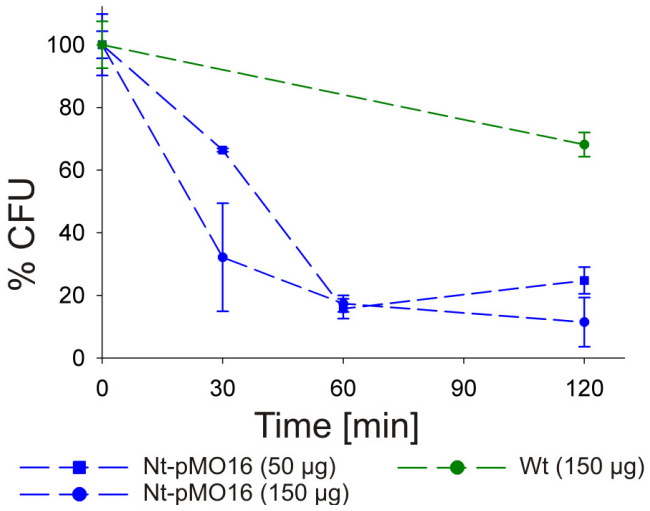

Fig. 25 Time course of bactericidal activity of PlyGBS monitored by decreasing the ability of *S. pyogenes* to form colonies. Plants from which total soluble protein was isolated as well as protein amounts added to the bacteria cell culture at time point 0 are indicated. A dilution series was used to obtain countable colony numbers which were normalized to the colony number at time point 0. Since more data could not be obtained, the graphs show averages of two replicates as well as the standard deviation for every time point.

3.1.6.3 Live/dead staining

To confirm the results obtained from the cell suspension clearing, a live/dead fluorescence staining using the LIVE/DEAD® *Bac*Light™ Bacterial Viability Kit was performed. The stains used in this kit differ in their ability to penetrate the cell membrane of bacteria.

Whereas the dye SYTO®9 is able to cross the membrane of living cells, and thus gives green fluorescence, the second dye, propidium iodide, can only enter the cell when the membrane is disrupted. Once propidium iodide has entered the cell, it suppresses the SYTO®9 stain, showing dying cells in red colour.

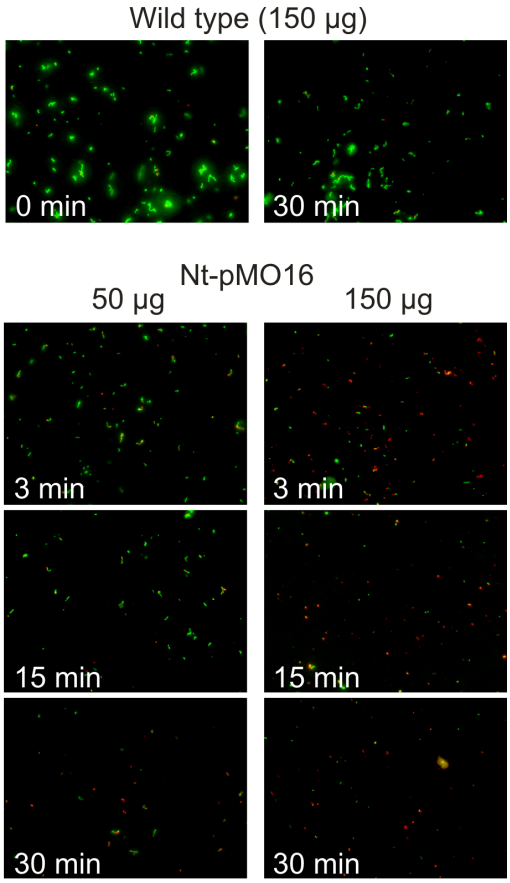

Fig. 26 Visualization of effective killing of *S. pyogenes* cells by live/dead fluorescence staining. Fluorescence images are shown for a wild type control and two different concentrations of PlyGBS-containing protein extracts. Live cells show green fluorescence while dying cells fluoresce red. Cells that have already lysed cannot be stained, explaining the decline in cell number seen over time in the two PlyGBS samples.

Fluorescence of bacterial cells mixed with different amounts of TSP derived from wild type and PlyGBS expressing plants was monitored over time, with respect to fluorescence colour and cell number (Fig. 26). It was clearly visible that no difference could be seen in samples with wild type protein confirming that proteins derived from wild type plants did not attack bacterial cell walls. In contrast, PlyGBS-containing samples showed a dose-dependent increase in the number of red fluorescing cells over time, indicating an increasing number of dying cells as shown for the two amounts of PlyGBS-containing TSP displayed (Fig. 26). The

decrease in cell number observed for the PlyGBS-containing samples can be explained by the fact that once cells are completely lysed they cannot be stained.

3.2 Pal and Cpl-1

Since very encouraging results were obtained for PlyGBS, the same strategy was employed for two phage lytic enzymes against *Streptococcus pneumoniae*, Pal and Cpl-1 (GenBank accession numbers: *pal*: EU450672, *cpl-1*: EU450673). Thus, as for PlyGBS, both genes were optimized for preferred codon usage by tobacco chloroplasts and re-synthesized.

3.2.1 Cloning into expression cassette pHK20

To obtain successful expression in the chloroplast, *pal* and *cpl-1* were inserted as *Nde*I/*Xba*I fragments into the expression pHK20 cassette (6.3.1), whose promoter is also active in *E. coli* cells. However, insertion of the transgenes into the cassette could not be achieved. All constructs derived from this cloning procedure showed unexpected RFLP analysis results.

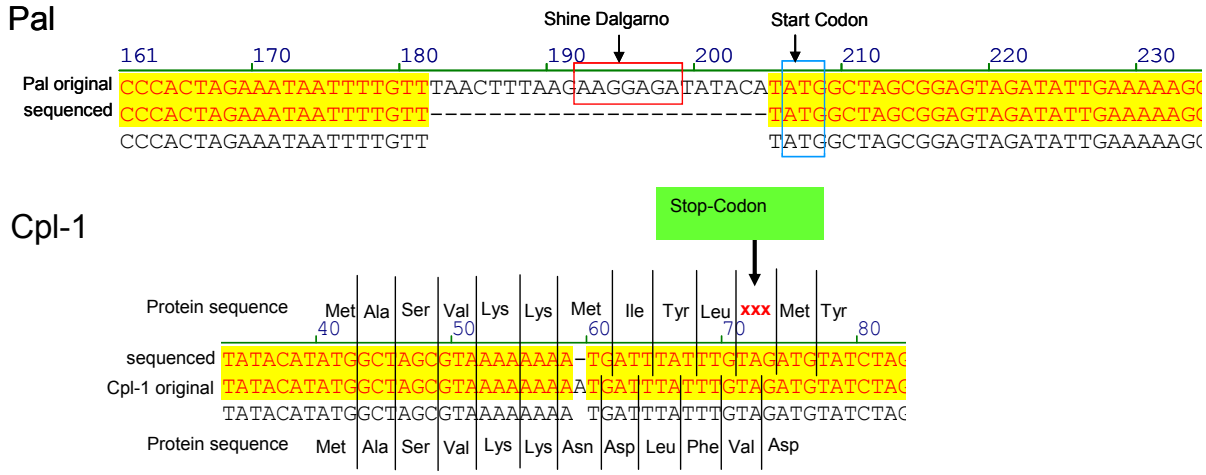

Fig. 27 Mutation examples in sequences derived from *pal* and *cpl-1* cloning into plasmid pHK20. **"**Pal- and Cpl-1 original", respectively, display the *in silico* sequence of the plasmids. "sequenced" shows the plasmid sequence derived from transformed *E. coli* cells. In the *pal*-containing plasmid, a sequence including the Shine-Dalgarno sequence was deleted, whereas in the *cpl-1* carrying plasmid, a point mutation occurred resulting in a frame shift leading to the formation of a stop codon.

Sequencing revealed that, in all plasmids, mutations had occurred. Fig. 27 shows sequences obtained from cloning procedures ("sequenced") in comparison to the *in silico* sequence ("Pal and Cpl-1 original", respectively). Thus, it was assumed that Pal and Cpl-1 are toxic when expressed in *E. coli* cells and, therefore, cannot be successfully cloned into pHK20.

3.2.2 Toxin shuttle construction

To transform chloroplasts with the transgenes *pal* and *cpl-1*, it was necessary to first construct a toxin shuttle vector (pTox; GenBank accession number EU450674) that suppresses transgene transcription in *E. coli* and allows restoration of transcription via marker gene deletion once the plasmid is integrated into the chloroplast genome. Using this construct, the gene of interest should not be transcribed in *E. coli* as long as the terminators function as transcription block.

A detailed protocol for the construction of the pTox vector is described in 2.8.5. Briefly, pTox harbours the tobacco rRNA operon promoter (P*rrn*) followed by the selectable marker *aadA*. The *aadA* is framed by a 5' UTR derived from the tobacco *rbcL* gene and a 3' UTR consisting of two fused *E. coli* terminators, the intrinsic rrnB T1 (T*int*) and the rho-factor-dependent tR1 terminator from the *cro* gene of phage λ (T*rho*). To facilitate excision of the *aadA* and the two *E. coli* terminators at a later stage, two directly orientated *loxP* sites were integrated 3 bp upstream of the Shine-Dalgarno sequence and downstream of the *E. coli* rho-dependent terminator.

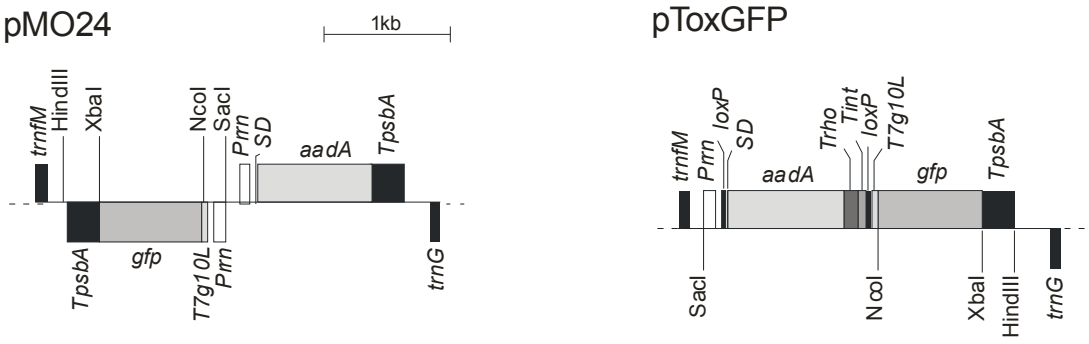

Fig. 28 Maps of transformation vectors pMO24 and pToxGFP. pMO24 is based on the transformation vector pRB95 (GenBank accession number AJ312393) and carries the transgene *gfp* driven by the rRNA operon promoter (P*rrn*) fused to a 5' UTR derived from T7 phage gene 10 (*T7g10l*). The 3' UTR derived from *psbA* (T*psbA*) serves to stabilise the transcript. The expression cassette of the antibiotic resistance gene *aadA* consists of a P*rrn* promoter fused to the 5' UTR of *rbcL* containing an appropriate Shine-Dalgarno (*SD*) sequence and the 3' UTR from *psbA*.
The chloroplast transformation vector pToxGFP consists of the ribosomal RNA operon promoter (P*rrn*) fused to the 5' UTR of the plastid *rbcL* gene followed by the selectable marker gene *aadA*. The *aadA* gene is followed by a fused *E. coli* terminator consisting of the rho-dependent λtR1 (T*rho*) and the intrinsic *rrn*B T1 (T*int*) terminators. This expression cassette is flanked by two directly orientated *loxP* sites, one located 3 base pairs upstream of the *rbcL* Shine-Dalgarno sequence and one directly behind the intrinsic terminator. The transgene following the *loxP* site is fused to a 5' UTR derived from the gene 10 of phage T7 (*T7g10l*) and the 3' UTR of the plastid *psbA* gene (T*psbA*).

This expression cassette was followed by the gene 10 leader sequence of the *E. coli* phage T7 (*T7g10l*) followed by the gene of interest and a 3' UTR from tobacco *psbA* (T*psbA*) to enhance transcript stability. The complete cassette was flanked by plastome sequences to facilitate later insertion into the chloroplast by homologous recombination.

Firstly, to test the efficiency of the construct, a non-toxic reporter gene, *gfp,* was inserted (pToxGFP).

As an expression control, a second plasmid, pMO24 (6.3.5), was constructed. For pMO24, which is based on pRB95 (Ruf et al., 2001), the transgene *gfp* is driven by the tobacco P*rrn* promoter fused to the T7g10 leader (T*7g10l*). The 3' UTR, derived from tobacco *psbA* (T*psbA*), serves as a transcript stabilizer. Fig. 28 shows plasmid maps of pTox as well as pMO24 carrying *gfp* as a reporter gene.

3.2.3 Efficiency test of the toxin shuttle

To gain further insights into the suppression of protein expression with the pToxGFP vector, GFP expression of both constructs (pMO24 and pToxGFP) was monitored in *E. coli* using Western blotting. Total soluble proteins were extracted from *E. coli* carrying the plasmids pToxGFP and pMO24, respectively, applied as dilution series on an SDS acrylamide gel and separated electrophoretically. Separated proteins were blotted to a nylon membrane and GFP was identified by immunodetection using an anti-GFP antibody derived from mouse. The secondary antibody, anti-mouse, derived from goat and linked to a horseradish peroxidase, allowed luminescence detection of GFP after PS-3 acridan substrate addition.

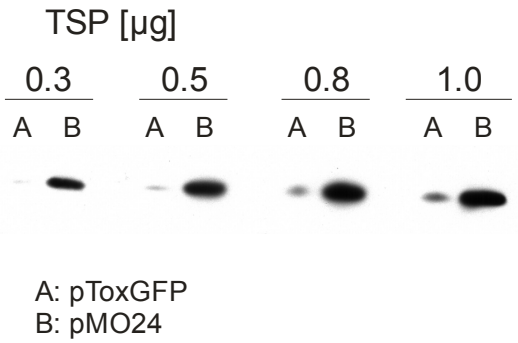

Fig. 29 Immunoblot analysis of total soluble protein extracted from *E. coli* carrying the plasmids pToxGFP (A) and pMO24 (B), respectively. The loaded amount of total soluble protein is indicated above each pair of lanes. Scion Image for Windows software quantification showed that GFP accumulation was less than 1% in the pToxGFP samples compared to the pMO24 samples.

Fig. 29 shows the obtained Western blot. The amount of GFP derived from pToxGFP was drastically reduced compared to pMO24 (less than 1% in pToxGFP compared to pMO24), indicating that the transcription block functions and *gfp* transcription is drastically reduced. Since it is known that GFP protein is relatively stable and even small translated amounts accumulate within the cell (Prasher et al., 1992; Kain et al., 1995) it can be assumed that the huge decrease in GFP as observed for pToxGFP should be even more significant at the level of *gfp* mRNA.

3.2.4 Toxicity test for Pal and Cpl-1

In previous experiments (3.2.1) it was postulated that Pal and Cpl-1 have toxic effects on *E. coli* when expressed inside the bacterial cell. Since the pTox vector showed strongly decreased transcription for the inserted gene of interest, it could be used to analyze the toxicity of Pal and Cpl-1 based on co-cloning tests. Both genes, *pal* and *cpl-1*, were cloned in a 1:1 ratio together with a non-toxic gene, here *gfp*, into the plasmids pMO24 and pTox. Obtained colonies were tested using RFLP analysis for successful integration of *pal*, *gfp* and *cpl-1*, respectively. Whereas samples derived from the plasmid pMO24 showed exclusively *gfp* insertions, samples from pTox showed integration of *gfp* as well as *pal* and *cpl-1*, respectively, at a ratio of around 50% each. Tab. 3 shows precise colony numbers as well as percentages of insertions into pMO24 and pTox, respectively.

Tab. 3 Co-cloning of the *pal* and *cpl-1* genes together with *gfp* into the plasmids pMO24 and pTox. The vector backbones used are indicated while the inserted gene combinations are shown in bold and italics. Numbers of colonies obtained as well as percentages carrying a specific gene are indicated.

Backbone	**pMO24**		**pTox**	
inserts	***pal***	***gfp***	***pal***	***gfp***
colonies	-	40	29	24
insertions	-	100%	55%	45%
inserts	***cpl-1***	***gfp***	***cpl-1***	***gfp***
colonies	-	40	13	22
insertions	-	100%	37%	63%

3.2.5 Generation of transplastomic plants with pTox derivatives

To insert *pal* and *cpl-1* into the pTox vector, the 5' *Nde*I restriction site was replaced by an *Nco*I restriction site using polymerase chain reaction and the primers Pal-F, Cpl-1-NcoI and M13-rev. Derived fragments were inserted as *Nco*I/*Xba*I fragments into the pTox vector resulting in pToxPal and pToxCpl-1, respectively.

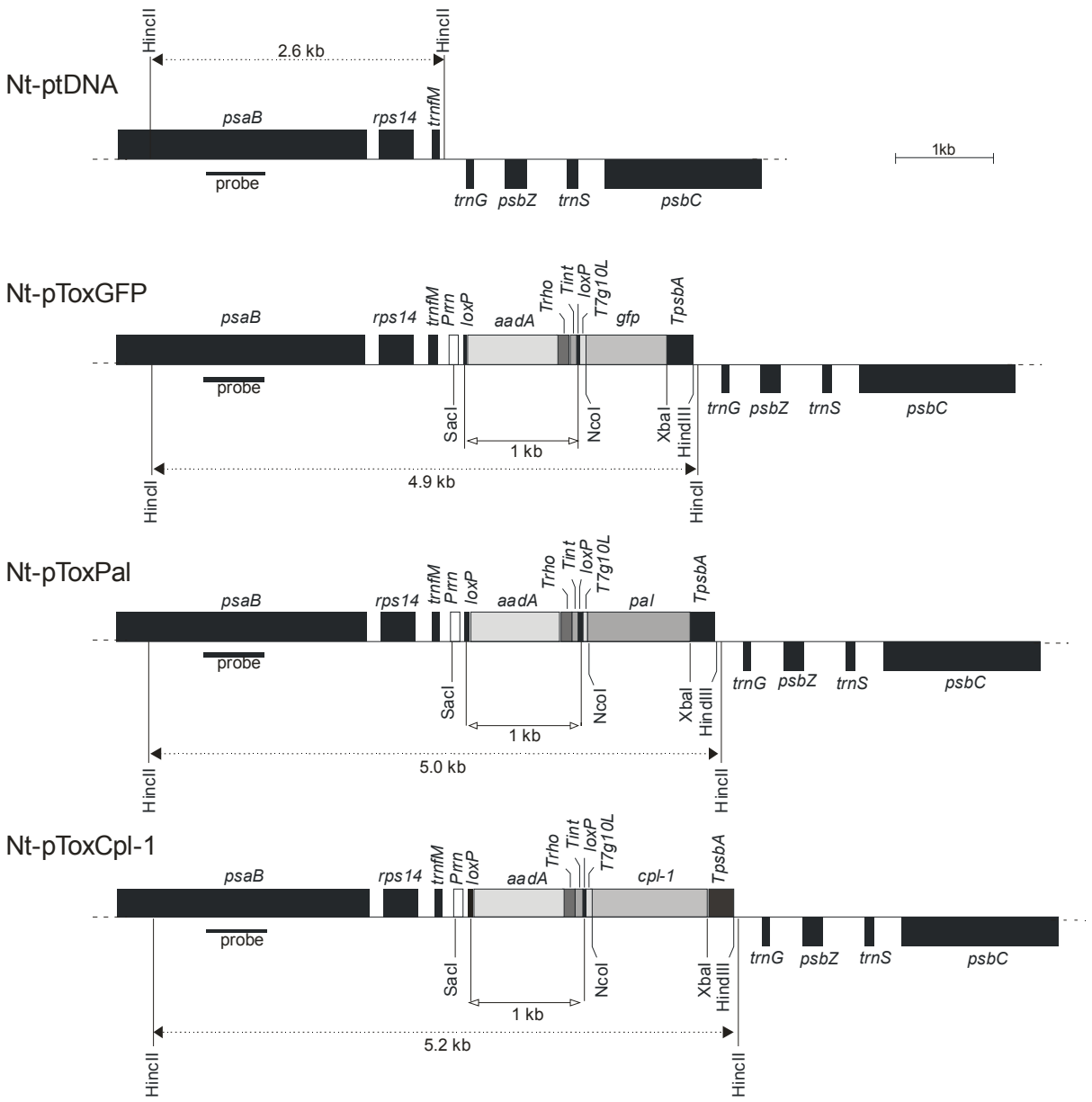

Fig. 30 Physical map of the targeted region of the plastid genome for the introduction of the transgenes *gfp, pal* or *cpl-1* between the plastid genes *trnfM* and *trnG*. Transplastomic lines were generated with transformation vectors pToxGFP, pToxPal and pToxCpl-1, which carried the transgenes *gfp, pal* or *cpl-1*. The resulting transplastomic lines were named Nt-pToxGFP, Nt-pToxPal and Nt-pToxCpl-1. Expected sizes of DNA fragments in RFLP analyses with the restriction enzyme *Hinc*II as well as sizes of the *aadA* blocks that are excised by CRE-mediated deletion are indicated. The location of the RFLP probe is shown as a black bar.

The pTox plasmids carrying the *gfp*, *pal* and *cpl-1* genes were used to biolistically transform *Nicotiana tabacum cv. petit havana* leaves resulting in Nt-pToxGFP, Nt-pToxPal and Nt-pToxCpl-1 plants (T_0 generation). Independent transplastomic lines were obtained after several rounds of regeneration and stringent antibiotic selection on spectinomycin containing medium. 2 lines of each construct (Nt-pToxGFP #3 and #8, Nt-pToxPal #2 and #18 and Nt-pToxCpl-1 #8 and #20) were characterized in detail. Physical maps of the insertion region of wild type and transplastomic lines as well as restriction sites used for cloning or RFLP analysis and resulting fragment sizes are shown in Fig. 30.

For RFLP analysis, genomic DNA was digested with *Hinc*II and fragments were detected via Southern blotting using a radiolabelled *psaB* probe (6.1.1). To test whether the obtained plants show homoplasmy, a seed assay was performed. RFLP analyses as well as seed assays revealed successful integration of the transgenes as well as homoplasmy of the tested plants (Fig. 41, Fig. 42). These data are presented under 3.2.9.1 and 3.2.9.2.

3.2.6 Protein analysis and identification of Pal and Cpl-1

To test whether Pal and Cpl-1 accumulated to high amounts, total soluble protein was extracted from Nt-pToxPal and Nt-pToxCpl-1 plants and separated electrophoretically by SDS-PAGE. Using colloidal Coomassie staining, clear bands corresponding to the size of Pal (35 kDa) and Cpl-1 (40 kDa) could be seen, whereas no such band could be detected in the wild type sample (Fig. 47).

To confirm that these bands were indeed the lytic enzymes Pal and Cpl-1, the bands were excised from the gel and the extracted proteins tryptically digested. Standard mass spectrometry was then used to analyse and identify the proteins using the Mascot software. These analyses, kindly done by Dr. Waltraud Schulze (Max Planck Institute of Molecular Plant Physiology, Golm, Germany), showed that the protein bands indeed were Pal and Cpl-1. Peptide coverage for Pal and Cpl-1 was 63% and 61%, respectively.

3.2.7 Activity tests of Pal and Cpl-1

To examine whether the obtained homoplasmic plants produced active bactericidal proteins, total soluble protein isolated from Nt-pToxPal and Nt-pToxCpl-1 plants was tested for its ability to kill *Streptococcus pneumoniae*, the target bacteria for the two lytic enzymes (Loeffler et al., 2001; Loeffler et al., 2003).

3.2.7.1 Cell density decrease

The potential of the lysins to kill *S. pneumoniae* was first tested by monitoring the clearance of a bacterial cell suspension. Over a time course, the dose-dependent decrease in optical density at 600 nm (OD_{600}) was measured when different amounts of total soluble protein extract from Nt-pToxPal, Nt-pToxCpl-1 and wild type plants were added to the bacteria cells. The obtained data clearly showed a dose-dependent decrease of OD_{600} in samples containing either Pal or Cpl-1, whereas no significant decrease in wild type protein containing samples could be seen (Fig. 31). These results indicated that Pal and Cpl-1 derived from transplastomic plants were able to clear bacterial cell cultures in a dose-dependent manner.

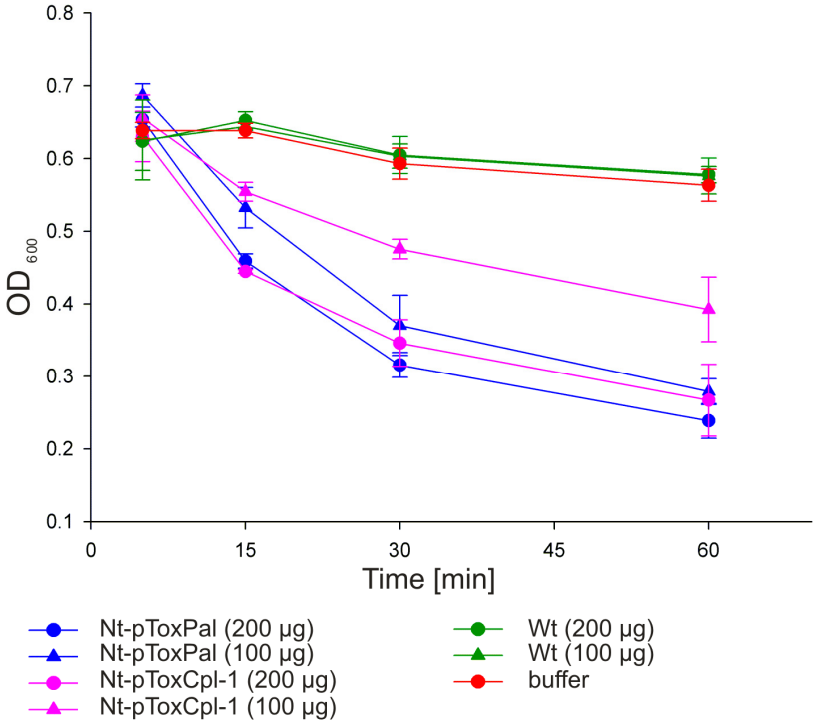

Fig. 31 Time course of bacterial cell death caused by Pal and Cpl-1 monitored by clearing of cell cultures of *S. pneumoniae*. Plants from which total soluble protein was obtained as well as amounts of total soluble protein added to the bacterial cell culture at time point 0 are indicated. Optical density was measured at 600 nm (OD_{600}). The graphs show averages of two sets of experiments with three replicates each as well as the standard deviation for every time point.

Since Pal, an amidase, and Cpl-1, a lysozyme, show different modes of action, they should be able to act synergistically as shown by Loeffler and Fischetti (2003). To examine this effect, different amounts of total soluble protein (100 and 150 µg each) from Pal and Cpl-1 expressing plants were mixed and tested for their ability to kill *S. pneumonia*. To show that both enzymes together killed the bacteria faster than one protein alone, total soluble protein of Nt-pToxPal was used as reference.

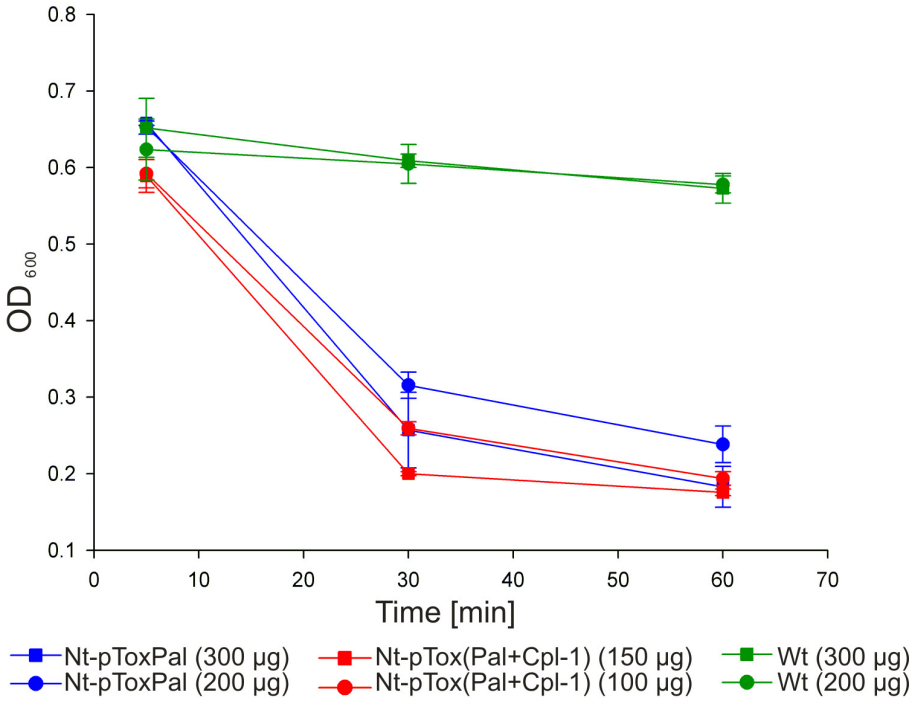

Fig. 32 Time course of synergistic bactericidal activity of Pal and Cpl-1 monitored as clearance of cell cultures of *S. pneumoniae*. Plants from which protein was isolated as well as amounts of total soluble protein added to the bacterial cell culture at time point 0 are indicated. The red line shows the effect of Pal and Cpl-1 combination; protein amounts of each protein are indicated. Optical density was measured at 600 nm (OD_{600}). The graphs show averages of three replicates as well as the standard deviation for every time point.

Data obtained from the clearing of the bacteria cell culture showed that total soluble protein containing both Pal and Cpl-1 (150 µg each) were able to decrease OD_{600} as fast as 300 µg of Pal-containing total soluble protein (Fig. 32). Since the graph for 150 µg of Pal and Cpl-1 combined showed a plateau at 30 min (OD_{600} = 0.2, which was assumed to be the final OD caused by cell debris), whereas 300 µg of TSP with Pal still showed a decrease from 30 to 60 minutes, it was assumed that Pal and Cpl-1 indeed act synergistically. However, a more detailed time course has to be implemented to further investigate and confirm this.

In further experiments, it was tested whether the formerly observed toxic effect of Pal and Cpl-1 when expressed in *E. coli* could also be seen by monitoring cell density of *E. coli* suspension cultures supplemented with total soluble protein derived from Nt-pToxPal and Nt-pToxCpl-1 plants.

Interestingly, no effect on the cell density from either Pal or Cpl-1-containing protein samples could be seen (Fig. 33). Thus, Pal and Cpl-1 were not able to kill *E. coli* cells from the

outside, leading to the assumption that the toxic effect of Pal and Cpl-1 is not caused by lysin attack to the cell wall.

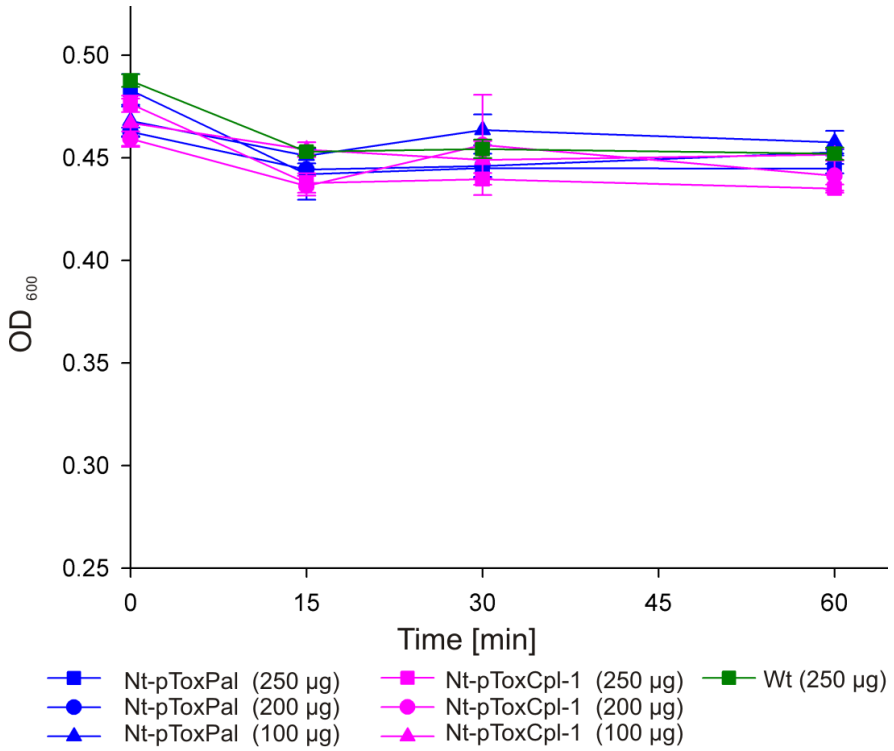

Fig. 33 Test of bactericidal activity of Pal and Cpl-1 on *E. coli* cell cultures. Amounts of total soluble plant protein added to the bacterial cell culture at time point 0 are indicated. Optical density was measured at 600 nm (OD_{600}). The graphs show averages of three replicates as well as the standard deviation for every time point.

3.2.7.2 Viability tests

To further confirm the bacteriolytic effect of Pal and Cpl-1, bacterial cells exposed to different amounts of lysin containing total soluble protein were examined for their ability to form colonies. It was assumed that if Pal and Cpl-1 attack and degrade the cell wall of *S. pneumoniae*, cells were no longer able to divide and form colonies. To better compare the obtained results, all colony numbers were normalized to the colony number derived from time point 0. Results obtained from this experiment indeed showed a decrease in a time and dose-dependent manner indicating that Pal and Cpl-1-containing total soluble proteins lyse *S. pneumoniae* and inhibit colony formation (Fig. 34).

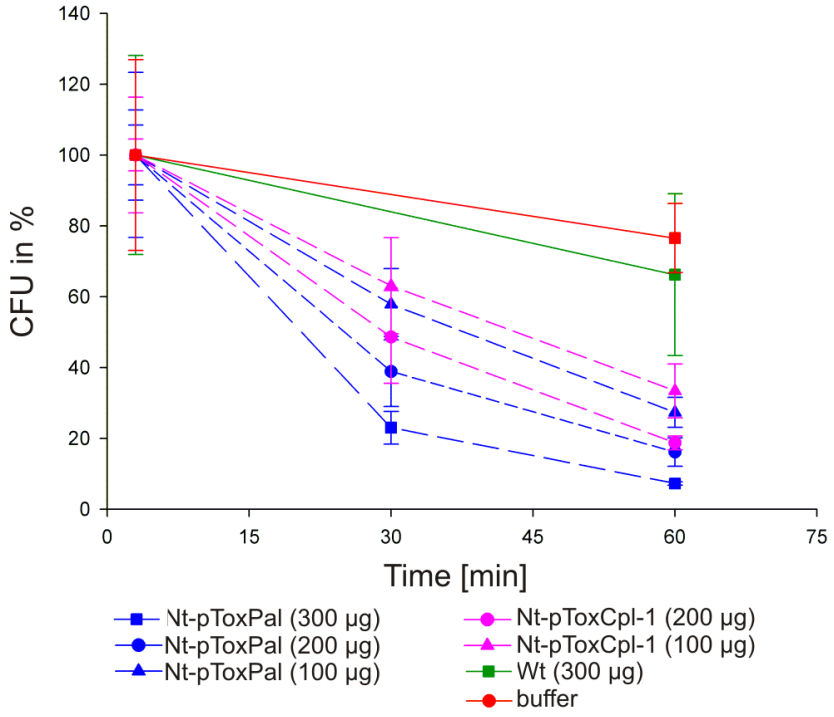

Fig. 34 Time course of bactericidal activity of Pal and Cpl-1 monitored by the decreasing ability of *S. pneumoniae* to form colonies. Plants from which total soluble protein was isolated as well as protein amounts added to the bacterial cell culture at time point 0 are indicated. A dilution series of the culture was plated out and obtained colony numbers were normalized to the colony number derived from time point 0. The graphs show averages of two sets of experiments with two to three dilutions each.

3.2.7.3 Live/dead staining

Direct visualization of the integrity of bacterial cell walls and a confirmation of the results obtained from the OD decrease and CFU determination can be obtained by the live/dead staining assay described in 3.1.6.3. Already lyzed cells are not stained with this approach but instead result in a visible decrease in cell number. Whereas cell suspensions with wild type protein showed predominantly green fluorescing, living cells, fluorescence microscopy of bacterial samples supplemented with lytic enzymes showed increasing numbers of red fluorescing cells, indicating increasing destruction of cell wall structures. As seen in the previous experiments, the increase of red fluorescing cells as well as the decrease in cell number occurs in a time and dose-dependent manner (Fig. 35).

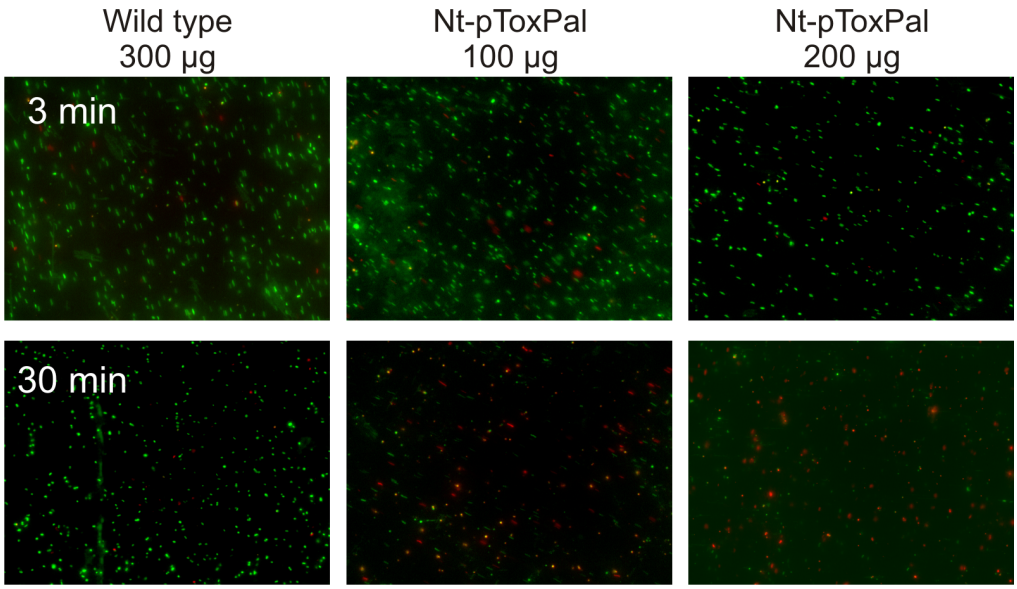

Fig. 35 Visualization of effective killing of *S. pneumoniae* cells by live/dead fluorescence staining. Fluorescence images are shown for the wild type control and two different concentrations of Pal-containing total soluble protein. Live cells show green fluorescence, while damaged cells fluoresce red. Already lysed cells cannot be stained, explaining the decline in cell number over time in the Pal samples.

3.2.8 Removal of aadA via the CRE-lox system

To remove the undesired *aadA* marker gene cassette and to test the effect of the transcription block, transplastomic plants were pollinated with a homozygous nuclear transformed CRE expressing plant (2.6.2) resulting in plants termed Nt-pTox-Cre (T_1 generation) (2.6.2). The *Cre* gene expression was driven by the P2' promoter of the *Agrobacterium* mannopine synthase (Corneille et al., 2001). To mediate later import of the CRE into the chloroplast, the protein is fused to a transit peptide derived from the pea Rubisco small subunit.

3.2.8.1 Identification of putative marker-free plants

Seeds resulting from crossings of transplastomic lines with CRE expressing plants were tested for recombination events on spectinomycin containing medium. Deletion of the *aadA* marker gene caused by the site-specific recombinase would lead to loss of antibiotic resistance and thus, due to the translation inhibiting effect of spectinomycin, to white leaf tissue. Indeed, seedlings with white patches were obtained under selection pressure (Fig. 36).

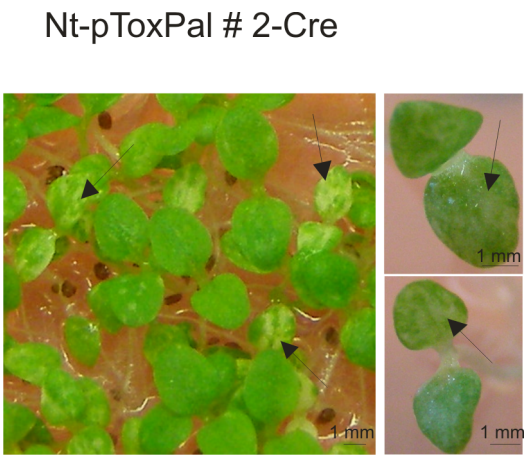

Fig. 36 Mottled pattern of CRE expressing Nt-pToxPal-Cre seedlings. Seedlings were grown on spectinomycin containing medium. Arrows indicate white areas; a 1 mm scale bar is shown for size comparison.

Assuming spectinomycin sensitivity of the white areas, mottled Nt-pToxGFP-Cre seedlings grown on antibiotic containing medium were examined by fluorescence microscopy using proper wavelengths to show GFP (excitation filter 470 nm/emission filter 505-530 nm) as well as chlorophyll fluorescence (excitation filter 450-490 nm/emission filter 520 nm - long pass emission).

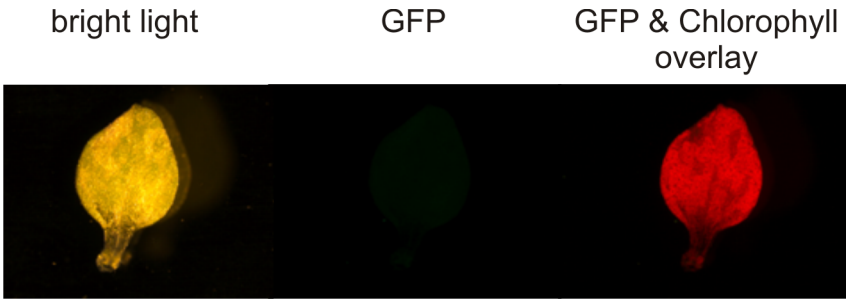

Fig. 37 Autofluorescence studies of cotyledons of GFP-free mottled Nt-pToxPal-Cre seedlings grown on spectinomycin. Bright field as well as fluorescence microscopic images were taken at the appropriate wavelengths for GFP and chlorophyll fluorescence detection as indicated above.

In theory, white areas resulting from *aadA* deletion should also show reduced GFP fluorescence due to the translation inhibition caused by spectinomycin. To obtain reliable results from fluorescence microscopy, background fluorescence at the wavelength used for GFP fluorescence detection was determined using GFP-free plants (Nt-pToxPal-Cre, Fig. 36) grown on spectinomycin containing medium (Fig. 37).

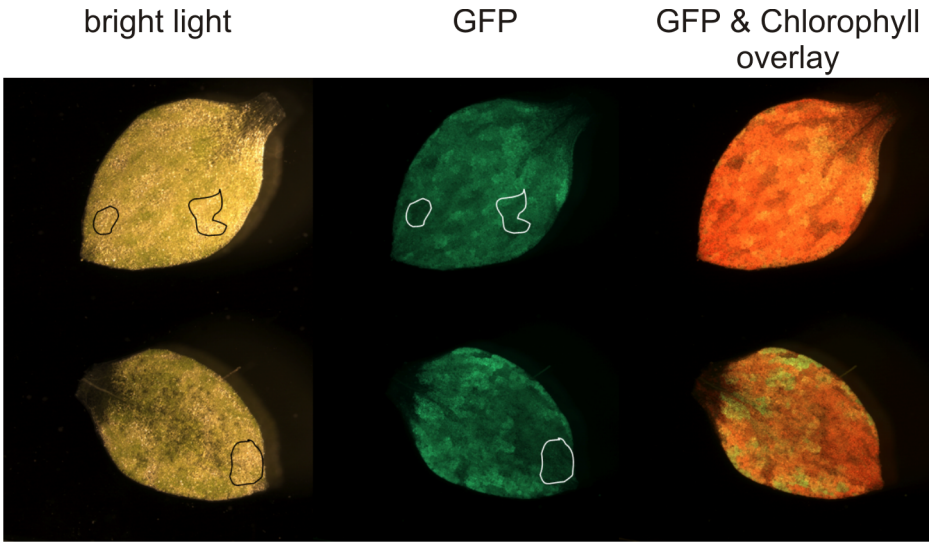

Fig. 38 Fluorescence studies of cotyledons of CRE expressing mottled Nt-pToxGFP-Cre seedlings grown on spectinomycin. Bright field as well as fluorescence microscopic images were taken at the appropriate wavelengths for GFP and chlorophyll fluorescence detection as indicated above. White areas seen in the bright field image are marked for comparison.

Detailed examination of GFP expressing plants showed that indeed, white areas correspond to decreased GFP fluorescence indicating successful deletion of the *aadA* gene as well as the *E. coli* terminator region (Fig. 38).

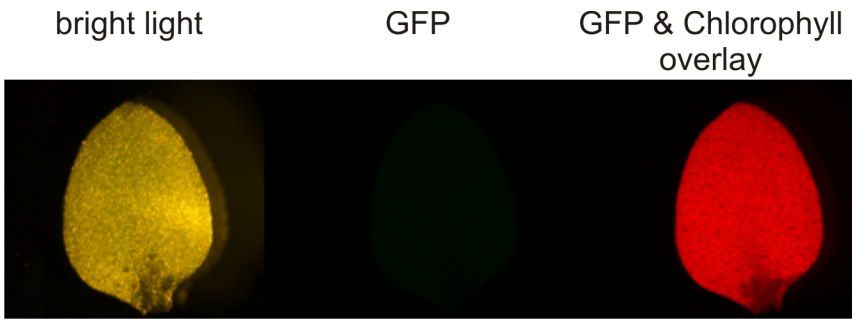

Fig. 39 Autofluorescence studies of cotyledons of GFP-free Nt-pToxPal-Cre seedlings grown on kanamycin. Bright field as well as fluorescence microscopic images were taken at the appropriate wavelengths for GFP and chlorophyll fluorescence detection as indicated above.

As a second confirmation that the white areas with less GFP fluorescence are not caused by mutations leading to impaired transcription or translation, pToxGFP-Cre seedlings were also germinated on kanamycin containing medium. Kanamycin resistance should be inherited from the CRE expressing plant used for pollination.

GFP-free plants (Nt-pToxPal-Cre) grown on kanamycin containing medium were again used to determine background fluorescence at the wavelength used for GFP fluorescence (Fig. 39). Seedlings grown on kanamycin containing medium showed no white patches whereas the mottled GFP fluorescence still could be seen even in primary leaves indicating that CRE activity influences GFP expression (Fig. 40A, B).

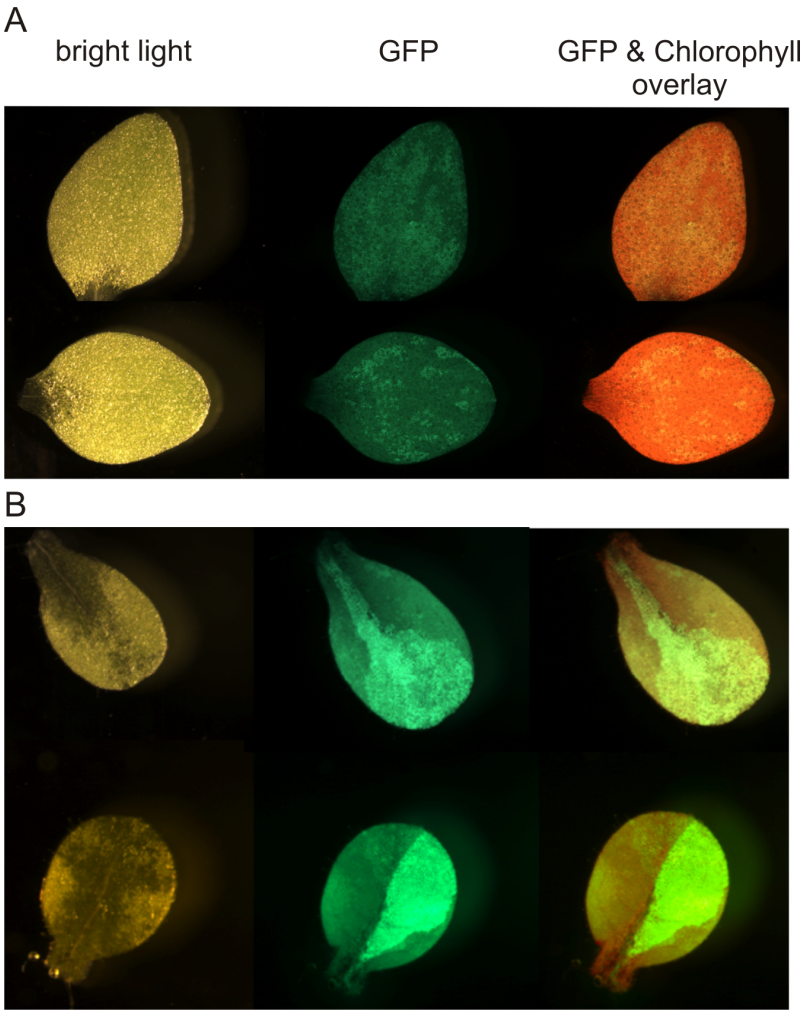

Fig. 40 Fluorescence studies of Nt-pToxGFP-Cre seedlings grown on kanamycin containing medium. Bright field as well as fluorescence microscopic images were taken at the appropriate wavelengths for GFP and chlorophyll fluorescence detection as indicated above for cotyledons (A) and primary leaves (B). The dark areas in the bright field image from primary leaves are due to the use of forceps for harvesting.

The fluorescence pattern of the seedlings indicated that the CRE-mediated recombination was not complete and thus the seedlings examined are still heteroplasmic. Since further growth on spectinomycin containing medium forces the plants to keep the *aadA* for survival, plants were transferred to soil and grown to maturity to allow for completion of site-specific recombination.

3.2.9 Molecular analysis of marker-free transplastomic plants

3.2.9.1 Southern blotting

To test whether site-specific recombination has been completed in mature plants, total DNA was extracted from wild type, transplastomic Nt-pTox ("selfed") as well as Nt-pTox-Cre plants ("Cre"), digested with *Hinc*II over night and used for Southern blotting using a *psaB* probe (6.1.1) that hybridized to flanking plastome sequences (Fig. 30). In general, two different fragment lengths were obtained for all three constructs (pToxCpl-1, pToxPal and pToxGFP) showing the long *aadA*-containing fragment in the transplastomic Nt-pTox plants at sizes of 5.2 kb, 5.0 kb and 4.9 kb, respectively, and the shorter fragment in the Nt-pTox-Cre plants at the size of 4.2 kb, 4.0 kb and 3.9 kb, respectively (Fig. 41).

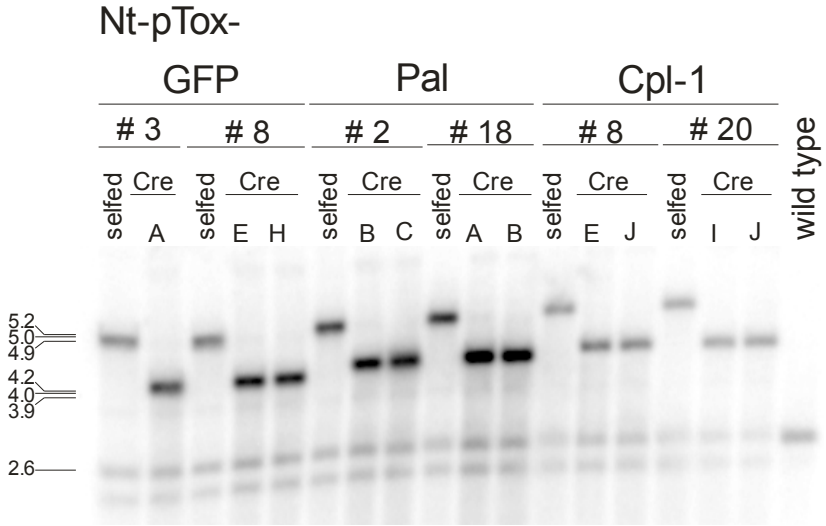

Fig. 41 RFLP analysis of transplastomic Nt-pTox tobacco lines. Total cellular DNA was digested with *Hinc*II and hybridized to a radiolabelled probe detecting the region of the plastid genome that flanks the transgene insertion site (Fig. 30). Fragment sizes for the wild type and the different transplastomic lines are indicated in kb. The inserted transgene and numbers of independently generated transplastomic lines and plants are shown above the blot. T_1 plants termed "selfed" indicate plants obtained from self pollination; "Cre" indicates plants obtained from crossings with *Cre* nuclear transformed plants where the *aadA* is recombined out. Differences in fragment sizes correspond to the size of the *aadA* and terminator sequences (1 kb).

The size differences between Nt-pTox and Nt-pTox-Cre plants correspond to the size of the *aadA* containing block (1 kb, Fig. 30) deleted by site-specific recombination. Wild type plants showed band sizes corresponding to the plastome sequence without insertion of a transgene. The slightly visible wild type-like bands in the transplastomic lines were again suspected to

be signals derived from nuclear copies of the plastome target region. Signal intensities tentatively suggested that the transplastomic plants were homoplasmic.

3.2.9.2 Confirmation of homoplasmy by seed assay

To confirm homoplasmy of the marker-free Nt-pTox-Cre plants, seed assays on spectinomycin containing as well as antibiotic-free medium were performed using seeds obtained from the Nt-pTox-Cre plants ("Nt-pTox-Cre-selfed", T_2 generation) (2.6.2).

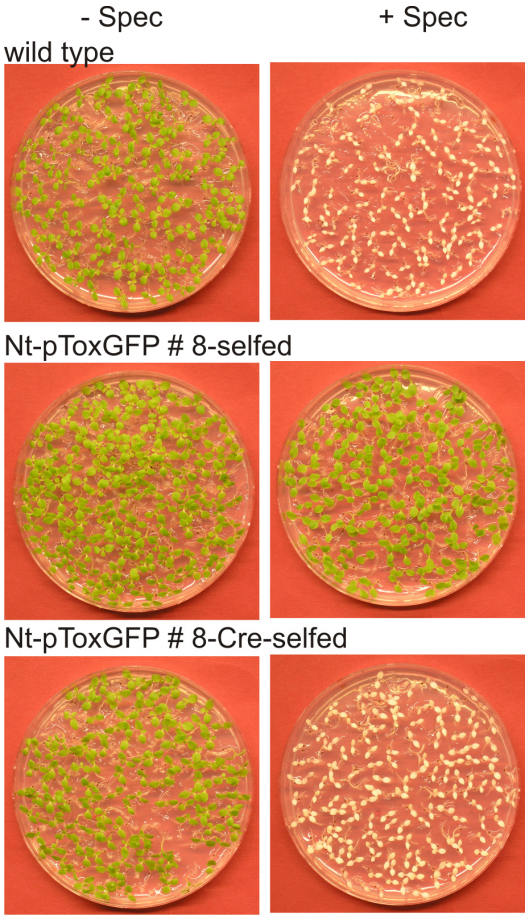

Fig. 42 Seed assay to confirm homoplasmy and complete CRE-mediated deletion of *aadA* in Nt-pTox-Cre plants. –Spec and +Spec indicate presence or absence of spectinomycin in the germination medium. Wild type seedlings were compared to seedlings obtained from transplastomic plants Nt-pToxGFP #8 ("Nt-pToxGFP#8-selfed", T_1 generation) and Nt-pToxGFP #8-Cre by self pollination ("Nt-pToxGFP#8-Cre-selfed", T_2 generation). Green seedlings in +Spec medium show resistance whereas white seedlings are sensitive to the antibiotic. The white phenotype of Nt-pToxGFP #8-Cre plants grown on +spec medium indicated complete *aadA* deletion.

As a control, wild type seedlings as well as Nt-pTox seedlings ("Nt-pTox-selfed") were used. Wild type seedlings showed a green phenotype on antibiotic-free medium, whereas spectinomycin in the medium led to white seedlings that ceased to grow (Fig. 42). Nt-pTox seedlings developed normally in both the absence and presence of the antibiotic in the culture

medium indicating presence of the *aadA* gene that confers antibiotic resistance. In contrast, Nt-pTox-Cre-selfed seedlings show a green phenotype on spectinomycin-free medium, whereas when grown on antibiotic containing medium, they were white and ceased to grow. This wild type-like phenotype indicates absence of the resistance-providing *aadA* gene, which confirms the results obtained from the Southern blot.

3.2.9.3 Northern blotting

Northern blotting was used to identify *gfp*, *pal* and *cpl-1*-specific mRNAs. Total RNA from wild type, Nt-pTox and Nt-pTox-Cre plants was isolated, blotted and hybridized to a gene-specific probe (full coding region of *gfp*, *pal* and *cpl-1*, respectively) (Fig. 43). As expected, in all wild type samples transgene mRNA could not be detected.

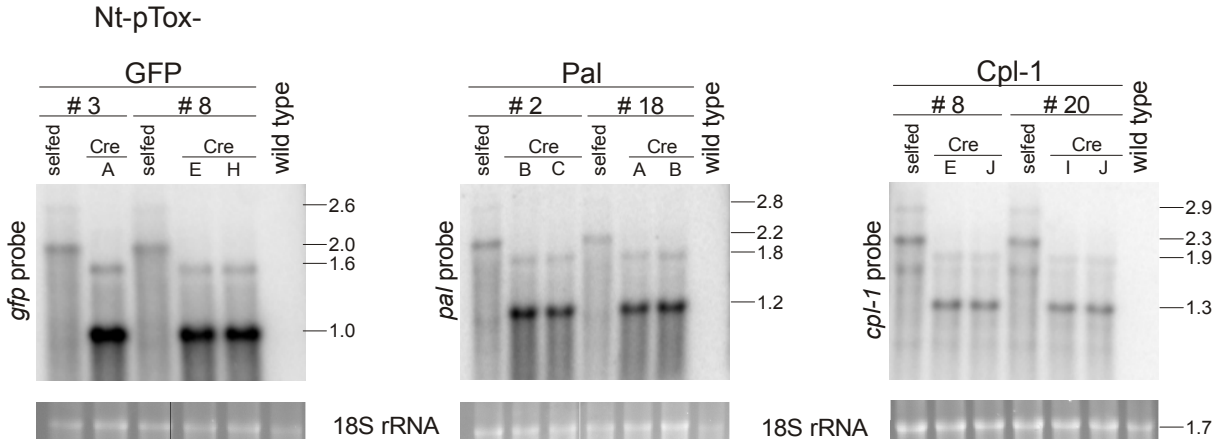

Fig. 43 RNA blot analyses of *gfp*, *pal* and *cpl-1* mRNA accumulation. 3 µg of total RNA were separated in a formaldehyde containing 1% agarose gel and blotted. Obtained fragment sizes are indicated in kb. Major transcripts were detected by gene-specific probes at the size of 1.0 kb (Nt-pToxGFP-Cre), 2.0 kb (Nt-pToxGFP-selfed), 1.2 kb (Nt-pToxPal-Cre), 2.2 kb (Nt-pToxPal-selfed), 1.3 kb (Nt-pToxCpl-1-Cre) and 2.3 kb (Nt-pToxCpl-1-selfed). In all cases additional minor transcripts can be seen 0.6 kb larger than the major transcript, indicating read-through transcription. 18S rRNA bands from the gel used for blotting are shown and serve as a control for equal RNA loading.

In all Nt-pToxGFP, Nt-pToxPal and Nt-pToxCpl-1 plants slight amounts of transcripts corresponding to the sizes of 2.0, 2.2 and 2.3 kb, respectively, indicated that read-through transcription over the fused *E. coli* terminator had occurred. Interestingly, a larger second transcript with the sizes of 2.6, 2.8 and 2.9 kb, respectively, could also be seen in small amounts indicating that additional read-through transcription terminated further downstream. Nt-pToxGFP-Cre, Nt-pToxCpl-1-Cre and Nt-pToxPal-Cre plants showed that the major transcripts detected were 1.0, 1.2 and 1.3 kb, respectively, in length. The size differences of the transcript compared to the Nt-pTox plants, which lack CRE, correspond to the expected

sizes for P*rrn* mediated expression after *aadA* elimination (1 kb). Again a second 0.6 kb larger transcript could also be detected resulting from read-through transcription. Comparing the signal intensity in all plants, major transcripts derived from CRE expressing Nt-pToxGFP-Cre and Nt-pToxPal-Cre plants appeared to be much stronger than the transcript from selfed Nt-pToxGFP plants, whereas Nt-pToxCpl-1-Cre plants showed almost the same amounts of major transcript when compared to CRE-free Nt-pToxCpl-1 plants. Interestingly, additional bands could be detected in all Nt-pToxCpl-1 and Nt-pToxCpl-1-Cre plants. The mRNA analysis of *cpl-1* showed possible processing sites that may result in unstable transcripts. However, these results indicated that loss of *aadA* influences and increases mRNA accumulation depending on the inserted gene.

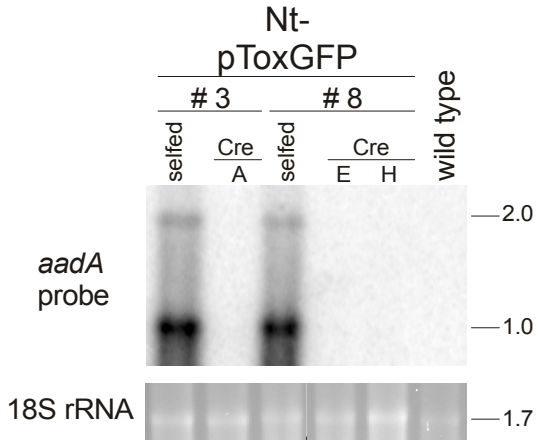

Fig. 44 RNA blot analysis of *aadA* mRNA accumulation. 3 µg of total RNA were separated in a formaldehyde containing 1% agarose gel and blotted. An *aadA*-specific hybridization probe detected major transcripts of 1.0 kb in the Nt-pToxGFP plants ("selfed") and a minor transcript of 2.0 kb resulting from read-through transcription to the *TpsbA* 3' UTR. No *aadA* mRNA was detected in Nt-pToxGFP-Cre plants ("Cre"), indicating successful CRE-mediated deletion. Nt-pToxGFP lines and plants are indicated above. 18S rRNA bands from the gel used for blotting are shown and serve as a control for equal RNA loading.

To further demonstrate complete deletion of the selection marker gene, *aadA* mRNA accumulation was tested (Fig. 44). As previously described, total RNA was isolated, blotted and hybridized to an *aadA*-specific probe (6.1.1). In contrast to wild type samples, where no *aadA* mRNA could be detected, Nt-pTox plants showed a major transcript at 1 kb as expected from transcription initiated from the P*rrn* promoter as well as a minor transcript of larger size resulting from read-through transcription to the 3' UTR of the gene of interest (Stern and Gruissem, 1987). Nt-pTox-Cre plants did not show any *aadA* transcript, indicating successful recombinase-mediated marker gene elimination.

3.2.10 Recombinant protein quantification in the marker-containing and marker-free transplastomic plants

3.2.10.1 GFP fluorescence and protein accumulation

To examine and quantify GFP accumulation in Nt-pToxGFP and Nt-pToxGFP-Cre plants, fluorescence microscopy was performed with seedlings at proper wavelengths to visualize GFP and chlorophyll fluorescence. Wild type plants were used as a non-fluorescing control. As expected from the Northern blot analysis Nt-pToxGFP-selfed seedlings (T_1 generation) showed less GFP fluorescence compared to Nt-pToxGFP-Cre-selfed seedlings (T_2 generation) (Fig. 45).

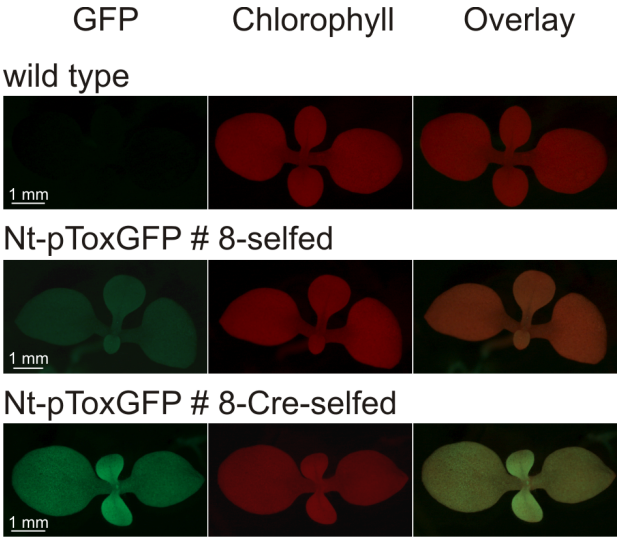

Fig. 45 GFP and chlorophyll fluorescence of GFP-containing Nt-pTox plants with and without CRE-mediated marker gene elimination. Plant lines as well as measured fluorescence are indicated. The overlay shows the combination of GFP and chlorophyll fluorescence.

Since GFP amounts in the Nt-pToxGFP or Nt-pToxGFP-Cre plants were too low to be directly visualized by SDS-PAGE and Coomassie staining, total soluble protein was extracted from homoplasmic plants and Western blotting was used for protein quantification. For immunodetection the antibodies already mentioned (3.2.3) were used. Measured signal intensities, analysed using the Scion Image for Windows software, showed 4-5 times higher GFP accumulation in the Nt-pToxGFP-Cre compared to Nt-pToxGFP plants (Fig. 46) confirming the results obtained from the Northern blot (3.2.9.3). Using purified GFP protein (Oliver Drechsel, Max Planck Institute of Molecular Plant Physiology, Golm, Germany) as a reference, GFP was calculated to accumulate to up to 7-10% of total soluble cellular protein in Nt-pToxGFP-Cre plants.

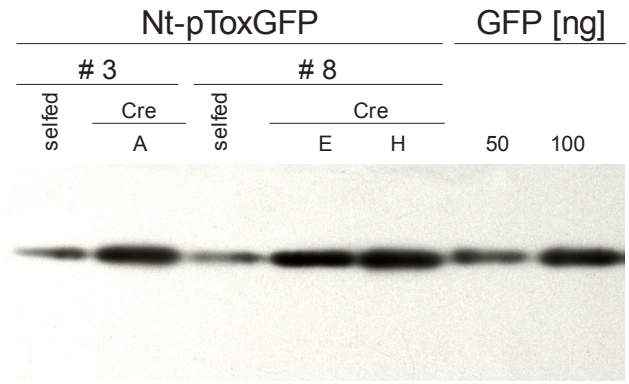

Fig. 46 Analysis of GFP protein accumulation in transplastomic plants. 3 µg of TSP from Nt-pToxGFP ("selfed"), Nt-pToxGFP-Cre ("Cre") plants and purified GFP from *E. coli* as reference were blotted and detected by an anti-GFP antibody derived from mouse using the ECL detection system (1 s exposure time). Nt-pToxGFP lines and plants as well as loaded amounts of purified GFP are indicated.

3.2.10.2 Pal and Cpl-1 protein quantification

To determine Pal and Cpl-1 contents, total soluble protein was isolated from Nt-pToxPal, Nt-pToxPal-Cre, Nt-pToxCpl-1 and Nt-pToxCpl-1-Cre plants, electrophoretically separated on an SDS-containing polyacrylamide gel and stained using a colloidal Coomassie stain.

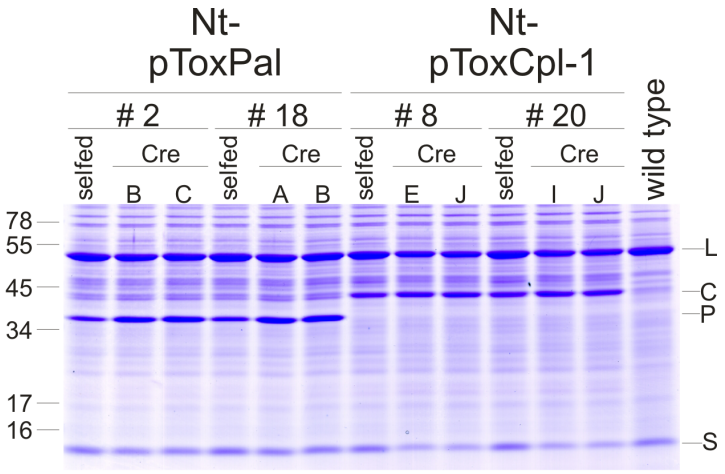

Fig. 47 Pal and Cpl-1 protein accumulation in Nt-pTox and Nt-pTox-Cre plants monitored by Coomassie staining. 15 µg of total soluble protein was extracted from Pal and Cpl-1 expressing plants, electrophoretically separated and stained with colloidal Coomassie. Marker band sizes are given in kDa. Identified proteins are indicated as follows: L, large subunit of Rubisco; S, small subunit of Rubisco; P, Pal protein; C, Cpl-1 protein.

As described previously (3.2.6), clear bands at the expected size for Pal (35 kDa) and Cpl-1 (40 kDa) could be detected in all the samples from Pal and Cpl-1 expressing plants. TSP extracted from Nt-pToxPal-Cre plants showed 2-3 times higher Pal accumulation compared to Nt-pToxPal plants, whereas Nt-pToxCpl-1-Cre plants did not show significantly higher Cpl-1 accumulation compared to Nt-pToxCpl plants (Fig. 47).

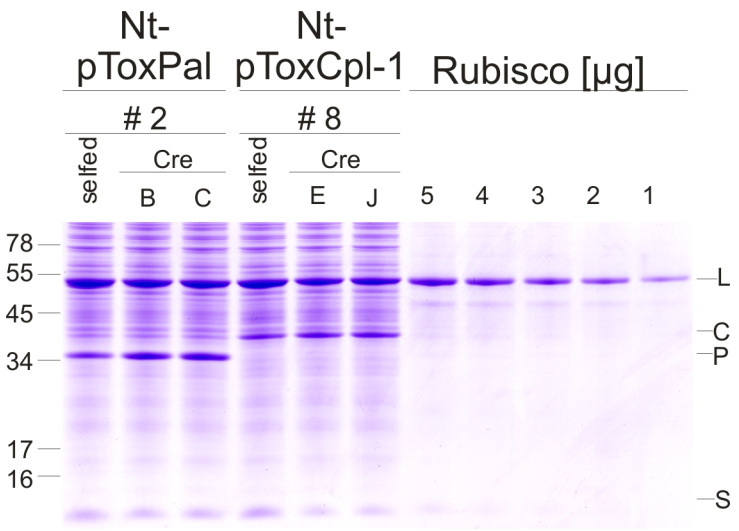

Fig. 48 Quantification of Pal and Cpl-1 protein accumulation in Nt-pTox and Nt-pTox-Cre plants by comparison to a dilution series of purified Rubisco protein. For Nt-pTox plants 15 µg TSP were loaded; Rubisco amounts are indicated above. Protein bands indicated as follows: L, large subunit of Rubisco; S, small subunit of Rubisco; P, Pal protein; C, Cpl-1 protein.

These observations were in line with the results obtained from Northern blotting (3.2.9.3). Interestingly, Rubisco levels seemed to decrease in the Nt-pToxCpl-1-Cre plants.

Quantification of Pal and Cpl-1 protein accumulation in Nt-pTox and Nt-pTox-Cre plants, respectively, was estimated by comparing band intensities. More specifically, 15 µg of total soluble protein extracted from Pal and Cpl-1 expressing plants as well as a dilution series of commercially available Rubisco were separated by SDS-PAGE and stained with Coomassie (Fig. 48).

Since Pal and Cpl-1 are less stainable with Coomassie than the Rubisco large subunit due to amino acid composition (basic amino acids: Pal: 30; Cpl-1: 29; RbcL: 55) and isoelectric point (Pal: 5.02; Cpl-1: 4.66; RbcL: 6.4) (Tab. 4), Pal protein content was estimated to be 10-20% and 30-40% of TSP in Nt-pToxPal and Nt-pToxPal-Cre plants, respectively, whereas the Cpl-1 content was approximately 10-20% of TSP in both Nt-pToxCpl-1 and Nt-pToxCpl-1-Cre plants.

Tab. 4 Amino acid composition of Pal, Cpl-1 and Rubisco large subunit. Amino acids are indicated by the one-letter code and are classified according to their properties. The sum of amino acids belonging to a given group is indicated.

Amino Acids	Pal	Cpl-1	Rubisco (RbcL)
Charged (RKHYCDE)	109	106	155
Acidic (DE)	41	45	59
Basic (KR)	30	29	55
Polar (NCQSTY)	84	107	101
Hydrophobic (AILFWV)	91	104	173

3.2.11 Protein stability of Pal and Cpl-1

As mentioned previously, for pharmaceutical production, stability of the proteins in the production platform is of high importance.

Fig. 49 Sampling of leaves from mature transplastomic Nt-pToxPal-Cre and Nt-pToxCpl-1-Cre plants and leaf numbering.

Since it is known that protein biosynthesis decreases in older leaves (Daniell et al., 2001), changes in foreign protein content over leaf aging can serve as an indicator of protein stability. Thus, protein stability of Pal and Cpl-1 over leaf age was determined using equal amounts of TSP from leaves of mature plants (Fig. 49).

Similar to PlyGBS, Pal and Cpl-1 appeared to be stable through plant development since no significant decrease in protein content could be detected in leaves of different age (Fig. 50).

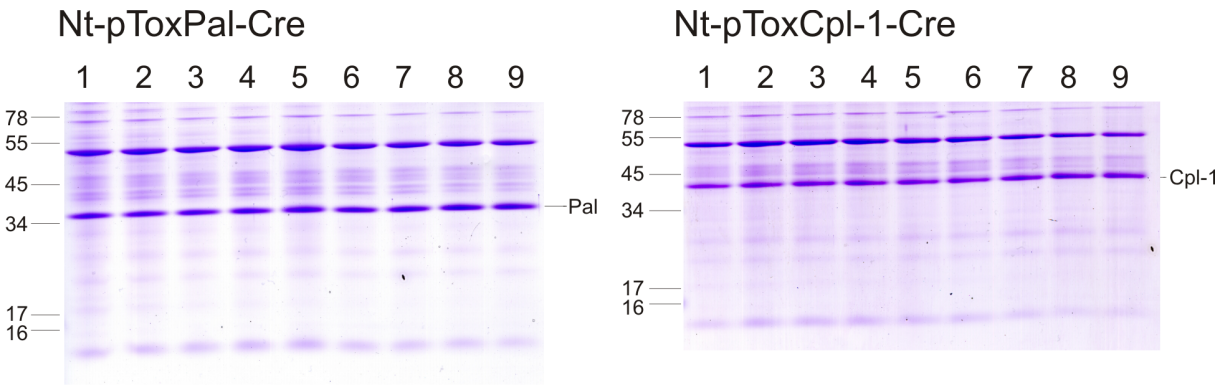

Fig. 50 Pal and Cpl-1 protein accumulation is independent of leaf age. Comparison of Pal and Cpl-1 in a developmental series of 9 leaves from the top to the bottom of Nt-pToxPal-Cre and Nt-pToxCpl-1-Cre plants, respectively. Foreign protein accumulation does not decline with leaf age, indicating that Pal and Cpl-1 protein levels are extremely stable in chloroplasts.

3.2.12 Protein quantification - recombined plants vs. pMO24

To check whether the presence or absence of a *loxP* site at the 5' end upstream of the T7 gene 10 leader has any effect on mRNA stability and/or protein accumulation, GFP expression of 4 week old homoplasmic *aadA*-free Nt-pToxGFP-Cre plants ("Nt-pToxGFP-Cre-selfed", T_2 generation) (2.6.2) and plants transformed with pMO24 (3.2.2) ("Nt-pMO24-selfed", T_1 generation) was studied using fluorescence microscopy. Homoplasmy of Nt-pMO24 plants was confirmed by Yvonne Weber (Max Planck Institute of Molecular Plant Physiology, Golm, Germany) using a seed assay described in 2.7.2. Plants were not further characterized. Interestingly, the GFP fluorescence in Nt-pToxGFP-Cre-selfed leaves appeared to be higher than in Nt-pMO24-selfed leaves, as shown in Fig. 51.

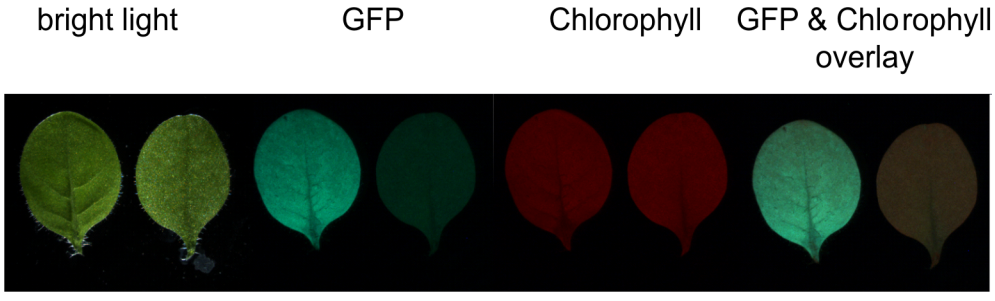

Fig. 51 Microscopy studies of Nt-pMO24 and maker-free Nt-pToxGFP-Cre plant leaves. Leaves obtained from 4 week old Nt-pToxGFP-Cre-selfed (left) and Nt-pMO24-selfed plants (right) are shown using bright field as well as fluorescence microscopy at the appropriate wavelengths for GFP and chlorophyll fluorescence as indicated above.

To compare GFP protein accumulation, a Western blot was performed using total soluble protein extracted from pooled leaves from Nt-pMO24-selfed and Nt-pToxGFP-Cre-selfed plants. Immunodetection of GFP protein confirmed 3-4 times higher GFP accumulation within the Nt-pToxGFP-Cre-selfed compared to the Nt-pMO24-selfed plants (Fig. 52).
From the Western blot shown in 3.2.10.1 a GFP content of about 1-2% of TSP was estimated for the Nt-pMO24-selfed plants.
These results led to the assumption that higher fluorescence due to higher GFP accumulation may result from increased *gfp* mRNA accumulation since the hairpin structure of the *loxP* site shows potential transcript stabilizing properties. However, other reasons, such as orientation of the open reading frame have not yet been excluded.

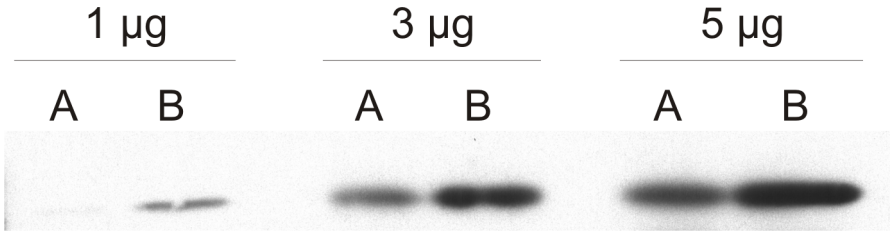

Fig. 52 Western blot comparing GFP protein accumulation of Nt-pMO24-selfed (A) and Nt-pToxGFP-Cre-selfed (B) plants. Loaded amounts of total soluble protein are indicated above.

4 Discussion

The increasing incidence of bacterial resistance against common antibiotics causes concomitant problems in the treatment of bacterial generated diseases. Hence it is very important to discover and establish new antimicrobial drugs. In addition to high effectiveness, new antimicrobial drugs should be easily producible in terms of cost efficiency, easy handling, low number of necessary purification steps and easy up-scaling. Furthermore, exclusion of resistance development against new antimicrobial drugs is crucial. As shown from production in bacteria, phage lytic enzymes may offer a useful alternative to commonly used antibiotics since they have the potential to efficiently kill their target bacteria. Lysins show advantages, such as highly efficient bactericidal activity regardless of bacterial sensitivity to antibiotics. Additionally, due to their mode of action, lysins have very narrow target spectra avoiding the disturbance of the natural bacterial flora. However, it has been found already that lysins may be toxic to bacteria (Sheehan et al., 1997) and thus expression in bacterial cultures, which requires fermenter systems, is relatively cost intensive and not easy to handle (Kusnadi et al., 1997).

The increasing importance of plants as a production platform for pharmaceuticals is mainly based on their advantages, such as easy handling, low production costs and the capability to express large amounts of foreign protein (McBride et al., 1995; Ye et al., 2001; Tregoning et al., 2003; Zhou et al., 2008). Additionally, they also may show an alternative platform for the expression of proteins which are toxic for bacteria (e.g. Pal (3.2.1). Chloroplasts provide a prokaryotic expression system and a huge genome copy number which can provide a high number of transgene copies after transformation. They also offer a high safety standard for transgene containment due to their maternal inheritance. The transformation strategy is easy and allows precise integration of the transgene into the plastome. Taking into account these features, chloroplasts theoretically provide a perfect expression system for the production of phage lytic enzymes. In summary, production of phage lytic enzymes in plant chloroplasts would meet all requirements for an attractive alternative to existing antibiotics.

Three candidates were chosen to be investigated in the present study: Pal and Cpl-1 are lytic enzymes that attack *Streptococcus pneumoniae*, whereas PlyGBS attacks group A and B streptococci. Group A streptococci and *S. pneumoniae* belong to the ten pathogens causing the highest morbidity and mortality rates world wide (Carapetis et al., 2005) and already a huge number of these strains show antibiotic resistance (Henning et al., 1997). In this work,

the capability of chloroplasts to produce active phage lytic enzymes (PlyGBS, Pal and Cpl-1) was investigated.

4.1 Expression in Escherichia coli

Since the aim of this thesis was to express the phage lytic enzymes in the tobacco chloroplast, *plyGBS*, *pal* and *cpl-1* genes were adjusted to the codon usage preferred by chloroplasts and cloned into a chloroplast expression cassette. This cassette harboured the promoter P*rrn,* which due to the eubacterial ancestry of chloroplasts, is also active in *E. coli*. Whereas *plyGBS* containing plasmids could be easily obtained, no *E. coli* colony could be found with the correct expression cassette containing the *pal* or *cpl-1* genes (3.2.1). Sequencing analysis revealed that several sequence modifications or deletions had occurred which prevented proper expression of the protein and suggested that, when expressed in the cell, Pal and Cpl-1 are toxic to *E. coli* (Fig. 27). Interestingly, this effect has been observed before by Sheehan et al. (1997), who were also not able to clone the *pal* gene and also observed sequence deletions within the plasmids. However, DNA amplification in *E. coli* cells is necessary for the transformation of foreign genes inside chloroplasts. Since the strongest known promoter in chloroplasts is the P*rrn* promoter a system had to be found that is inactive in *E. coli* cells, to avoid expression of the toxic proteins in bacteria, but allows high foreign protein expression in chloroplasts.

One possibility would be the usage of bacteria as provided by Lucigen® cooperation (Middleton, Wisconsin, USA) which are optimized for protein overexpression and can be used to express toxic proteins. However, these bacteria are not optimized for cloning and thus, presence of endonucleases, possible recombination activity and low transformation rate make them inappropriate for DNA amplification.

Furthermore, several strategies have been used to control expression of toxic proteins in bacteria. The most common system for toxic protein expression in bacteria is the isopropylthio-beta-D-galactoside (IPTG) inducible promoter system (Jacob and Monod, 1961; Donovan et al., 1996; Sheehan et al., 1997; Hansen et al., 1998), which allows the cultivation of transformed bacterial cells and the induction of foreign protein production after addition of IPTG. In this system a repressor protein is expressed that binds to the operator sequence within the promoter of the regulated gene and thereby should prevent its transcription (Jacob and Monod, 1961). Once IPTG is present it binds to the repressor protein and prevents its binding to the promoter allowing transcription of the controlled gene to occur. The IPTG inducible promoter system meets the requirements regarding protein expression suppression

in bacteria and is also a known system for inducible gene expression in chloroplasts (Muhlbauer and Koop, 2005). However, while expression induction in chloroplasts resulted in a 20-fold increase (from 0.05% to 1% of total soluble protein) in this case, the final foreign protein content did not exceed 1% of total soluble protein, which is far too low for commercial purposes.

A second known system for induced foreign protein production in chloroplasts which avoids protein expression in *E. coli* cells, is based on the usage of a promoter that is recognized by a bacteriophage T7 RNA polymerase (Magee et al., 2004; Lossl et al., 2005). The promoter is not active in *E. coli* cells and thus, no toxic protein is produced. In chloroplasts transcription is induced by the expression of a nuclear encoded T7 RNA polymerase that is subsequently targeted to the chloroplast. However, this system had not yet been shown to be appropriate to express high amounts of foreign protein. A major drawback is that T7 RNA polymerase mediated transcription can cause disruption of plastid gene expression and thus, causes a pale green mutant phenotype (Magee et al., 2007).

Since both previously presented strategies rely on transcription induction, it cannot be excluded that toxic protein is produced nevertheless, due to promoter leakage (McKinney et al., 2001; Uicker et al., 2007), read-through transcription from an upstream located promoter (e.g. from a resistance gene) or cryptic promoters in the plasmid backbone sequence (Jechlinger et al., 2004; Guo et al., 2007).

Thus, to circumvent the previously mentioned problems, a shuttle vector (pTox) was constructed that was based on transcription suppression of the genes encoding toxic proteins rather than an inducible system (3.2.2).

Therefore, the 3' end of the marker gene *aadA* was fused to a synthetically constructed transcription block consisting of an *E. coli* rho-factor-dependent terminator derived from the *cro* genes of phage λ (*rutA* and *rutB* box as well as *boxB* and two transcription stops) and an intrinsic *E. coli* terminator *rrnB T1*. Both terminators showed individual termination efficiencies in *E. coli* of 97.1% and >90%, respectively, and thus should represent efficient transcription terminators (Reynolds et al., 1992; Richardson and Richardson, 1996; Vieu and Rahmouni, 2004; Nojima et al., 2005).

The marker gene with a 5' UTR and the *E. coli* transcription block was flanked by two directly orientated *loxP* sites facilitating later excision of the *aadA* marker gene and the transcription block. Further downstream of the transcription block and the second *loxP* site, the gene of interest was fused to a 5' UTR known to enhance translation (leader sequence of the phage T7 gene 10) and a plastid 3' UTR taken from the tobacco gene *psbA*. The complete

construct was fused to the tobacco plastid rRNA operon promoter P*rrn* and flanked by chloroplast homologous regions to allow integration into the chloroplast genome. In theory, in *E. coli* the mRNA of the *aadA* gene should be produced until transcription is terminated at the combined *E. coli* terminator and thus, no putative toxic gene, here the gene of interest, should be expressed. After insertion of the construct into the chloroplast genome via homologous recombination, elimination of the *aadA* marker gene as well as the *E. coli* transcription block using the CRE-lox recombination system allows smooth expression of the gene of interest.
An overview of the theoretical functionality of the toxin shuttle (pTox) is shown in Fig. 53.

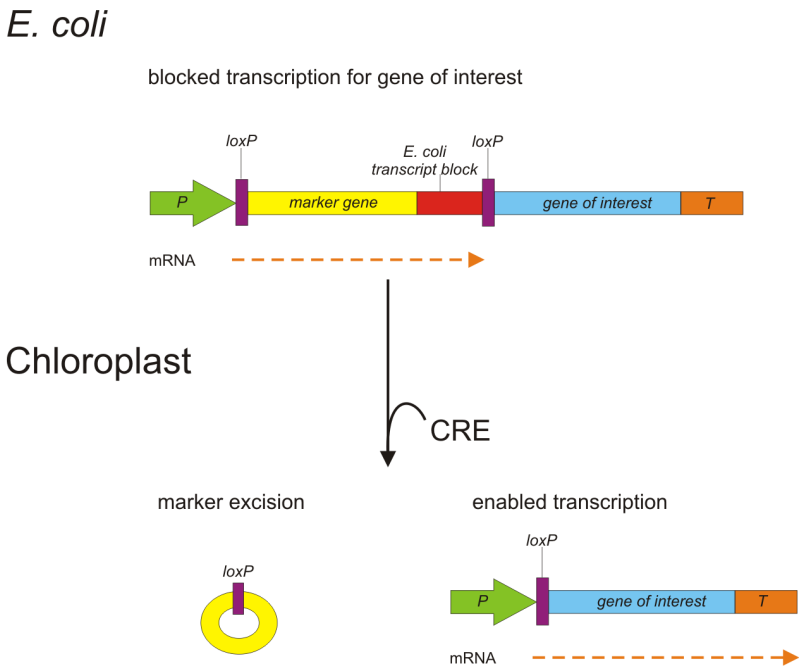

Fig. 53 Schematic structure and theoretical functionality of the toxin shuttle pTox in *E. coli* and chloroplasts. The marker gene fused to two strong *E. coli* terminators (*E. coli* transcription block) is flanked by two directly orientated *loxP* sites. In *E. coli* the strong transcription terminator allows only transcription of the marker gene. Transcripts are displayed by dashed lines. Once the pTox vector is transformed into chloroplasts, expression of a CRE recombinase leads to recombination between the two *loxP* sites resulting in marker gene elimination. Once the marker including the transcription block is removed, the second gene of interest can be transcribed. The chloroplast derived P*rrn* promoter (P) and the 3' UTR of *psbA* (T) are indicated.

In addition to the benefit of suppressed expression in bacteria and possible transcription restoration in chloroplasts, the system has the advantage that the strong P*rrn* promoter can be used and that marker gene deletion occurs concomitantly. Furthermore, inducible expression of the nuclear *Cre* gene would enable the system to be developed into an inducible chloroplast expression system.

Using *gfp* as a reporter gene, it could be shown that, when transformed into *E. coli* cells, the pTox vector (pToxGFP) was indeed able to drastically reduce the GFP expression in comparison to the pMO24 plasmid, which was used as control. As expected from the termination efficiency of both *E. coli* terminators in the transcription block, band intensities showed that the GFP that accumulates in the pToxGFP samples is less than 1% compared to GFP levels for pMO24 (Fig. 29). It is known that GFP protein is highly stable (Prasher et al., 1992; Kain et al., 1995) and accumulates in the cell even if the transcription level is low. Thus, given the large decrease in GFP protein level, as observed for the pToxGFP construct (100-fold), it was expected that *gfp* transcription level was suppressed to a greater extent in the pToxGFP samples and that *gfp* mRNA abundance is extremely low. With increasing amount of loaded total soluble protein, the differences between the two plasmids appear to be less severe, which is due to already saturated signals in the pMO24 samples. In summary, these results show that the toxin shuttle pTox can successfully be used to shuttle toxic genes into the chloroplasts with drastically decreased protein expression in the *E. coli* cell.

Since only indications for the toxicity of Pal and Cpl-1 had been reported, a co-cloning experiment was established to precisely show whether Pal and Cpl-1 are toxic to *E. coli* (3.2.4). As the pTox vector appeared to largely suppress expression of the gene of interest located downstream of the *E. coli* transcription block, the *pal* and *cpl-1* genes were cloned together with the non-toxic *gfp* gene in a 1:1 ratio into the pTox vector as well as into the pMO24 vector as a control. As expected from previous observations, almost 50% of all colonies derived from the transformation with the pTox vector carried *pal* or *cpl-1*, whereas no colonies carrying either *pal* or *cpl-1* with the pMO24 backbone could be identified (Tab. 3). Instead all colonies carried the non-toxic *gfp* gene. These results show that Pal and Cpl-1 indeed have a toxic effect on *E. coli* cells and that an inhibited transcription of *pal* and *cpl-1* allows DNA amplification, which is necessary for subsequent chloroplast transformation.

Although Pal and Cpl-1 are the best studied lytic enzymes and their binding sites as well as their cleavage substrate have been identified, the reason for their toxicity is unknown. The synthesis pathway of peptidoglycan may give possible explanations. The biochemical synthesis of peptidoglycan can be divided into three basic steps. The first step takes place in the bacterial cytosol and includes the formation of two nucleotide sugar-linked precursors, UDP-N-acetylmuramyl-pentapeptide (UDP-MurNAc-pentapeptide) and UDP-N-acetyl-glucosamine (UDP-GlcNAc) (Scheffers and Pinho, 2005). Pal, which is an N-acetyl-muramoyl-L-alanine amidase, cleaves the bond between the muramic acid and the first amino

acid in the pentapeptide (L-alanine). Based on this fact it is possible that Pal attacks the peptidoglycan precursor UDP-MurNAc-pentapeptide in the cell and thus inhibits proper cell wall formation. In a second step of peptidoglycan biosynthesis, which is located at the cytosolic membrane, the UDP-MurNAc-pentapeptide precursor is bound to the membrane acceptor bactoprenol to form a lipid intermediate. Subsequently, GlcNAc from UDP-GlcNAc is linked to the MurNAc-intermediate resulting in GlcNAc-β-(1,4)-MurNAc-(pentapeptide)-pyrophosphoryl-undecaprenol. To speculate about the possible reason for the toxic effect of Cpl-1, it is important to know that Cpl-1 is a lysozyme and thus cleaves the β-(1,4) glycosidic bond between MurNAc and GlcNAc. The last step forming this target glycosidic bond, the transglycosylation, is located at the outer side of the cytosolic membrane and thus should not be accessible to Cpl-1 mediated cleavage. Nevertheless, it has been shown that Cpl-1 is able to interact with the precursor and thus, may prevent proper translocation of the precursor and subsequent cell wall synthesis (Perez-Dorado et al., 2007).

In contrast to Pal and Cpl-1, PlyGBS did not show any toxic effects when expressed in the *E. coli* cells, although the catalytic domain of PlyGBS showed 27% identity to the catalytic domain of Ply187, an *N*-acetylmuramoyl-L-alanine amidase and 46% identity with the catalytic domain of Cpl-1 (Cheng et al., 2005). Thus, an effect of PlyGBS expression on the peptidoglycan precursors may have been expected. However, the lack of knowledge about the precise cleavage site of PlyGBS within the peptidoglycan does not allow further speculation regarding the putative effects of PlyGBS in comparison to Pal and Cpl-1.

4.2 Molecular Analysis

4.2.1 Molecular analyses of transplastomic plants

4.2.1.1 Genome analysis

In the course of the project, chloroplast transformants for *pal*, *cpl-1* and *plyGBS* were obtained and characterized in detail. Precise information regarding successful integration of the transgenes via homologous recombination was presented by RFLP analysis shown in Fig. 15 for PlyGBS and Fig. 41 for Pal, Cpl-1 and GFP, whose transformation was performed using the transformation vector pTox.

With respect to the utilized restriction enzymes, the obtained Southern blots showed fragment sizes that were expected for wild type and transplastomic plants and which exactly corresponded to the fragment sizes expected for successful integration of the transgenes. Pal,

Cpl-1 and GFP expressing plants derived from pollination with nuclear CRE expressing plants showed a smaller fragment exactly corresponding to the size expected after *aadA* deletion (Fig. 30). Corneille et al. (2001) described the CRE expressing plants (Nt-Cre2-200), which were used in this work for pollination, as plants with weak CRE activity that only showed complete CRE-mediated deletion if excision was advantageous (e.g. removal of a toxic gene). However, in the present study complete elimination of the *aadA* gene was observed. In addition, no recombination events were detected, as reported for protocols such as introduction of CRE by *Agrobacterium* transformation (Corneille et al., 2003; Lutz et al., 2006), supporting the selection of the more laborious pollination protocol. These results confirmed that CRE-mediated deletion in the chloroplast genome is a useful tool as previously shown (Corneille et al., 2001). Combined with this approach, the use of pTox as a transformation vector may offer the additional benefit of harbouring only a single promoter and terminator for the expression of two transgenes, since it has been shown previously that the introduction of plastid sequences (e.g. promoters, UTRs) could lead to homologous recombination events within the plastome (Rogalski et al., 2006).

As expected from previous data, a faint wild type-like signal could be observed (Fig. 15, Fig. 41), which presumably resulted from known nuclear copies of the chloroplast target sequence (Ayliffe and Timmis, 1992). The ~ 200 bp long mitochondrial sequence, which is homologous to a part of the *psaB* probe (as identified by alignment of ptDNA and mtDNA), could be excluded as the origin of the signal. The fragments derived from mitochondrial DNA digested with *Bam*HI or *Hinc*II would give ~ 11 kb and ~ 3.4 kb fragments, respectively, which are much larger fragments compared to the observed wild type-like signals. Nevertheless, a homoplasmic status of the plant cannot be predicated exclusively by Southern blot. Although comparisons of the band intensities can provide some preliminary indications regarding the homoplasmic and heteroplasmic status, it cannot be fully excluded that residual wild type copies of the plastome are present in the plant.

Since chloroplasts are maternally inherited in tobacco plants (Bock, 2007; Ruf et al., 2007), a seed assay could be performed to confirm homoplasmy of the mother plant. Therefore, seeds were germinated on spectinomycin containing medium. Compared to numbers in a mesophyll cell, less plastome copies are inherited in each seed (Stephanie Ruf, Max Planck Institute of Molecular Plant Physiology, Golm, Germany, personal communication), and thus, screening seedling coloration on antibiotic containing medium gives a precise resolution of the plastome composition of the mother plant. With this, reliable evidence for homoplasmy can be obtained since seeds harbouring the *aadA* marker gene appear green, whereas seeds containing wild

type plastome copies bleach out and cease to grow. However, all tested plants (Nt-pMO16, Nt-pToxPal, Nt-pToxCpl-1 and Nt-pToxGFP) showed homoplasmy in the seed assays (Fig. 16, Fig. 42) and thus, confirmed the data obtained by Southern blots (Fig. 15, Fig. 41). Interestingly, seedlings derived from Nt-pMO16 plants showed a pale green phenotype. Since no unexpected bands were seen in the Southern blot, plastome rearrangements as a possible reason for this could be excluded. It was assumed that the expression of PlyGBS may impose a large burden on the plant, since it was previously observed that high protein expression of proteins, even those known to be non-toxic such as GUS, led to the generation of pale green plants (Herz et al., 2005).

A seed assay was also used for the identification of CRE-mediated recombination events as described in Lutz et al. (2006). The seedlings derived from crosses with nuclear CRE expressing plants showed a mottled phenotype when germinated on spectinomycin containing medium (Fig. 36). It could be shown that the mottled phenotype was due to incomplete recombination and thus, to translation inhibition due to *aadA* deletion in the white sectors and *aadA* mediated resistance within the green sectors. Since the *Agrobacterium* mannopine synthase promoter, which is driving CRE expression, seems to increase in activity during leaf development (Langridge et al., 1989), it was assumed that CRE expression did not take place early enough in seedling development to cause complete recombination. Nevertheless, constitutive expression of CRE and consecutive recombination should result in marker-free plants, which was indeed shown to be the case by Southern blot and seed assays (Fig. 41, Fig. 42).

4.3 Protein expression and biological activity

4.3.1 Transcription, translation and stability of lysins in plants

4.3.1.1 PlyGBS expression

In chloroplasts, gene expression is mainly regulated at posttranscriptional levels. It is well established that mRNA accumulation, stability and processing are important for foreign protein expression (Bollenbach et al., 2007). It was shown that Nt-pMO16 transplastomic plants expressed high amounts of *plyGBS* mRNA (Fig. 17) indicating that the fused transcript-stabilizing elements (5' and 3' UTRs) stabilize the mRNA and allow accumulation. As expected from previous studies where endogenous 3' UTRs were shown to be unable to facilitate termination efficiently (Stern and Gruissem, 1987), an additional longer transcript

caused by read-through transcription could be detected. In contrast, the detection of *rbcL* mRNA showed that only one transcript with the expected size of 1.6 kb was expressed as described in Monde et al. (2000), where no read-through transcription could be detected from the *accD* gene, which is located downstream of the *rbcL* gene. When comparing the mRNA levels of *rbcL* from the wild type and transplastomic plants, the proportion of *rbcL* in all plants was found to be similar (Fig.18) since for all samples same amounts of RNA was loaded. However, it was noticed that from transplastomic plants slightly less total RNA could be obtained compared to wild type plants from the same amounts of leaf material, although this observation was not further analyzed regarding significance and reproducibility.

The subsequent step in chloroplast gene expression, translation, is a complex process regulated by a multitude of different strategies. To determine expressed protein amounts, total soluble protein from transplastomic plants was extracted and analyzed via SDS-PAGE for the presence of foreign protein bands (Fig. 19), which were then used to confirm the presence of the desired protein by mass spectrometry. For PlyGBS, a prominent band at the expected size could be identified. Quantification measurements revealed that PlyGBS accumulated to more than 70% of total soluble protein (73.% ± 3.3%), which is the highest amount of foreign protein accumulation obtained from stable plant (chloroplast) transformation so far described (Fig. 20) (De Cosa et al., 2001). Interestingly, only low amounts of the Rubisco large subunit could be detected in the transplastomic lines indicating that the high accumulation of PlyGBS was accompanied by a sharp decrease in plastid-encoded proteins.

It could be reasoned that the observed decrease in the amount of total RNA may explain the decrease in RbcL accumulation in the transplastomic lines. However, there are reasons arguing against this hypothesis. First, RbcL translation rate is dependent on the nuclear expression rate and assembly with the small nuclear encoded subunit (Wostrikoff and Stern, 2007). Since *rbcL* mRNA is chloroplast encoded and plastids possess an abundance of gene copy numbers, of which most if not all are transcriptionally active (Eberhard et al., 2002), *rbcL* mRNA in any event is overrepresented in comparison to protein content. In addition to this, analyses performed with *C. reinhardtii* showed that a reduction in plastome copy number, and, more precisely, *rbcL* transcript decreases to 24% of normal levels did not show any effect on protein accumulation (Eberhard et al., 2002). Taken together, it can be assumed that a decrease in *rbcL* mRNA will not lead to a proportional decrease in RbcL accumulation and thus, translational rather than transcriptional reasons are responsible for the decline in chloroplast protein expression.

Presumably, the decrease in Rubisco content indicates an overall decrease in chloroplast encoded proteins, which in turns leads to impaired photosynthesis and assimilation rates. Regarding this, the appearance of a certain phenotype was expected. A phenotype usually gives a good visible indication of how a plant responds to genetic or environmental changes. In the case of Nt-pMO16 plants, a pale green phenotype as well as retarded growth could be observed (Fig. 21). Previous studies have already shown that a decrease in Rubisco content (as shown in Fig. 19 and Fig 20) to 30% of normal level caused growth retardation and a pale green phenotype of photoautotrophically grown plants, which increased in severity with further decreasing Rubisco contents (Rodermel et al., 1988; Hudson et al., 1992; Kanevski and Maliga, 1994; Marc Aurel Schöttler, Max Planck Institute of Molecular Plant Physiology, Golm, Germany, personal communication).

In terms of foreign protein expression, plants sometimes show a pale green phenotype (Magee et al., 2004; Glenz et al., 2006) indicating that protein production can display an enormous burden to the plant. However, it was assumed in these cases that toxic effects of the protein were the reason for the phenotype since in other cases even higher protein accumulation was observed without development of a pale green phenotype (De Cosa et al., 2001; Kuroda and Maliga, 2001). Supporting this hypothesis, nuclear expression of a protein that causes a pale green phenotype when expressed in the chloroplasts, with subsequent chloroplast import did not show the development of a chlorotic phenotype, probably due to lower toxic protein concentrations (Teodoro Cardi, personal communication).

In the present study, with respect to the high amount of PlyGBS quantified by Coomassie staining (Fig. 19, Fig. 20), it was assumed that exhausted translation capacity rather than toxicity was the reason for the phenotype.

It is possible that the protein itself or more precisely its composition is responsible for the exhaustion of translation capacity. Factors necessary for translation e.g. tRNAs or certain amino acids, may become limiting for proper chloroplast protein synthesis. It is often the case that rarely used tRNAs are required for foreign protein expression and hence, these tRNAs can become limiting. However, in the work presented here the coding sequence of the foreign genes was adjusted to the codon usage preferred by chloroplasts and thus, to frequently used tRNAs. Nevertheless, it is possible that, even if a tRNA pool is sufficient for the production of chloroplast proteins, it can become limiting especially if the foreign protein is expressed in high amounts like PlyGBS. This hypothesis is supported by the fact that some plastid-encoded tRNAs can become limiting when *de novo* synthesis of large quantities of photosynthesis proteins are required (Kanamaru and Tanaka, 2004). Comparison of plastome-encoded tRNA

levels (Kerstin Petersen, Max Planck Institute of Molecular Plant Physiology, Golm, Germany) with the frequencies of the codons in the three lysin genes showed that tRNAs of low abundance, such as those for serine or proline are often used in the lysin genes. Thus, the tRNA abundance may be sufficient for plastid proteins but become limiting when used more frequently for foreign protein expression. Additionally, when comparing the amino acid frequency in chloroplast proteins to the amino acid frequency in the lytic enzymes, it was indeed found that some amino acids e.g. Ala, Asn, Asp, Trp and Tyr appeared more frequently in the lysins. In bacteria, it has also been observed that in the case of protein expression with a prevalent usage of one amino acid, e.g. His-tag, that this amino acid can become limiting (Stefan Kempa, Max Planck Institute of Molecular Plant Physiology, Golm, Germany, personal communication). An additional fact supporting this hypothesis is the rescue of the reduced growth of Nt-pMO16 plants by grafting onto a wild type stock, which then presumably compensates the deficiency of the PlyGBS expressing plants and thereby, rescues growth rate and seed development (Fischer et al., 1998; Lalonde et al., 2003) (Fig. 22).

Since grafting is not suitable for large-scale biomass production, it may be possible to rescue the phenotype by reducing foreign protein expression (Allison and Maliga, 1995; Eibl et al., 1999; Herz et al., 2005). However, it is unclear whether high protein yield from slowly growing plants or decreased protein expression from normal developing plants is more fruitful.

Since foreign protein expression to up to the level reported here has not been previously described, it was assumed that exhaustion of translation capacity rather than toxicity may be a reason for the observed phenotype. However, possible toxic effects of the protein as shown for a recombinant lipophilic protein, which localizes to the thylakoid membrane and thus impairs photosynthesis (Hennig et al., 2007), cannot fully be excluded and have to be examined in further detail.

4.3.1.2 Pal, Cpl-1 and GFP expression

Since the pTox vector in bacteria efficiently inhibited expression of a gene of interest downstream of the transcription block, it was of great interest to determine transcription of *pal* and *cpl-1* in chloroplasts.

Analyses of *gfp* and *pal* mRNAs extracted from Nt-pTox plants revealed a slight accumulation of mRNA corresponding to the size of the dicistronic mRNA containing *aadA* and the gene of interest (Fig. 43). In comparison to the high *aadA* transcript accumulation

detected in Fig. 44, *gfp* and *pal* mRNA content appeared to be drastically reduced. This was indicated by the low amounts of read-through transcript corresponding exactly to the size and the amount of the dicistronic mRNA seen in Fig. 43. Although it is not clear whether the *E. coli* block has any function in chloroplasts, these results indicate that, in chloroplasts, the *E. coli* transcriptional block also led to decreased transcript accumulation of a downstream located gene. However, it is not known whether the *E. coli* transcription block indeed functions as a transcription terminator, since in chloroplasts, 3' termini can be formed either by direct termination or by nucleolytic activity (Stern and Kindle, 1993).

First, the *E. coli* terminator block, displaying several inverted repeats forming hairpin structures, could serve as a processing site and stabilizing structure as known from inverted repeats located in the 3' UTR of chloroplast genes. In this case, the downstream mRNA is degraded and the *E. coli* block prevents further 3' to 5' exonucleolytic activity (Stern and Gruissem, 1987; Rott et al., 1996; Monde et al., 2000). This functionality is possible, because for most inverted repeats located in plastid 3' UTRs this mode of action is known. It has been reported that 3' UTR maturation is a two step reaction, where endonucleolytic cleavage takes place first with subsequent 3' to 5' exonucleolytic mRNA degradation. The downstream product is highly unstable and cannot be detected (Rott et al., 1996; Hicks et al., 2002). Given that read-through transcript can be detected it is assumed that endonucleolytic cleavage is the limiting step (Monde et al., 2000), leaving visible amounts of uncleaved mRNA.

A second possible function of the *E. coli* block is indeed transcription termination. Although *in vivo* and *in vitro* approaches have shown that many chloroplast 3' UTRs with inverted repeats are incapable of terminating transcription efficiently (Monde et al., 2000; Hicks et al., 2002), some examples, such as *petD*, show efficient inverted repeat mediated transcription termination. It was found that in cases of efficient termination the inverted repeat was followed by a uridine-rich region, similar to *E. coli* intrinsic terminators (Platt, 1986; Stern and Gruissem, 1987). Since the *E. coli* block is composed of the *E. coli tR1* rho-dependent terminator (Richardson and Richardson, 1996; Vieu and Rahmouni, 2004) consisting of 2 stem-loop structures with subsequent uridine-rich regions (t1 and t2) known to serve as termination sites in *E. coli*, followed by the *E. coli* rho-independent terminator *rrnB* T1 (Reynolds et al., 1992; Nojima et al., 2005) with one hairpin structure, it is possible that this combination can indeed lead to substantial levels of transcription termination. However, the exact mechanism of how the *E. coli* transcription block prevents accumulation of the mRNA of the downstream gene is not known.

As expected from these results, the deletion of the *aadA* marker gene and the *E. coli* transcription block in Nt-pTox-Cre plants led to a drastic increase of mature *gfp* and *pal* mRNA, indicating that the *E. coli* block indeed suppressed mRNA accumulation of downstream genes.

In contrast to these results obtained from *gfp* and *pal* containing transformants, *cpl-1* mRNA accumulated to comparable amounts as *pal* and *gfp* within the Nt-pTobCpl-1 plants, but did not, as expected, significantly increase in Nt-pToxCpl-1-Cre plants. Instead, additional bands approximately 500 bp smaller than the dicistronic mRNA in the Nt-pToxCpl-1 (1.7 kb) and the mature mRNA in the Nt-pToxCpl-1-Cre plants (0.8 kb) could be detected (Fig.43). Sequence analysis using the Software Mfold version 3.2 (Mathews et al., 1999; Zuker, 2003) revealed a potential hairpin structure around 650 bp downstream of the start codon, as seen in Fig. 54.

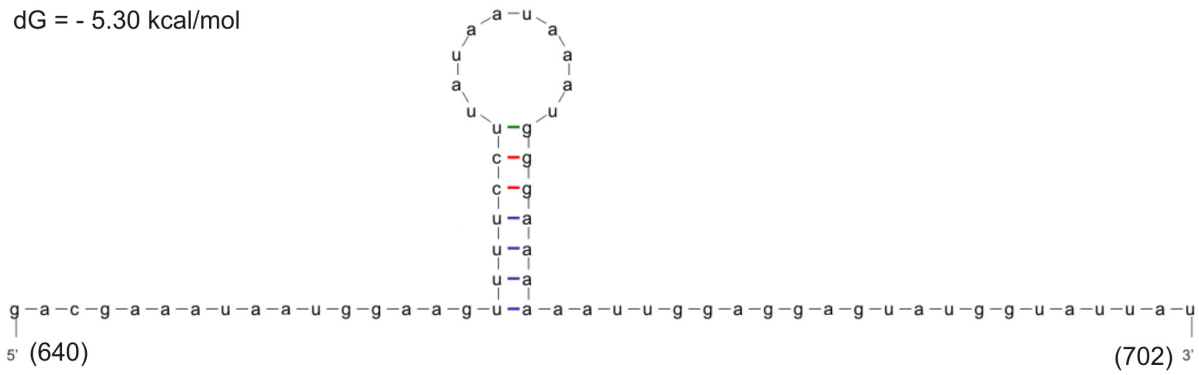

Fig. 54 RNA hairpin structure in the coding region of *cpl-1*. The sequence section displayed is indicated by base pairs counted from the start codon. Free enthalpy of the hairpin structure is indicated above.

It is known that the mRNA degradation machinery uses hairpin structures for targeted processing within the untranslated regions (Zhou et al., 2007). Although the effect of hairpin structures within coding regions is unclear, it is possible that in the case of *cpl-1* the stem-loop structure within the mRNA displayed a cryptic target structure non-specifically recognized for mRNA processing and degradation. Although, in general, the amount of non-specifically processed mRNA should be comparable in Nt-pToxCpl-1 and Nt-pToxCpl-1-Cre plants, the probability of *cpl-1* mRNA to be a target of this non-specific degradation would increase with the increasing number of *cpl-1* mRNA molecules after *E. coli* block deletion. It is possible that the increased amount of mRNA due to the transcription block deletion would

lead to an increased protein accumulation surpassing a threshold for harmful amounts of a foreign protein, in terms of exhausting the capacities to produce proteins needed for photosynthesis. Impaired photosynthesis could cause oxidative stress which, in turn, may increase mRNA degradation (Salvador et al., 1993; Salvador and Klein, 1999). Thus, the theoretical increase in *cpl-1* mRNA in the Nt-pToxCpl-1-Cre plants could have been masked by an increased probability to be a target of non-specific processing at the stem-loop structure within the coding region. In that case, it is possible that non-specific degradation and increased mRNA accumulation are balanced and, therefore, *cpl-1* mRNA contents do not differ from Nt-pToxCpl-1 plants. Whether *cpl-1* mRNA is indeed processed or 3' to 5' degraded can probably be shown by Northern blotting using large amounts of RNA to detect intermediates. However, reasons for the lack of an increase in *cpl-1* mRNA levels in the Nt-pToxCpl-1-Cre plants (as expected from the *gfp* and *pal* results) are only speculative without further investigations.

Since it is not clear how frequent stem-loop structures appear within the coding region of a gene and neither *pal* nor *plyGBS* mRNA showed any of these potential stem-loop structures, it may be possible that *plyGBS* mRNAs were not affected by increased mRNA degradation due to oxidative stress. Nevertheless, it is possible that decrease in total RNA levels in the PlyGBS expressing plants is due to increased RNA degradation caused by oxidative stress.

Protein expression data from transplastomic plants transformed with *pal* and *cpl-1*, respectively, showed that additional bands could be detected at the expected sizes for Pal (35 kDa) and Cpl-1 (40 kDa). These results indicated that the proteins accumulate to a high level (Fig. 47, Fig 48), although the protein accumulation was not as high as seen for PlyGBS. Likewise, GFP accumulation within Nt-pTox plants was detected (Fig. 45, Fig. 46).

In accordance with the phenotype of the Pal and Cpl-1 expressing Nt-pTox plants, the amount of Rubisco large subunit was comparable to wild type plants showing that the expression level of Pal and Cpl-1 did not affect protein expression in chloroplasts.

In comparison to Nt-pToxPal plants, Pal content increased 2-3 fold by CRE-mediated deletion of the *aadA* block in Nt-pToxPal-Cre plants. These results indicated that, in the case of Pal expression, transcript accumulation was indeed limiting since increased *pal* mRNA accumulation in Nt-pToxPal-Cre plants (Fig. 43) corresponded to an increase in protein amount. The same results could be seen in Nt-pToxGFP-Cre plants, whose *gfp* mRNA amount increased 4-5 fold, proportional to GFP protein accumulation, once the *aadA* block had been removed by recombination (Fig. 43, Fig. 46).

The content of Cpl-1 in Nt-pToxCpl-1 and Nt-pToxCpl-1-Cre plants was found to be similar, as expected from the *cpl-1* mRNA levels (Fig. 43). Interestingly, in contrast to Pal and GFP expressing plants, the content of small Rubisco subunit decreased in the Nt-pToxCpl-1-Cre plants, although no phenotype could be seen. The small Rubisco subunit is proteolytically degraded once the large subunit of Rubisco is not present in adequate proportion for assembly (Schmidt and Mishkind, 1983; Kanevski and Maliga, 1994). It was therefore assumed that, as previously mentioned, the total chloroplast protein expression rate was decreased, as indicated by the lower RbcL content. Furthermore, it is possible that Cpl-1 expression in Nt-pToxCpl-1 plants was already at the highest level possible for this protein. An increase of *cpl-1* mRNA, caused by the deletion of the *aadA* block (as expected from *pal* and *gfp* data), could lead to a harmful amount of Cpl-1 expression or an exhaustion of the chloroplast translation capacity. In both cases, a decrease in RbcL could cause stress and increased mRNA degradation, which may have impeded further accumulation non-specifically. In contrast to Cpl-1, increased *pal* mRNA and protein expression did not lead to harmful protein accumulation levels or an exhaustion of expression capacity and thus, did not cause reduced chloroplast protein expression. Nevertheless, regarding these effects, it would be interesting to determine RbcL accumulation levels in Nt-pToxGFP-Cre plants, since GFP is known to be nontoxic for chloroplasts and the increase in protein accumulation due to transcript block deletion is even higher than that observed for Pal.

4.3.1.3 Lysin stability in plants

As shown in Fig. 23 and Fig. 50, all three lytic enzymes appeared to be very stable within the chloroplast and could even be found in older leaves where it had been previously demonstrated that protein expression capacity usually decreases (Daniell et al., 2001; Birch-Machin et al., 2004; Zhou et al., 2008). However, these results were not surprising. Chloroplasts possess prokaryotic-like proteolytic machinery (Adam 2006, Adam 2007) and since lytic enzymes have been optimized over evolution to resist proteolytic degradation by their host bacterium, it was expected that they would be poor substrates for chloroplast proteases. It is possible that unknown stabilizing structures or sequences (e.g. protective N- or C-terminal sequences) or a lack of a motif or motifs recognised by proteases causes this high stability and accumulation. It would be of great interest to identify the structures or motifs conferring this stability and in case they can be localized to small regions at the termini, it may be possible to use this knowledge to stabilize proteins which are currently difficult to express in chloroplasts (Birch-Machin et al., 2004; Bellucci et al., 2005).

4.3.1.4 Putative expression-enhancing structures

The observation of increased GFP accumulation in the Nt-pToxGFP-Cre plants raised the question whether this protein accumulation is comparable to GFP accumulation from the expression cassette used for PlyGBS (*gfp* carrying construct pMO24; Fig 28). Surprisingly, the accumulation of GFP in the leaves of plants which formerly carried an *aadA* block (Nt-pToxGFP-Cre) was 3-4 times higher (~10% TSP) compared to Nt-pMO24 plants (Fig. 51, Fig. 52). As mentioned previously, foreign protein expression in chloroplasts is dependent on features of the 5' UTR as well as transcript stability. Although both constructs carried the same 5' UTR derived from the phage T7 gene 10 leader, there was a significant difference in that an additional 5' extension of the mRNA was present in Nt-pTox-Cre plants. After deletion of the *aadA* block, the remaining *loxP* site upstream of the T7 gene 10 leader, probably forming a hair pin structure, may serve as an additional transcript stabilizing feature and thus, increase *gfp* mRNA and protein accumulation. A Northern blot is necessary to show that increased mRNA accumulation is indeed responsible for the increased GFP accumulation observed by microscopy and Western blotting. However, there are other slight differences between the constructs (e.g. orientation of the open reading frames), and therefore other reasons for the increased accumulation cannot be fully excluded. To determine the effect of the 5' *loxP* site, new transformation vectors differing only in the presence or absence of a *loxP* site upstream of the T7 gene 10 leader are currently under construction.

4.3.2 Biological activity of plant derived lytic enzymes

Another important part of this work was the bacteriolytic activity of the expressed proteins, which was determined in cooperation with the Department of Medical Microbiology and Hospital Hygiene from the Hospital of Rostock University. Although the chloroplasts should provide a prokaryotic environment, it was not clear whether the proteins would show correct folding and assembly. PlyGBS is active as a monomer (Cheng et al., 2005), whereas Pal functions as a dimer (Varea et al., 2004), and differences in their activity due to incorrect folding or assembly are possible. The activity of lytic enzymes is usually measured in units with one unit (1 U) defined as the reciprocal of the highest dilution that decreases the optical density of a bacterial culture of OD_{600} 0.5 by 50% within 15 minutes (Loeffler et al., 2003). For Pal and Cpl-1, 1 U corresponds to the amount of 1 µg of bacteria-derived enzyme. More precisely, 1 U/ml of purified bacteria-derived Pal was capable of reducing a bacterial culture by 1.99 $\log_{10}$ CFU/ml in 10 min (Loeffler and Fischetti, 2003). For PlyGBS, precise

measurements of enzyme amounts corresponding to the activity of 1 U have not been described.

To determine the bacteriolytic activity of chloroplast-derived lytic enzymes, total soluble protein extracted from wild type and transplastomic plants was used. Pal and Cpl-1 were estimated to be 20% of TSP and PlyGBS to be 70% of TSP. Protein extracts from Pal and Cpl-1 expressing plants were additionally dialyzed to roughly purify the extract and remove bacterial growth-promoting compounds (e.g. sugars) which could be present in the protein extracts. It is known that glycerol stabilizes proteins (Gekko and Timasheff, 1981; Sawano et al., 1992) and, therefore, the solution was supplemented with glycerol to support Pal and Cpl-1 activity. The activity of all three lytic enzymes could be visualized by monitoring cell culture clearing caused by cell lysis (Loeffler et al., 2001; Loeffler and Fischetti, 2003). Whereas wild type protein samples did not affect the cell density, a dose and time-dependent decrease in optical density could be observed for samples with proteins derived from transplastomic plants (Fig. 24, Fig. 31). These data demonstrated the bacteriolytic activity of Pal and Cpl-1, of which 200 µg of total soluble protein was sufficient to decrease bacterial cell density to 50% after 30 min. PlyGBS containing total soluble protein showed a higher bacteriolytic activity, since 150 µg of total soluble protein showed nearly an almost complete clearance of the bacterial suspension after 30 min (Fig. 24). The dramatic decrease in cell density observed in all samples containing lytic enzymes within the first 15-30 min was followed by a plateau in the cell density (Fig. 24, Fig. 31). One possible reason for this reduction in the rate of decrease of the optical density could be that after 30 min most or all susceptible cells are lysed and that the residual optical density is caused by the remaining cell debris (Fig. 24). Another possible reason might be that the tight binding of the enzymes to their substrate, which is comparable to immunoglobulin molecules, which renders them single-use molecules and thus, higher amounts of enzymes may be required to efficiently lyse all bacterial cells within the culture (Lopez et al., 1997; Fischetti, 2006). Thus, it may simply be that not enough enzymes had been added to the bacterial suspension (Entenza et al., 2005). To test this possibility and to additionally show the synergistic effect of Pal and Cpl-1 due to their different target sites, higher protein concentrations and combinations of Pal and Cpl-1-containing total soluble protein extracts were analyzed (Fig. 32).

It could clearly be shown that the increased addition of Pal-containing protein (300 µl) indeed resulted in lower optical density after 30 min (compared to 200 µl of Pal-containing protein), which showed that in the previous experiment, not all bacterial cells could be lysed due to insufficient enzyme concentration.

Pal and Cpl-1 in combination (150 µg each) were able to lyse as much bacteria as double the amount of Pal alone (300 µg of Pal-containing protein extract) after 30 min (Fig.32). Although the synergistic effect of Pal and Cpl-1 could not clearly be demonstrated by this data, the plateau in optical density expected for the presence of residual cell debris, suggested that the lysis reaction in the samples with Pal and Cpl-1 combined was complete after 30 min. In contrast, samples with Pal alone still showed decrease in optical density between 30 and 60 min after lysine application. Thus, the synergistic effect may be demonstrated by selection of earlier time points.

Since Pal and Cpl-1 showed toxic effects when expressed in *E. coli* cells, the ability of Pal and Cpl-1 to clear *E. coli* cell culture was tested, to analyse possible non-specific activities (Fig. 33). As expected from previous observations (Loeffler et al., 2003), cell culture clearing could not be observed either in samples containing Pal and Cpl-1 or in wild type samples, indicating that the toxic effect of Pal and Cpl-1 must be due to intracellular reasons, as explained previously. Thus, the characteristic feature of high target specificity of lysins (Garcia et al., 1988; Lopez et al., 1992; Lopez et al., 1997) was also confirmed.

The examination of the bacteriolytic activities of PlyGBS, Pal and Cpl-1 was additionally confimed by testing the ability of the treated bacterial cultures to form colonies. This is a common technique to determine bacterial viability after lysin application (Loeffler and Fischetti, 2003). Immediately after determination of optical density, the colony forming units (CFU) decrease over a time frame of 60 min was determined.

As expected, the CFU decreased in a dose and time-dependent manner confirming the results obtained from the optical density measurements (Fig. 25 and Fig. 34). The highest amounts of lysin (300 µg of total soluble protein containing Pal and 150 µg of total soluble protein containing PlyGBS) were capable of lysing their target bacteria to such extents that less than 7.5% and 16% for Pal and PlyGBS, repectively, of the initial CFU were able to form colonies after 60 minutes. These residual bacteria that were still able to form colonies may be non-dividing cells at the time of lysin treatment, since it was shown that the lytic effect is more pronounced when treating dividing cells (Tuomanen and Tomasz, 1990; Loeffler et al., 2001). As mentioned before, an increase in lysin concentration or a repeated application should eliminate residual bacteria. A slight decrease in CFU could also be observed in the wild type samples and the buffer control indicating that transfer of bacteria from culture medium to pure buffer applies stress and slightly decreases bacterial viability.

A final confirmation of lysin activity was obtained by visualizing live and moribund cells with the aid of two DNA intercalating stains that differ in their ability to permeate cell

membranes (Fig. 26, Fig. 35). The applied SYTO®9 stain is able to permeate intact cell membranes and thus, stains living bacterial cells green. The second stain, propidium iodide, is able to only enter cells with disrupted cell membranes and thus displaces the green SYTO®9 stain and results in red fluorescence of dying cells. Phage lytic enzymes cleave the cell wall which leads to an exposure of the bacterial cell to osmotic pressure, resulting in the cell bursting. Activity of lysins therefore can be visualized by combining these two stains (Köller et al., 2008). Whereas fluorescence microscopy of wild type samples showed live, green fluorescing bacteria 30 min after protein application, samples with lysin treatment showed an increasing number of red fluorescing cells. As expected, the number of red fluorescing cells after lysin application depended on the amount of applied protein and the amount of time that had elapsed after treatment. Indeed, only 3 minutes post-application, the culture exposed to 50 µg of TSP containing PlyGBS still showed high amounts of living cells while the culture treated with 150 µg of TSP containing PlyGBS already showed a huge number of red dying cells. Similarly, after 30 minutes, 100 µg of applied TSP containing Pal showed residual green fluorescing bacteria, whereas an increase of lysin content (200 µg of Pal-containing protein) resulted in almost exclusively red fluorescing cells. As seen for PlyGBS-containing samples, the 200 µg Pal-containing sample resulted in an overall decrease in cell number, which is not surprising since completely lysed cells can no longer be stained.

Although Pal, Cpl-1 and PlyGBS containing total soluble protein extracts showed bacteriolytic activity, it is difficult to compare the protein activities with each other and with the activities known from bacterial-derived proteins for several reasons. Firstly, purification of PlyGBS appeared to be impossible, since when using the described purification protocol (Cheng et al., 2005), plant-derived PlyGBS could only be obtained with wild type protein contamination, and thus, precise protein content determination could not be performed. A second reason for limited comparability is the lack of precise concentration information of bacterial-derived PlyGBS used for activity tests, since the authors only described dilution rates of purified protein used for activity determination (Cheng et al., 2005). Additionally, the experimental setup impeded the determination of lysin content equal to 1 U since culture clearance was measured with a bacterial culture of higher density. The lack of purification and thus, the ability to precisely determine protein content for Pal and Cpl-1 made it impossible to compare their bacteriolytic activities.

Since colony forming units were only determined 30 min after lysin treatment, where 40 µg (20% of 200 µg TSP) Pal and Cpl-1 was applied and shown to reduce bacterial culture by 7.9 and 7.7 $\log_{10}$ CFU/ml respectively (Fig. 34), bacteria-derived proteins and plant-derived

proteins could not be compared, because it was not possible to calculate CFU data for a 10 min treatment as described in (Loeffler and Fischetti, 2003). However, it was revealed that bacteriolytic activity was higher for the same amount of TSP containing PlyGBS compared to Pal or Cpl-1 containing TSP. Despite that, when the level of foreign protein accumulation as a proportion of TSP is taken into account, it is likely that Pal has a higher activity compared to PlyGBS since the amount of PlyGBS in 150 µg TSP would be approximately 105 µg of pure protein compared to the amount of Pal in 300 µg TSP which would be approximately 60 µg.
Taken together, a precise comparison of plant-derived lytic enzymes with bacteria-derived proteins is only possible if activity tests can be performed with purified proteins under comparable conditions. However, several experiments have shown that chloroplast-derived PlyGBS, Pal and Cpl-1 were able to specifically lyse their target bacteria *S. pyogenes* and *S. pneumoniae.* Thus, chloroplasts are suitable bioreactors for lysin production.

4.4 Economic efficiency and applications of plant-derived lysins

From the present study, phage lytic enzymes appear to be very good candidates for foreign protein expression within chloroplasts. Although dependent on the specific protein, it was shown overall that high amounts of functional protein could be produced within plants. For example, Nt-pMO16 plants were able to produce approximately 4.5 g of PlyGBS per kg of fresh leaf material (≙ 70% of TSP). According to Watson et al. (2004) approximately 20 000 tobacco plants (*c.v. petit havana*) can be grown per hectare resulting in ~ 5.4 t of fresh material. Assuming that Nt-pMO16 plants with their reduced growth would only produce half that amount of fresh weight (2.7 t), the yield of PlyGBS from one hectare would be ~ 12.3 kg of PlyGBS. Switching to a commercial cultivar producing ~ 50 t of fresh weight (Watson et al., 2004) would give ~ 225 kg PlyGBS per hectare. This amount could even be doubled by increasing growth density to 250 000 plants with impaired growth per hectare producing ~ 125 t of fresh weight resulting in ~ 560 kg of PlyGBS (CropTech Incorporation, 2000 (http://www.who.int/tobacco/framework/public_hearings/F0290029.pdf). Unfortunately, no precise amounts of PlyGBS protein suitable for medical treatment are known and thus, only amounts used for the bacterial assays can be used as a basis for calculations. The estimated amount produced of 560 kg of PlyGBS would result in 5.60 billion doses of 100 µg of pure protein as was used in the described assays.
The expressed lytic enzymes possess the capability of active destruction of target bacteria and thus, show potential for medical application. Since activity assays in the present thesis were

done with crude protein extract, it was assumed that topical application of the total soluble protein solution as a spray or cream may be possible. However, toxic or allergic reactions have to be ruled out before such an application becomes feasible.

For intravenous application as shown to be possible from experiments done with Pal and Cpl-1 (Entenza et al., 2005), purification is absolutely necessary, but can simply be carried out by affinity chromatography (Jado et al., 2003). Of course, it has to be tested whether plant derived lysins can also be used for intravenous application, although it is assumed that the protein's features are the same as that for those that are bacteria-derived.

Another possible application form would be the expression in plant tissue that can be used as food (e.g. tomato fruits) (Ruf et al., 2001). Due to the close relationship between tobacco and tomato, conclusions can be drawn that expression in tomato fruits may be possible. Since it is known that translation and transcription are gradually down regulated during fruit ripening in red tomatoes (Kahlau and Bock, 2008), the usage of edible green tomatoes, which probably retain photosynthetically and translationally active chloroplasts may be an alternative.

4.5 Alternatives to conventional antibiotics

The increase in resistance mechanisms developed by bacteria against common antibiotics and the fact that only 3 new classes of antibiotics were developed in the last 40 years (Marr et al., 2006) make it necessary to find appropriate alternatives.

Three alternatives have been proposed to potentially replace commonly used antibiotics in medical application.

The first promising alternative involves the use of bacteriophages. Bacteriophages, as the most abundant entities on earth, show advantages such as high target specificity even to multi-drug resistant bacteria and thus, no interference with the normal host bacterial flora (Merril et al., 2003). Due to their high mutation rate they can easily adapt to phage-resistant bacteria. An interesting usage of phages as antibiotics has already been shown (Hagens and Blasi, 2003; Hagens et al., 2004), where phages were modified by replacing genes involved in phage extrusion with a restriction endonuclease resulting in the efficient cleavage of DNA within the bacterial host cell. Bacteriophages have been shown to be capable of treating diseases caused by gram-positive as well as gram-negative bacteria (Bull et al., 2002; Stone, 2002).

Additionally, the lower costs needed for development of phage therapy compared to the developmental costs for new antibiotics as well as the relatively rare side effects during therapy make them an attractive alternative to common antibiotics (Matsuzaki et al., 2005).

Despite these advantages, there are also several disadvantages associated with phages as proper antibiotic alternatives. The usage of intact phages for therapy rapidly causes immunological responses, mainly directed to the capsid proteins, which restrict application to oral, topical or singular intravenous application (Summers, 2001). Additionally, the ability of some phages to transfer toxic genes to formerly toxin-less bacteria is of great concern (Broudy and Fischetti, 2003). Furthermore, the conversion of a lytic phage into lysogenic prophages and thus, immunization of the host bacterium as well as modification of the cell-surface receptor recognized by the phage and acquisition of systems degrading the phage nucleic acids can cause failure of phage therapy (Skurnik and Strauch, 2006).

A second promising tool to fight diseases caused by antibiotic-resistant bacteria may be so-called antimicrobial peptides (AMP) or peptide antibiotics. Peptide antibiotics are small (less than 100 amino acids long) peptide molecules with antimicrobial activity encoded by specific genes (Bals, 2000). Peptide antibiotics have different modes of action. Whereas some AMPs, due to their amphiphatic character, are able to form pores and channels in the plasma membrane of the bacterial cell and thus, cause membrane perturbation and loss of cell content (Li et al., 2005; Lohner and Blondelle, 2005; Toke, 2005), others cause inhibition of cell wall biosynthesis (Breukink and de Kruijff, 2006; Hasper et al., 2006) and DNase or RNase activity (Zarivach et al., 2002; Vankemmelbeke et al., 2005). Although there are great advantages of peptide antibiotics, such as bactericidal activity against drug-resistant bacteria combined with broad target spectra including bacteria, fungi and viruses, the potency against sensitive target bacteria is not as high as for conventional antibiotics and thus AMPs are unlikely to fully replace current treatments (Marr et al., 2006). The development of an impermeable outer membrane or development of specific proteases could result in resistant bacteria, although only low levels of resistance development have been reported so far (Gordon et al., 2005; Marr et al., 2006). It has also been suggested that therapeutic administration of peptide antibiotics may promote resistance to peptides of the host innate immune system and thus, increase vulnerability of humans to diseases caused by peptide-resistant bacteria (Bell and Gouyon, 2003). Additionally, the development of peptide antibiotics appears to be difficult since most peptides, although possessing high *in vitro* activity, lose their activity under *in vivo* conditions (Marr et al., 2006). Restriction to topical application due to potential toxicity caused by interactions with membranes, instability and immunogenicity together with high developmental and manufacturing costs ($50 – 400 per gram) (Bals, 2000; Marr et al., 2006) may disqualify AMPs for large commercial application strategies.

Thus, both AMPs and phage therapy may offer somewhat less promise than the third alternative: enzymes that cleave the bacterial cell wall. Cell wall hydrolases attack specific sites within the bacterial peptidoglycan leading to cell wall degradation and subsequent cell lysis (Masschalck and Michiels, 2003). Enzymes mediating these reactions can be found in eukaryotes, bacteria and phages. Most studies have been performed on proteins derived from eukaryotes (lysozymes) and phages (phage lysins), whereas, information pertaining to bacterial hydrolases is very rare. Lysozymes are commonly known hydrolases that are produced by eukaroytes and are present in various tissues (e.g. skin) and secretions (Masschalck and Michiels, 2003). Although it was shown that lysozymes have antimicrobial activity against bacteria, fungi and viruses (Reddy et al., 2004; Lee-Huang et al., 2005; Wang et al., 2005), the observation of acquired resistance against lysozymes of some gram-positive bacteria (Bera et al., 2005; Abdou et al., 2007) may make them less interesting as alternatives to antibiotic. In comparison, lytic enzymes from phages show great potential as an antibiotic alternative. Repeated application has shown that resistance development is highly unlikely, since rapid killing as well as essentiality of the enzyme substrate disallow modification of the enzyme targets and thus, resistance development. It has already been demonstrated that milli- to microgram levels of lysin within one litre of bacterial suspension can efficiently kill bacteria regardless of their antibiotic sensitivity (Fischetti, 2005; Fischetti et al., 2006). This efficient action at low-dosage levels is not only attractive regarding the therapy costs, but may also be the reason for the lack of neutralization by the immune response and severe allergic responses by the host. This makes lytic enzymes a promising treatment for topical as well as intestinal application, but also for long term therapy and repeated application (Fischetti, 2005). Although all currently identified phage lysins act against gram-positive bacteria, the abundance of phages makes it most likely that a phage lysin targeting gram-negative bacteria can also be identified. So far, the major obstacle preventing clinical application has been the relatively cost-intensive production (Parisien et al., 2008). Since production in plants is around 10-50 times cheaper than production in *E. coli* (even when expressed with lower efficiency) (Kusnadi et al., 1997), the work presented here describes a new cost efficient method to produce high amounts of lysins using plant chloroplasts as a production platform. This will help to facilitate the production of next-generation antibiotics.

5 Summary

Plants, more precisely their chloroplasts with their bacterial-like expression machinery inherited from their cyanobacterial ancestors, can potentially offer a cheap expression system for proteinaceous pharmaceuticals. This system would be easily scalable and provides appropriate safety due to chloroplasts maternal inheritance (Stoger et al., 2002; Fischer et al., 2004; Stoger et al., 2004; Ma et al., 2005; Stoger et al., 2005). In this work, it was shown that three phage lytic enzymes (Pal, Cpl-1 and PlyGBS) could be successfully expressed at very high levels and with high stability in tobacco chloroplasts. PlyGBS expression reached an amount of foreign protein accumulation (> 70% TSP) that has never been obtained before. Although the high expression levels of PlyGBS caused a pale green phenotype with retarded growth, presumably due to exhaustion of plastid protein synthesis capacity, development and seed production were not impaired under greenhouse conditions.

Since Pal and Cpl-1 showed toxic effects when expressed in *E. coli,* a special plastid transformation vector (pTox) was constructed to allow DNA amplification in bacteria. The construction of the pTox transformation vector allowing a recombinase-mediated deletion of an *E. coli* transcription block in the chloroplast, leading to an increase of foreign protein accumulation to up to 40% of TSP for Pal and 20% of TSP for Cpl-1. High dose-dependent bactericidal efficiency was shown for all three plant-derived lytic enzymes using their pathogenic target bacteria *S. pyogenes* and *S. pneumoniae*. Confirmation of specificity was obtained for the endotoxic proteins Pal and Cpl-1 by application to *E. coli* cultures. These results establish tobacco chloroplasts as a new cost-efficient and convenient production platform for phage lytic enzymes and address the greatest obstacle for clinical application. The present study is the first report of lysin production in a non-bacterial system. The properties of chloroplast-produced lysins described in this work, their stability, high accumulation rate and biological activity make them highly attractive candidates for future antibiotics.

6 Literature and internet sources

6.1 Literatur

Abdallah F, Salamini F, Leister D (2000) A prediction of the size and evolutionary origin of the proteome of chloroplasts of *Arabidopsis*. Trends Plant Sci **5:** 141-142

Abdou AM, Higashiguchi S, Aboueleinin AM, Kim M, Ibrahim HR (2007) Antimicrobial peptides derived from hen egg lysozyme with inhibitory effect against *Bacillus* species. Food Control **18:** 173-178

Abremski K, Hoess R, Sternberg N (1983) Studies on the properties of P1 site-specific recombination: Evidence for topologically unlinked products following recombination. Cell **32:** 1301-1311

Adam Z (2007) Protein stability and degradation in plastids. *In* Cell and Molecular Biology of Plastids, pp 315-338

Adams DE, Bliska JB, Cozzarelli NR (1992) Cre-lox recombination in *Escherichia coli* cells mechanistic differences from the *in vitro* reaction. J Mol Biol **226:** 661-673

Allison LA, Maliga P (1995) Light-responsive and transcription-enhancing elements regulate the plastid *psbD* core promoter. Embo J **14:** 3721-3730

Ayliffe MA, Timmis JN (1992) Plastid DNA sequence homologies in the tobacco nuclear genome. Mol Gen Genet **236:** 105-112

Bals R (2000) Antimicrobial peptides and peptide antibiotics. Med Klin (Munich) **95:** 496-502

Barkan A, Walker M, Nolasco M, Johnson D (1994) A nuclear mutation in maize blocks the processing and translation of several chloroplast mRNAs and provides evidence for the differential translation of alternative mRNA forms. Embo J **13:** 3170-3181

Bateman JM, Purton S (2000) Tools for chloroplast transformation in *Chlamydomonas*: expression vectors and a new dominant selectable marker. Mol Gen Genet **263:** 404-410

Baumeister W, Walz J, Zuhl F, Seemuller E (1998) The proteasome: paradigm of a self-compartmentalizing protease. Cell **92:** 367-380

Bayley CC, Morgan M, Dale EC, Ow DW (1992) Exchange of gene activity in transgenic plants catalyzed by the Cre-lox site-specific recombination system. Plant Mol Biol **18:** 353-361

Bell G, Gouyon PH (2003) Arming the enemy: the evolution of resistance to self-proteins. Microbiology **149:** 1367-1375

Bellucci M, De Marchis F, Mannucci R, Bock R, Arcioni S (2005) Cytoplasm and chloroplasts are not suitable subcellular locations for beta-zein accumulation in transgenic plants. J Exp Bot **56:** 1205-1212

Bendich AJ (1987) Why do chloroplasts and mitochondria contain so many copies of their genome? Bioessays **6:** 279-282

Bera A, Herbert S, Jakob A, Vollmer W, Gotz F (2005) Why are pathogenic staphylococci so lysozyme resistant? The peptidoglycan O-acetyltransferase OatA is the major determinant for lysozyme resistance of *Staphylococcus aureus*. Mol Microbiol **55:** 778-787

Bertani G (1951) STUDIES ON LYSOGENESIS I.: The mode of phage liberation by lysogenic *Escherichia coli*. J Bacteriol **62:** 293-300

Bimboim HC, Doly J (1979) A rapid alkaline extraction procedure for screening recombinant plasmid DNA. Nucleic Acids Res **7:** 1513-1523

Birch-Machin I, Newell CA, Hibberd JM, Gray JC (2004) Accumulation of rotavirus VP6 protein in chloroplasts of transplastomic tobacco is limited by protein stability. Plant Biotechnol J **2:** 261-270

Bock R (2000) Sense from nonsense: how the genetic information of chloroplasts is altered by RNA editing. Biochimie **82:** 549-557

Bock R (2001) Transgenic plastids in basic research and plant biotechnology. J Mol Biol **312:** 425-438

Bock R (2006) Extranuclear inheritance: Gene transfer out of plastids. *In* Progress in Botany, pp 75-100

Bock R (2007) Structure, function, and inheritance of plastid genomes. *In* Cell and Molecular Biology of Plastids, pp 29-63

Bock R, Khan MS (2004) Taming plastids for a green future. Trends Biotechnol **22:** 311-318

Bock R, Kossel H, Maliga P (1994) Introduction of a heterologous editing site into the tobacco plastid genome: the lack of RNA editing leads to a mutant phenotype. Embo J **13:** 4623-4628

Bollenbach TJ, Schuster G, Portnoy V, Stern D (2007) Processing, degradation, and polyadenylation of chloroplast transcripts. *In* Cell and Molecular Biology of Plastids, pp 175-211

Bollenbach TJ, Schuster G, Stern DB (2004) Cooperation of endo- and exoribonucleases in chloroplast mRNA turnover. Prog Nucleic Acid Res Mol Biol **78:** 305-337

Bonen L, Vogel J (2001) The ins and outs of group II introns. Trends Genet **17:** 322-331

Borysowski J, Weber-Dabrowska B, Gorski A (2006) Bacteriophage endolysins as a novel class of antibacterial agents. Exp Biol Med **231:** 366-377

Boyer SK, Mullet JE (1988) Sequence and transcript map of barley chloroplast *psbA* gene. Nucleic Acids Res **16:** 8184

Boynton JE, Gillham NW, Harris EH, Hosler JP, Johnson AM, Jones AR, Randolph-Anderson BL, Robertson D, Klein TM, Shark KB, et a (1988) Chloroplast transformation in *Chlamydomonas* with high velocity microprojectiles. Science **240:** 1534-1538

Bradford MM (1976) A rapid and sensitive method for the quantitation of microgram quantities of protein utilizing the principle of protein-dye binding. Anal Biochem **72:** 248-254

Bradley D, Gatenby AA (1985) Mutational analysis of the maize chloroplast ATPase-beta subunit gene promoter: the isolation of promoter mutants in *E. coli* and their characterization in a chloroplast in vitro transcription system. Embo J **4:** 3641-3648

Breukink E, de Kruijff B (2006) Lipid II as a target for antibiotics. Nat Rev Drug Discov **5:** 321-332

Broudy TB, Fischetti VA (2003) In vivo lysogenic conversion of Tox(-) *Streptococcus pyogenes* to Tox(+) with lysogenic streptococci or free phage. Infect Immun **71:** 3782-3786

Buey R, Monterroso B, Menéndez M, Diakun G, Chacón P, Hermoso J, Díaz J (2007) Insights into molecular plasticity of choline binding proteins (Pneumococcal Surface Proteins) by SAXS. J Mol Biol **365:** 411-424

Bull JJ, Levin BR, DeRouin T, Walker N, Bloch CA (2002) Dynamics of success and failure in phage and antibiotic therapy in experimental infections. BMC Microbiol **2:** 35

Carapetis JR, Steer AC, Mulholland EK, Weber M (2005) The global burden of group A streptococcal diseases. Lancet Infect Dis **5:** 685-694

Carrer H, Hockenberry TN, Svab Z, Maliga P (1993) Kanamycin resistance as a selectable marker for plastid transformation in tobacco. Mol Gen Genet **241:** 49-56

Cerutti H, Johnson AM, Boynton JE, Gillham NW (1995) Inhibition of chloroplast DNA recombination and repair by dominant negative mutants of *Escherichia coli* RecA. Mol Cell Biol **15:** 3003-3011

Cerutti H, Osman M, Grandoni P, Jagendorf AT (1992) A homolog of *Escherichia coli* RecA protein in plastids of higher plants. Proc Natl Acad Sci U S A **89:** 8068-8072

Chang CC, Sheen J, Bligny M, Niwa Y, Lerbs-Mache S, Stern DB (1999) Functional analysis of two maize cDNAs encoding T7-like RNA polymerases. Plant Cell **11:** 911-926

Cheng Q, Nelson D, Zhu S, Fischetti VA (2005) Removal of group B streptococci colonizing the vagina and oropharynx of mice with a bacteriophage lytic enzyme. Antimicrob Agents Chemother **49:** 111-117

Chomczynski P, Sacchi N (2006) The single-step method of RNA isolation by acid guanidinium thiocyanate-phenol-chloroform extraction: twenty-something years on. Nat Protocols **1:** 581-585

Christoffersen RE (2006) Antibiotics-an investment worth making? Nat Biotechnol **24:** 1512-1514

Corneille S, Lutz KA, Svab Z, Maliga P (2001) Efficient elimination of selectable marker genes from the plastid genome by the CRE-lox site-specific recombination system. Plant J **27:** 171-178

Corneille S, Lutz KA, Azhagiri AK, Maliga P (2003) Identification of functional lox sites in the plastid genome. Plant J **35:** 753-762

Cundell DR, Masure HR, Tuomanen EI (1995) The molecular basis of pneumococcal infection: a hypothesis. Clin Infect Dis **21 Suppl 3:** S204-211

Cundell DR, Gerard NP, Gerard C, Idanpaan-Heikkila I, Tuomanen EI (1995) *Streptococcus pneumoniae* anchor to activated human cells by the receptor for platelet-activating factor. Nature **377:** 435-438

d'Herell F (1917) Sur un microbe invisible antagoniste des bacilles dysentériques. C.R. Acad. Sci. Paris **165:** 373–375

Dale EC, Ow DW (1991) Gene transfer with subsequent removal of the selection gene from the host genome. Proc Natl Acad Sci U S A **88:** 10558-10562

Daniell H (2002) Molecular strategies for gene containment in transgenic crops. Nat Biotech **20:** 581-586

Daniell H, Kumar S, Dufourmantel N (2005) Breakthrough in chloroplast genetic engineering of agronomically important crops. Trends Biotechnol **23:** 238-245

Daniell H, Lee SB, Panchal T, Wiebe PO (2001) Expression of the native cholera toxin B subunit gene and assembly as functional oligomers in transgenic tobacco chloroplasts. J Mol Biol **311:** 1001-1009

Daniell H, Streatfield SJ, Wycoff K (2001) Medical molecular farming: production of antibodies, biopharmaceuticals and edible vaccines in plants. Trends Plant Sci **6:** 219-226

De Cosa B, Moar W, Lee SB, Miller M, Daniell H (2001) Overexpression of the Bt cry2Aa2 operon in chloroplasts leads to formation of insecticidal crystals. Nat Biotechnol **19:** 71-74

Djurkovic S, Loeffler JM, Fischetti VA (2005) Synergistic killing of *Streptococcus pneumoniae* with the bacteriophage lytic enzyme Cpl-1 and penicillin or gentamicin depends on the level of penicillin resistance. Antimicrob Agents Chemother **49:** 1225-1228

Donovan RS, Robinson CW, Glick BR (1996) Review: optimizing inducer and culture conditions for expression of foreign proteins under the control of the lac promoter. J Ind Microbiol **16:** 145-154

Eberhard S, Drapier D, Wollman FA (2002) Searching limiting steps in the expression of chloroplast-encoded proteins: relations between gene copy number, transcription, transcript abundance and translation rate in the chloroplast of *Chlamydomonas reinhardtii*. Plant J **31:** 149-160

Eibl C, Zou Z, Beck a, Kim M, Mullet J, Koop HU (1999) *In vivo* analysis of plastid *psbA*, *rbcL* and *rpl32* UTR elements by chloroplast transformation: tobacco plastid gene expression is controlled by modulation of transcript levels and translation efficiency. Plant J **19:** 333-345

Eisermann A, Tiller K, Link G (1990) *In vitro* transcription and DNA binding characteristics of chloroplast and etioplast extracts from mustard (*Sinapis alba*) indicate differential usage of the *psbA* promoter. Embo J **9:** 3981-3987

Emanuel C, Weihe A, Graner A, Hess WR, Borner T (2004) Chloroplast development affects expression of phage-type RNA polymerases in barley leaves. Plant J **38:** 460-472

Entenza JM, Loeffler JM, Grandgirard D, Fischetti VA, Moreillon P (2005) Therapeutic effects of bacteriophage Cpl-1 lysin against *Streptococcus pneumoniae* endocarditis in rats. Antimicrob Agents Chemother **49:** 4789-4792

Farley MM, Harvey C, Stull T, Smith JD, Schuchat A, Wenger JD, Stephens DS (1993) A population-based assessment of invasive disease due to group B streptococcus in nonpregnant adults. N Engl J Med **328:** 1807-1811

Fernandez-Tornero C, Garcia E, de Pascual-Teresa B, Lopez R, Gimenez-Gallego G, Romero A (2005) Ofloxacin-like antibiotics inhibit pneumococcal cell wall-degrading virulence factors. J Biol Chem **280:** 19948-19957

Fernandez M, Hickman ME, Baker CJ (1998) Antimicrobial susceptibilities of group B streptococci isolated between 1992 and 1996 from patients with bacteremia or meningitis. Antimicrob Agents Chemother **42:** 1517-1519

Fischer N, Stampacchia O, Redding K, Rochaix J (1996) Selectable marker recycling in the chloroplast. Mol Gen Genet **251:** 373-380

Fischer R, Stoger E, Schillberg S, Christou P, Twyman RM (2004) Plant-based production of biopharmaceuticals. Curr Opin Plant Biol **7:** 152-158

Fischer W-N, André B, Rentsch D, Krolkiewicz S, Tegeder M, Breitkreuz K, Frommer WB (1998) Amino acid transport in plants. Trends Plant Sci **3:** 188-195

Fischetti VA (2005) Bacteriophage lytic enzymes: novel anti-infectives. Trends Microbiol **13:** 491-496

Fischetti VA (2006) Using phage lytic enzymes to control pathogenic bacteria. BMC Oral Health **6:** S16

Fischetti VA, Nelson D, Schuch R (2006) Reinventing phage therapy: are the parts greater than the sum? Nat Biotechnol **24:** 1508-1511

Garcia E, Garcia JL, Garcia P, Arraras A, Sanchez-Puelles JM, Lopez R (1988) Molecular evolution of lytic enzymes of *Streptococcus pneumoniae* and its bacteriophages. Proc Natl Acad Sci U S A **85:** 914-918

Garcia P, Garcia JL, Garcia E, Sanchez-Puelles JM, Lopez R (1990) Modular organization of the lytic enzymes of *Streptococcus pneumoniae* and its bacteriophages. Gene **86:** 81-88

Gatenby AA, Castleton JA, Saul MW (1981) Expression in *E. coli* of maize and wheat chloroplast genes for large subunit of ribulose bisphosphate carboxylase. Nature **291:** 117-121

Gekko K, Timasheff SN (1981) Mechanism of protein stabilization by glycerol: preferential hydration in glycerol-water mixtures. Biochemistry **20:** 4667-4676

Ghosh K, Van Duyne GD (2002) Cre-loxP biochemistry. Methods **28:** 374-383

Giglione C, Meinnel T (2001) Organellar peptide deformylases: universality of the N-terminal methionine cleavage mechanism. Trends Plant Sci **6:** 566-572

Giglione C, Vallon O, Meinnel T (2003) Control of protein life-span by N-terminal methionine excision. Embo J **22:** 13-23

Glenz K, Bouchon B, Stehle T, Wallich R, Simon MM, Warzecha H (2006) Production of a recombinant bacterial lipoprotein in higher plant chloroplasts. Nat Biotechnol **24:** 76-77

Gold L (1988) Posttranscriptional regulatory mechanisms in *Escherichia coli*. Annu Rev Biochem **57:** 199-233

Goldschmidt-Clermont M (1991) Transgenic expression of aminoglycoside adenine transferase in the chloroplast: a selectable marker of site-directed transformation of *Chlamydomonas*. Nucleic Acids Res **19:** 4083-4089

Gomord V, Chamberlain P, Jefferis R, Faye L (2005) Biopharmaceutical production in plants: problems, solutions and opportunities. Trends Biotechnol **23:** 559-565

Gordon YJ, Romanowski EG, McDermott AM (2005) A review of antimicrobial peptides and their therapeutic potential as anti-infective drugs. Curr Eye Res **30:** 505-515

Gram HC (1884) Über die isolierte Färbung der Schizomyceten in Schnitt- und Trockenpräparaten. Fortschr. Med. **2:** 185-189

Gray MW (1993) Origin and evolution of organelle genomes. Curr Opin Genet Dev **3:** 884-890

Gruissem W (1989) Chloroplast gene expression: how plants turn their plastids on. Cell **56:** 161-170

Gums JG (2004) Redefining appropriate use of antibiotics. Am Fam Physician **69:** 35, 39-40

Guo F, Gopaul DN, van Duyne GD (1997) Structure of Cre recombinase complexed with DNA in a site-specific recombination synapse. Nature **389:** 40-46

Guo Y, German TL, Schultz RD (2007) A cryptic promoter in potato virus X vector interrupted plasmid construction. BMC Mol Biol **8:** 17

Hagens S, Blasi U (2003) Genetically modified filamentous phage as bactericidal agents: a pilot study. Lett Appl Microbiol **37:** 318-323

Hagens S, Habel A, von Ahsen U, von Gabain A, Blasi U (2004) Therapy of experimental *Pseudomonas* infections with a nonreplicating genetically modified phage. Antimicrob Agents Chemother **48:** 3817-3822

Hager M, Bock R (2000) Enslaved bacteria as new hope for plant biotechnologists. Appl Microbiol Biotechnol **54:** 302-310

Hajdukiewicz PT, Allison LA, Maliga P (1997) The two RNA polymerases encoded by the nuclear and the plastid compartments transcribe distinct groups of genes in tobacco plastids. Embo J **16:** 4041-4048

Hajdukiewicz PT, Gilbertson L, Staub JM (2001) Multiple pathways for Cre/lox-mediated recombination in plastids. Plant J **27:** 161-170

Hansen LH, Knudsen S, Sorensen SJ (1998) The effect of the *lacY* gene on the induction of IPTG inducible promoters, studied in *Escherichia coli* and *Pseudomonas fluorescens*. Curr Microbiol **36:** 341-347

Hasper HE, Kramer NE, Smith JL, Hillman JD, Zachariah C, Kuipers OP, de Kruijff B, Breukink E (2006) An alternative bactericidal mechanism of action for lantibiotic peptides that target lipid II. Science **313:** 1636-1637

Hayes R, Kudla J, Gruissem W (1999) Degrading chloroplast mRNA: the role of polyadenylation. Trends Biochem Sci **24:** 199-202

Hayes R, Kudla J, Schuster G, Gabay L, Maliga P, Gruissem W (1996) Chloroplast mRNA 3'-end processing by a high molecular weight protein complex is regulated by nuclear encoded RNA binding proteins. Embo J **15:** 1132-1141

Heberer T (2002) Occurrence, fate, and removal of pharmaceutical residues in the aquatic environment: a review of recent research data. Toxicology Letters **131:** 5-17

Hedtke B, Borner T, Weihe A (1997) Mitochondrial and chloroplast phage-type RNA polymerases in *Arabidopsis*. Science **277:** 809-811

Hedtke B, Borner T, Weihe A (2000) One RNA polymerase serving two genomes. EMBO Rep **1:** 435-440

Hedtke B, Wagner I, Borner T, Hess WR (1999) Inter-organellar crosstalk in higher plants: impaired chloroplast development affects mitochondrial gene and transcript levels. Plant J **19:** 635-643

Hennig A, Bonfig K, Roitsch T, Warzecha H (2007) Expression of the recombinant bacterial outer surface protein A in tobacco chloroplasts leads to thylakoid localization and loss of photosynthesis. Febs J **274:** 5749-5758

Henning C, Bengtsson L, Jorup C, Engquist S (1997) Antibiotic resistance in *Streptococcus pneumoniae*, *Haemophilus influenzae* and *Streptococcus pyogenes* in respiratory tract infections in outpatients. Scand J Infect Dis **29:** 559-563

Hermoso JA, Monterroso B, Albert A, Galan B, Ahrazem O, Garcia P, Martinez-Ripoll M, Garcia JL, Menendez M (2003) Structural basis for selective recognition of pneumococcal cell wall by modular endolysin from phage Cp-1. Structure **11:** 1239-1249

Herz S, Fussl M, Steiger S, Koop HU (2005) Development of novel types of plastid transformation vectors and evaluation of factors controlling expression. Transgenic Res **14:** 969-982

Hicks A, Drager RG, Higgs DC, Stern DB (2002) An mRNA 3' processing site targets downstream sequences for rapid degradation in *Chlamydomonas* chloroplasts. J Biol Chem **277:** 3325-3333

Hirose T, Fan H, Suzuki JY, Wakasugi T, Tsudzuki T, Kossel H, Sugiura M (1996) Occurrence of silent RNA editing in chloroplasts: its species specificity and the influence of environmental and developmental conditions. Plant Mol Biol **30:** 667-672

Hirose T, Sugiura M (1997) Both RNA editing and RNA cleavage are required for translation of tobacco chloroplast ndhD mRNA: a possible regulatory mechanism for the expression of a chloroplast operon consisting of functionally unrelated genes. Embo J **16:** 6804-6811

Hormann F, Soll J, Bolter B (2007) The chloroplast protein import machinery: a review. Methods Mol Biol **390:** 179-194

Huang FC, Klaus, Klaus S, Herz, Herz S, Zou, Zou Z, Koop, Koop HU, Golds, Golds T (2002) Efficient plastid transformation in tobacco using the *aphA-6* gene and kanamycin selection. Mol Gen Genomics **268:** 19-27

Hudson GS, Evans JR, von Caemmerer S, Arvidsson YB, Andrews TJ (1992) Reduction of ribulose-1,5-bisphosphate carboxylase/oxygenase content by antisense RNA reduces photosynthesis in transgenic tobacco plants. Plant Physiol **98:** 294-302

Iamtham S, Day A (2000) Removal of antibiotic resistance genes from transgenic tobacco plastids. Nat Biotech **18:** 1172-1176

Ikeda TM, Gray MW (1999) Characterization of a DNA-binding protein implicated in transcription in wheat mitochondria. Mol Cell Biol **19:** 8113-8122

Inada M, Sasaki T, Yukawa M, Tsudzuki T, Sugiura M (2004) A systematic search for RNA editing sites in pea chloroplasts: an editing event causes diversification from the evolutionarily conserved amino acid sequence. Plant Cell Physiol **45:** 1615-1622

Jacob F, Monod J (1961) Genetic regulatory mechanisms in the synthesis of proteins. J Mol Biol **3:** 318-356

Jado I, Lopez R, Garcia E, Fenoll A, Casal J, Garcia P (2003) Phage lytic enzymes as therapy for antibiotic-resistant *Streptococcus pneumoniae* infection in a murine sepsis model. J Antimicrob Chemother **52:** 967-973

Jechlinger W, Azimpour Tabrizi C, Lubitz W, Mayrhofer P (2004) Minicircle DNA immobilized in bacterial ghosts: in vivo production of safe non-viral DNA delivery vehicles. J Mol Microbiol Biotechnol **8:** 222-231

Jia H, Pang Y, Chen X, Fang R (2006) Removal of the selectable marker gene from transgenic tobacco plants by expression of Cre recombinase from a tobacco mosaic virus vector through agroinfection. Transgenic Res **15:** 375-384

Kahlau S, Bock R (2008) Plastid transcriptomics and translatomics of tomato fruit development and chloroplast-to-chromoplast differentiation: chromoplast gene expression largely serves the production of a single protein. Plant Cell **20:** 856-874

Kain SR, Adams M, Kondepudi A, Yang TT, Ward WW, Kitts P (1995) Green fluorescent protein as a reporter of gene expression and protein localization. Biotechniques **19:** 650-655

Kanamaru K, Tanaka K (2004) Roles of chloroplast RNA polymerase sigma factors in chloroplast development and stress response in higher plants. Biosci Biotechnol Biochem **68:** 2215-2223

Kanevski I, Maliga P (1994) Relocation of the plastid *rbcL* gene to the nucleus yields functional ribulose-1,5-bisphosphate carboxylase in tobacco chloroplasts. Proc Natl Acad Sci U S A **91:** 1969-1973

Kavanagh TA, Thanh ND, Lao NT, McGrath N, Peter SO, Horvath EM, Dix PJ, Medgyesy P (1999) Homeologous plastid DNA transformation in tobacco is mediated by multiple recombination events. Genetics **152:** 1111-1122

Kay E, Vogel TM, Bertolla F, Nalin R, Simonet P (2002) *In situ* transfer of antibiotic resistance genes from transgenic (transplastomic) tobacco plants to bacteria. Appl Environ Microbiol **68:** 3345-3351

Khan MS, Maliga P (1999) Fluorescent antibiotic resistance marker for tracking plastid transformation in higher plants. Nat Biotech **17:** 910-915

Kim KS, Kaplan EL (1985) Association of penicillin tolerance with failure to eradicate group A streptococci from patients with pharyngitis. J Pediatr **107:** 681-684

Kittiwongwattana C, Lutz K, Clark M, Maliga P (2007) Plastid marker gene excision by the phiC31 phage site-specific recombinase. Plant Mol Biol **64:** 137-143

Klaus SM, Huang FC, Golds TJ, Koop HU (2004) Generation of marker-free plastid transformants using a transiently cointegrated selection gene. Nat Biotechnol **22:** 225-229

Kobayashi Y, Dokiya Y, Kumazawa Y, Sugita M (2002) Non-AUG translation initiation of mRNA encoding plastid-targeted phage-type RNA polymerase in *Nicotiana sylvestris*. Biochem Biophys Res Commun **299:** 57-61

Kobayashi Y, Dokiya Y, Sugita M (2001) Dual targeting of phage-type RNA polymerase to both mitochondria and plastids is due to alternative translation initiation in single transcripts. Biochem Biophys Res Commun **289:** 1106-1113

Kobayashi Y, Dokiya Y, Sugiura M, Niwa Y, Sugita M (2001) Genomic organization and organ-specific expression of a nuclear gene encoding phage-type RNA polymerase in *Nicotiana sylvestris.* Gene **279:** 33-40

Köller T, Nelson D, Nakata M, Kreutzer M, Fischetti VA, Glocker MO, Podbielski A, Kreikemeyer B (2008) PlyC, a novel bacteriophage lysin for compartment-dependent proteomics of group A streptococci. Proteomics **8:** 140-148

Koya V, Moayeri M, Leppla SH, Daniell H (2005) Plant-based vaccine: mice immunized with chloroplast-derived anthrax protective antigen survive anthrax lethal toxin challenge. Infect Immun **73:** 8266-8274

Kozak M (2005) Regulation of translation via mRNA structure in prokaryotes and eukaryotes. Gene **361:** 13-37

Krause K, Krupinska K (2000) Molecular and functional properties of highly purified transcriptionally active chromosomes from spinach chloroplasts. Physiologia Plantarum **109:** 188-195

Kresse H, Belsey MJ, Rovini H (2007) The antibacterial drugs market. Nat Rev Drug Discov **6:** 19-20

Kühn R, M. Torres R (2002) Cre/ loxP recombination system and gene targeting. Methods Mol Biol **180:** 175-204

Kuhn R, Schwenk F, Aguet M, Rajewsky K (1995) Inducible gene targeting in mice. Science **269:** 1427-1429

Kuroda H, Maliga P (2001) Complementarity of the 16S rRNA penultimate stem with sequences downstream of the AUG destabilizes the plastid mRNAs. Nucleic Acids Res **29:** 970-975

Kuroda H, Maliga P (2003) The plastid clpP1 protease gene is essential for plant development. Nature **425:** 86-89

Kuroiwa T (1989) The nuclei of cellular organelles and the formation of daughter organelles by the "plastid-dividing ring". J Plant Res **102:** 291-329

Kuroiwa T (1991) The replication, differentiation, and inheritance of plastids with emphasis on the concept of organelle nuclei. Int Rev Cytol **128:** 1-&

Kusnadi AR, Nikolov ZL, Howard JA (1997) Production of recombinant proteins in transgenic plants: Practical considerations. Biotechnol Bioeng **56:** 473-484

Kusumi K, Yara A, Mitsui N, Tozawa Y, Iba K (2004) Characterization of a rice nuclear-encoded plastid RNA polymerase gene OsRpoTp. Plant Cell Physiol **45:** 1194-1201

Kyhse-Andersen J (1984) Electroblotting of multiple gels: a simple apparatus without buffer tank for rapid transfer of proteins from polycrylamide to nitrocellulose. J Biochem Biophys Methods **10:** 203-209

Lalonde S, Tegeder M, Throne-Holst M, Frommer WB, Patrick JW (2003) Phloem loading and unloading of sugars and amino acids. Plant Cell Environ **26:** 37-56

Lambowitz AM, Zimmerly S (2004) Mobile group II introns. Annu Rev Genet **38:** 1-35

Lancefield RC (1933) A serological differentiation of human and other groups of haemolytic streptococci. J Exp Med **57:** 571-595

Langridge WH, Fitzgerald KJ, Koncz C, Schell J, Szalay AA (1989) Dual promoter of *Agrobacterium tumefaciens* mannopine synthase genes is regulated by plant growth hormones. Proc Natl Acad Sci U S A **86:** 3219-3223

Lee-Huang S, Maiorov V, Huang PL, Ng A, Lee HC, Chang YT, Kallenbach N, Huang PL, Chen HC (2005) Structural and functional modeling of human lysozyme reveals a unique nonapeptide, HL9, with anti-HIV activity. Biochemistry **44:** 4648-4655

Legen J, Kemp S, Krause K, Profanter B, Herrmann RG, Maier RM (2002) Comparative analysis of plastid transcription profiles of entire plastid chromosomes from tobacco attributed to wild-type and PEP-deficient transcription machineries. Plant J **31:** 171-188

Li J, Aroutcheva AA, Faro S, Chikindas ML (2005) Mode of action of lactocin 160, a bacteriocin from vaginal *Lactobacillus rhamnosus*. Infect Dis Obstet Gynecol **13:** 135-140

Li W, Ruf S, Bock R (2006) Constancy of organellar genome copy numbers during leaf development and senescence in higher plants. Mol Gen Genomics **275:** 185-192

Liere K, Börner T (2007) Transcription and transcriptional regulation in plastids. *In* Cell and Molecular Biology of Plastids, pp 121-174

Lindahl M, Yang DH, Andersson B (1995) Regulatory proteolysis of the major light-harvesting chlorophyll a/b protein of photosystem II by a light-induced membrane-associated enzymic system. Eur J Biochem **231:** 503-509

Loeffler JM, Djurkovic S, Fischetti VA (2003) Phage lytic enzyme Cpl-1 as a novel antimicrobial for pneumococcal bacteremia. Infect Immun **71:** 6199-6204

Loeffler JM, Fischetti VA (2003) Synergistic lethal effect of a combination of phage lytic enzymes with different activities on penicillin-sensitive and -resistant *Streptococcus pneumoniae* strains. Antimicrob Agents Chemother **47:** 375-377

Loeffler JM, Nelson D, Fischetti VA (2001) Rapid killing of *Streptococcus pneumoniae* with a bacteriophage cell wall hydrolase. Science **294:** 2170-2172

Loessner MJ (2005) Bacteriophage endolysins--current state of research and applications. Curr Opin Microbiol **8:** 480-487

Lohner K, Blondelle SE (2005) Molecular mechanisms of membrane perturbation by antimicrobial peptides and the use of biophysical studies in the design of novel peptide antibiotics. Comb Chem High Throughput Screen **8:** 241-256

Lohse M, Drechsel O, Bock R (2007) OrganellarGenomeDRAW (OGDRAW): a tool for the easy generation of high-quality custom graphical maps of plastid and mitochondrial genomes. Curr Genet **52:** 267-274

Lopez-Juez E, Pyke KA (2005) Plastids unleashed: their development and their integration in plant development. Int J Dev Biol **49:** 557-577

Lopez R (2004) *Streptococcus pneumoniae* and its bacteriophages: one long argument. Int Microbiol **7:** 163-171

López R, García E (2004) Recent trends on the molecular biology of pneumococcal capsules, lytic enzymes, and bacteriophage. FEMS Microbiol Rev **28:** 553-580

Lopez R, Garcia E, Garcia P, Garcia JL (1997) The pneumococcal cell wall degrading enzymes: a modular design to create new lysins? Microb Drug Resist **3:** 199-211

Lopez R, Garcia JL, Garcia E, Ronda C, Garcia P (1992) Structural analysis and biological significance of the cell wall lytic enzymes of *Streptococcus pneumoniae* and its bacteriophage. FEMS Microbiol Lett **79:** 439-447

Lossl A, Bohmert K, Harloff H, Eibl C, Muhlbauer S, Koop HU (2005) Inducible trans-activation of plastid transgenes: expression of the *R. eutropha phb* operon in transplastomic tobacco. Plant Cell Physiol **46:** 1462-1471

Lutz KA, Bosacchi MH, Maliga P (2006) Plastid marker-gene excision by transiently expressed CRE recombinase. Plant J **45:** 447-456

Lutz KA, Svab Z, Maliga P (2006) Construction of marker-free transplastomic tobacco using the Cre-loxP site-specific recombination system. Nat Protoc **1:** 900-910

Ma JK, Barros E, Bock R, Christou P, Dale PJ, Dix PJ, Fischer R, Irwin J, Mahoney R, Pezzotti M, Schillberg S, Sparrow P, Stoger E, Twyman RM (2005) Molecular farming for new drugs and vaccines. Current perspectives on the production of pharmaceuticals in transgenic plants. EMBO Rep **6:** 593-599

Magee AM, Coyne S, Murphy D, Horvath EM, Medgyesy P, Kavanagh TA (2004) T7 RNA polymerase-directed expression of an antibody fragment transgene in plastids causes a semi-lethal pale-green seedling phenotype. Transgenic Res **13:** 325-337

Magee AM, MacLean D, Gray JC, Kavanagh TA (2007) Disruption of essential plastid gene expression caused by T7 RNA polymerase-mediated transcription of plastid transgenes during early seedling development. Transgenic Res **16:** 415-428

Maliga P (2003) Progress towards commercialization of plastid transformation technology. Trends Biotechnol **21:** 20-28

Maliga P (2004) Plastid transformation in higher plants. Annu Rev Plant Biol **55:** 289-313

Marillonnet S, Giritch A, Gils M, Kandzia R, Klimyuk V, Gleba Y (2004) *In planta* engineering of viral RNA replicons: efficient assembly by recombination of DNA modules delivered by *Agrobacterium*. Proc Natl Acad Sci U S A **101:** 6852-6857

Marr AK, Gooderham WJ, Hancock RE (2006) Antibacterial peptides for therapeutic use: obstacles and realistic outlook. Curr Opin Pharmacol **6:** 468-472

Martin W, Herrmann RG (1998) Gene transfer from organelles to the nucleus: how much, what happens, and Why? Plant Physiol **118:** 9-17

Martin W, Rujan T, Richly E, Hansen A, Cornelsen S, Lins T, Leister D, Stoebe B, Hasegawa M, Penny D (2002) From the cover: Evolutionary analysis of *Arabidopsis*, cyanobacterial, and chloroplast genomes reveals plastid phylogeny and thousands of cyanobacterial genes in the nucleus. Proc Natl Acad Sci U S A **99:** 12246-12251

Masschalck B, Michiels CW (2003) Antimicrobial properties of lysozyme in relation to foodborne vegetative bacteria. Crit Rev Microbiol **29:** 191-214

Mathews DH, Sabina J, Zuker M, Turner DH (1999) Expanded sequence dependence of thermodynamic parameters improves prediction of RNA secondary structure. J Mol Biol **288:** 911-940

Matsuzaki S, Rashel M, Uchiyama J, Sakurai S, Ujihara T, Kuroda M, Ikeuchi M, Tani T, Fujieda M, Wakiguchi H, Imai S (2005) Bacteriophage therapy: a revitalized therapy against bacterial infectious diseases. J Infect Chemother **11:** 211-219

Mayfield SP, Cohen A, Danon A, Yohn CB (1994) Translation of the *psbA* mRNA of *Chlamydomonas reinhardtii* requires a structured RNA element contained within the 5' untranslated region. J Cell Biol **127:** 1537-1545

McBride KE, Svab Z, Schaaf DJ, Hogan PS, Stalker DM, Maliga P (1995) Amplification of a chimeric *Bacillus* gene in chloroplasts leads to an extraordinary level of an insecticidal protein in tobacco. Biotechnology (N Y) **13:** 362-365

McCormac DJ, Barkan A (1999) A nuclear gene in maize required for the translation of the chloroplast atpB/E mRNA. Plant Cell **11:** 1709-1716

McCullers JA, Tuomanen EI (2001) Molecular pathogenesis of pneumococcal pneumonia. Front Biosci **6:** D877-889

McKinney J, Guerrier-Takada C, Wesolowski D, Altman S (2001) Inhibition of *Escherichia coli* viability by external guide sequences complementary to two essential genes. Proc Natl Acad Sci U S A **98:** 6605-6610

Merril CR, Scholl D, Adhya SL (2003) The prospect for bacteriophage therapy in western medicine. Nat Rev Drug Discov **2:** 489-497

Monde RA, Greene JC, Stern DB (2000) The sequence and secondary structure of the 3′-UTR affect 3′-end maturation, RNA accumulation, and translation in tobacco chloroplasts. Plant Mol Biol **44:** 529-542

Monde RA, Schuster G, Stern DB (2000) Processing and degradation of chloroplast mRNA. Biochimie **82:** 573-582

Montagnani F, Fanetti A, Stolzuoli L, Croci L, Arena F, Zanchi A, Cellesi C (2008) Pneumococcal disease in a paediatric population in a hospital of central Italy: a clinical and microbiological case series from 1992 to 2006. J Infect **56:** 179-184

Monterroso B, Albert A, Martinez-Ripoll M, Garcia P, Garcia JL, Menendez M, Hermoso JA (2002) Crystallization and preliminary X-ray diffraction studies of the complete modular endolysin from Cp-1, a phage infecting *Streptococcus pneumoniae*. Acta Crystallogr D Biol Crystallogr **58:** 1487-1489

Muhlbauer SK, Koop HU (2005) External control of transgene expression in tobacco plastids using the bacterial lac repressor. Plant J **43:** 941-946

Navarre WW, Schneewind O (1999) Surface proteins of gram-positive bacteria and mechanisms of their targeting to the cell wall envelope. Microbiol Mol Biol Rev **63:** 174-229

Nelson D, Loomis L, Fischetti VA (2001) Prevention and elimination of upper respiratory colonization of mice by group A streptococci by using a bacteriophage lytic enzyme. Proc Natl Acad Sci U S A **98:** 4107-4112

Newman SM, Boynton JE, Gillham NW, Randolph-Anderson BL, Johnson AM, Harris EH (1990) Transformation of chloroplast ribosomal RNA genes in *Chlamydomonas*: Molecular and genetic characterization of integration events. Genetics **126:** 875-888

Nojima T, Lin AC, Fujii T, Endo I (2005) Determination of the termination efficiency of the transcription terminator using different fluorescent profiles in green fluorescent protein mutants. Anal Sci **21:** 1479-1481

Odell JT, Hoopes JL, Vermerris W (1994) Seed-specific gene activation mediated by the Cre/lox site-specific recombination system. Plant Physiol **106:** 447-458

Palmer JD (1983) Chloroplast DNA exists in two orientations. Nature **301:** 92-93

Palmer JD, Thompson WF (1982) Chloroplast DNA rearrangements are more frequent when a large inverted repeat sequence is lost. Cell **29:** 537-550

Parisien A, Allain B, Zhang J, Mandeville R, Lan CQ (2008) Novel alternatives to antibiotics: bacteriophages, bacterial cell wall hydrolases, and antimicrobial peptides. J Appl Microbiol **104:** 1-13

Peled-Zehavi H, Danon A (2007) Translation and translational regulation in chloroplasts. *In* Cell and Molecular Biology of Plastids, pp 249-281

Perez-Dorado I, Campillo NE, Monterroso B, Hesek D, Lee M, Paez JA, Garcia P, Martinez-Ripoll M, Garcia JL, Mobashery S, Menendez M, Hermoso JA (2007) Elucidation of the molecular recognition of bacterial cell wall by modular pneumococcal phage endolysin Cpl-1. J Biol Chem **282:** 24990-24999

Petrides D, Sapidou E, Calandranis J (1995) Computer-aided process analysis and economic evaluation for biosynthetic human insulin production - A case study. Biotechnol Bioeng **48:** 529-541

Platt T (1986) Transcription termination and the regulation of gene expression. Annu Rev Biochem **55:** 339-372

Prasher DC, Eckenrode VK, Ward WW, Prendergast FG, Cormier MJ (1992) Primary structure of the *Aequorea victoria* green-fluorescent protein. Gene **111:** 229-233

Prieß P (2002) Molekulare Charakterisierung und pathogene Bedeutung von cholinbindenden Proteinen von *Streptococcus pneumoniae*. Dissertation. Technische Universität Carolo-Wilhelmina, Brunswick, Germany

Qin PZ, Pyle AM (1998) The architectural organization and mechanistic function of group II intron structural elements. Curr Opin Struct Biol **8:** 301-308

Randerath O, König D, Saalmann M, Jansen B, Pulverer G (2000) Prophylaxe gegen Infektionen durch *Streptococcus pneumoniae*. Medizinische Klinik **95:** 678-682

Reddy KV, Yedery RD, Aranha C (2004) Antimicrobial peptides: premises and promises. Int J Antimicrob Agents **24:** 536-547

Reynolds R, Bermudez-Cruz RM, Chamberlin MJ (1992) Parameters affecting transcription termination by *Escherichia coli* RNA polymerase. I. Analysis of 13 rho-independent terminators. J Mol Biol **224:** 31-51

Richardson LV, Richardson JP (1996) Rho-dependent termination of transcription is governed primarily by the upstream Rho utilization (rut) sequences of a terminator. J Biol Chem **271:** 21597-21603

Ring A, Weiser JN, Tuomanen EI (1998) Pneumococcal trafficking across the blood-brain barrier. Molecular analysis of a novel bidirectional pathway. J Clin Invest **102:** 347-360

Rochaix JD, Kuchka M, Mayfield S, Schirmer-Rahire M, Girard-Bascou J, Bennoun P (1989) Nuclear and chloroplast mutations affect the synthesis or stability of the chloroplast *psbC* gene product in *Chlamydomonas reinhardtii*. Embo J **8:** 1013-1021

Rodermel SR, Abbott MS, Bogorad L (1988) Nuclear-organelle interactions: nuclear antisense gene inhibits ribulose bisphosphate carboxylase enzyme levels in transformed tobacco plants. Cell **55:** 673-681

Rogalski M, Ruf S, Bock R (2006) Tobacco plastid ribosomal protein S18 is essential for cell survival. Nucleic Acids Res **34:** 4537-4545

Rott R, Schuster G, Drager R, Stern D (1996) The 3′ untranslated regions of chloroplast genes in *Chlamydomonas reinhardtii* do not serve as efficient transcriptional terminators. Mol Gen Genet **252:** 676-683

Ruf S, Hermann M, Berger IJ, Carrer H, Bock R (2001) Stable genetic transformation of tomato plastids and expression of a foreign protein in fruit. Nat Biotechnol **19:** 870-875

Ruf S, Karcher D, Bock R (2007) Determining the transgene containment level provided by chloroplast transformation. Proc Natl Acad Sci U S A **104:** 6998-7002

Rujan T, Martin W (2001) How many genes in *Arabidopsis* come from cyanobacteria? An estimate from 386 protein phylogenies. Trends Genet **17:** 113-120

Russell SH, Hoopes JL, Odell JT (1992) Directed excision of a transgene from the plant genome. Mol Gen Genet **234:** 49-59

Salvador ML, Klein U (1999) The redox state regulates RNA degradation in the chloroplast of *Chlamydomonas reinhardtii*. Plant Physiol **121:** 1367-1374

Salvador ML, Klein U, Bogorad L (1993) Light-regulated and endogenous fluctuations of chloroplast transcript levels in *Chlamydomonas*. Regulation by transcription and RNA degradation. Plant J **3:** 213-219

Sambrook J, Fritsch EF, Maniatis T (1989) Molecular cloning : a laboratory manual. *In*. New York : Cold Spring Harbor Laboratory Press

Saraf-Levy T, Santoro SW, Volpin H, Kushnirsky T, Eyal Y, Schultz PG, Gidoni D, Carmi N (2006) Site-specific recombination of asymmetric lox sites mediated by a heterotetrameric Cre recombinase complex. Bioorganic and medicinal chemistry **14:** 3081-3089

Sawano H, Koumoto Y, Ohta K, Sasaki Y, Segawa S, Tachibana H (1992) Efficient in vitro folding of the three-disulfide derivatives of hen lysozyme in the presence of glycerol. FEBS Lett **303:** 11-14

Schagger H, von Jagow G (1987) Tricine-sodium dodecyl sulfate-polyacrylamide gel electrophoresis for the separation of proteins in the range from 1 to 100 kDa. Anal Biochem **166:** 368-379

Scheffers DJ, Pinho MG (2005) Bacterial cell wall synthesis: new insights from localization studies. Microbiol Mol Biol Rev **69:** 585-607

Schmidt GW, Mishkind ML (1983) Rapid degradation of unassembled ribulose 1,5-bisphosphate carboxylase small subunits in chloroplasts. Proc Natl Acad Sci U S A **80:** 2632-2636

Schmitz-Linneweber C, Barkan A (2007) RNA splicing and RNA editing in chloroplasts. *In* Cell and Molecular Biology of Plastids, pp 213-248

Schrag SJ, McGee L, Whitney CG, Beall B, Craig AS, Choate ME, Jorgensen JH, Facklam RR, Klugman KP, the Active Bacterial Core Surveillance T (2004) Emergence of *Streptococcus pneumoniae* with very-high-level resistance to penicillin. Antimicrob Agents Chemother **48:** 3016-3023

Schuch R, Nelson D, Fischetti VA (2002) A bacteriolytic agent that detects and kills *Bacillus anthracis*. Nature **418:** 884-889

Sheehan MM, Garcia JL, Lopez R, Garcia P (1997) The lytic enzyme of the pneumococcal phage Dp-1: a chimeric lysin of intergeneric origin. Mol Microbiol **25:** 717-725

Shevchenko A, Wilm M, Vorm O, Mann M (1996) Mass spectrometric sequencing of proteins from silver-stained polyacrylamide gels. Anal Chem **68:** 850-858

Shikanai T, Shimizu K, Ueda K, Nishimura Y, Kuroiwa T, Hashimoto T (2001) The chloroplast *clpP* gene, encoding a proteolytic subunit of ATP-dependent protease, is indispensable for chloroplast development in tobacco. Plant Cell Physiol **42:** 264-273

Shimda H, Sugiura M (1991) Fine structural features of the chloroplast genome: comparison of the sequenced chloroplast genomes. Nucleic Acids Res **19:** 983-995

Sijmons PC, Dekker BM, Schrammeijer B, Verwoerd TC, van den Elzen PJ, Hoekema A (1990) Production of correctly processed human serum albumin in transgenic plants. Biotechnology (N Y) **8:** 217-221

Skurnik M, Strauch E (2006) Phage therapy: facts and fiction. Int J Med Microbiol **296:** 5-14

Spellberg B, Powers JH, Brass EP, Miller LG, Edwards JE, Jr. (2004) Trends in antimicrobial drug development: implications for the future. Clin Infect Dis **38:** 1279-1286

Staub JM, Maliga P (1993) Accumulation of D1 polypeptide in tobacco plastids is regulated via the untranslated region of the *psbA* messenger-RNA. EMBO J **12:** 601-606

Stein DB, Palmer JD, Thompson WF (1986) Structural evolution and flip-flop recombination of chloroplast DNA in the fern genus *Osmunda*. Curr Genet **10:** 835-841

Stern DB, Gruissem W (1987) Control of plastid gene expression: 3' inverted repeats act as mRNA processing and stabilizing elements, but do not terminate transcription. Cell **51:** 1145-1157

Stern DB, Kindle KL (1993) 3'end maturation of the *Chlamydomonas reinhardtii* chloroplast *atpB* mRNA is a two-step process. Mol Cell Biol **13:** 2277-2285

Stoger E, Ma JK, Fischer R, Christou P (2005) Sowing the seeds of success: pharmaceutical proteins from plants. Curr Opin Biotechnol **16:** 167-173

Stoger E, Sack M, Fischer R, Christou P (2002) Plantibodies: applications, advantages and bottlenecks. Curr Opin Biotechnol **13:** 161-166

Stoger E, Schillberg S, Twyman RM, Fischer R, Christou P (2004) Antibody production in transgenic plants. Methods Mol Biol **248:** 301-318

Stone R (2002) Bacteriophage therapy. Stalin's forgotten cure. Science **298:** 728-731

Stratchounski LS, Andreeva IV, Ratchina SA, Galkin DV, Petrotchenkova NA, Demin AA, Kuzin VB, Kusnetsova ST, Likhatcheva RY, Nedogoda SV, Ortenberg EA, Belikov AS, Toropova IA (2003) The inventory of antibiotics in russian home medicine cabinets. Clin Infect Dis **37:** 498-505

Streatfield SJ (2006) Mucosal immunization using recombinant plant-based oral vaccines. Methods **38:** 150-157

Sugiura M (1989) The chloroplast chromosomes in land plants. Annu Rev Cell Biol **5:** 51-70

Sugiura M (1992) The chloroplast genome. Plant Mol Biol **19:** 149-168

Sulakvelidze A, Alavidze Z, Morris JG, Jr. (2001) Bacteriophage therapy. Antimicrob Agents Chemother **45:** 649-659

Summers WC (2001) Bacteriophage therapy. Annu Rev Microbiol **55:** 437-451

Svab Z, Hajdukiewicz P, Maliga P (1990) Stable transformation of plastids in higher plants. Proc Natl Acad Sci U S A **87:** 8526-8530

Svab Z, Maliga P (1993) High-frequency plastid transformation in tobacco by selection for a chimeric *aadA* gene. Proc Natl Acad Sci U S A **90:** 913-917

Svab Z, Maliga P (2007) From the cover: Exceptional transmission of plastids and mitochondria from the transplastomic pollen parent and its impact on transgene containment. Proc Natl Acad Sci U S A **104:** 7003-7008

Syrogiannopoulos GA, Grivea IN, Beratis NG, Spiliopoulou AE, Fasola EL, Bajaksouzian S, Appelbaum PC, Jacobs MR (1997) Resistance patterns of *Streptococcus pneumoniae* from carriers attending day-care centers in southwestern Greece. Clin Infect Dis **25:** 188-194

Tabb DL, McDonald WH, Yates JR (2002) DTASelect and contrast: tools for assembling and comparing protein identifications from shotgun proteomics. J Proteome Res **1:** 21-26

Tenover FC (2006) Mechanisms of antimicrobial resistance in bacteria. Am J Infect Control **34:** 3-10

Tewari KK, Wildman SG (1966) Chloroplast DNA from tobacco leaves. Science **153:** 1269-1271

Thiel K (2004) Old dogma, new tricks - 21st century phage therapy. Nat Biotech **22:** 31-36

Thomson D, Henry R (1995) Single-step protocol for preparation of plant tissue for analysis by PCR. Biotechniques **19:** 394-397, 400

Tillich M, Funk HT, Schmitz-Linneweber C, Poltnigg P, Sabater B, Martin M, Maier RM (2005) Editing of plastid RNA in Arabidopsis thaliana ecotypes. Plant J **43:** 708-715

Toke O (2005) Antimicrobial peptides: new candidates in the fight against bacterial infections. Biopolymers **80:** 717-735

Tregoning JS, Nixon P, Kuroda H, Svab Z, Clare S, Bowe F, Fairweather N, Ytterberg J, van Wijk KJ, Dougan G, Maliga P (2003) Expression of tetanus toxin fragment C in tobacco chloroplasts. Nucleic Acids Res **31:** 1174-1179

Tuomanen E (2006) *Streptococcus pneumoniae*. *In* The Prokaryotes, pp 149-162

Tuomanen E, Tomasz A (1990) Mechanism of phenotypic tolerance of nongrowing pneumococci to beta-lactam antibiotics. Scand J Infect Dis Suppl **74:** 102-112

Uicker WC, Schaefer L, Koenigsknecht M, Britton RA (2007) The essential GTPase YqeH is required for proper ribosome assembly in *Bacillus subtilis*. J Bacteriol **189:** 2926-2929

Vankemmelbeke M, Healy B, Moore GR, Kleanthous C, Penfold CN, James R (2005) Rapid detection of colicin E9-induced DNA damage using *Escherichia coli* cells carrying SOS promoter-lux fusions. J Bacteriol **187:** 4900-4907

Varea J, Monterroso B, Saiz JL, Lopez-Zumel C, Garcia JL, Laynez J, Garcia P, Menendez M (2004) Structural and thermodynamic characterization of Pal, a phage natural chimeric lysin active against pneumococci. J Biol Chem **279:** 43697-43707

Vieu E, Rahmouni AR (2004) Dual role of boxB RNA motif in the mechanisms of termination/antitermination at the lambda tR1 terminator revealed *in vivo*. J Mol Biol **339:** 1077-1087

Wakasugi T, Tsudzuki J, Ito S, Nakashima K, Tsudzuki T, Sugiura M (1994) Loss of all *ndh* genes as determined by sequencing the entire chloroplast genome of the black pine *Pinus thunbergii*. Proc Natl Ac Sci **91:** 9794-9798

Wakasugi T, Tsudzuki T, Sugiura M (2001) The genomics of land plant chloroplasts: Gene content and alteration of genomic information by RNA editing. Photosynth Res **70:** 107-118

Wang S, Ng TB, Chen T, Lin D, Wu J, Rao P, Ye X (2005) First report of a novel plant lysozyme with both antifungal and antibacterial activities. Biochem Biophys Res Commun **327:** 820-827

Watson J, Koya V, Leppla SH, Daniell H (2004) Expression of *Bacillus anthracis* protective antigen in transgenic chloroplasts of tobacco, a non-food/feed crop. Vaccine **22:** 4374-4384

Welte T, Marre R, Suttorp N (2003) CAPNet--network of competence for community acquired pneumonia: structures and aims. Pneumologie **57:** 34-41

Witte W, Cuny C, Klare I, Nubel U, Strommenger B, Werner G (2008) Emergence and spread of antibiotic-resistant Gram-positive bacterial pathogens. Int J Med Microbiol **298:** 365-377

Wostrikoff K, Stern D (2007) Rubisco large-subunit translation is autoregulated in response to its assembly state in tobacco chloroplasts. Proc Natl Acad Sci U S A **104:** 6466-6471

Yamaguchi K, Subramanian AR (2000) The plastid ribosomal proteins. Identification of all the proteins in the 50S subunit of an organelle ribosome (chloroplast). J Biol Chem **275:** 28466-28482

Yamaguchi K, von Knoblauch K, Subramanian AR (2000) The plastid ribosomal proteins. Identification of all the proteins in the 30S subunit of an organelle ribosome (chloroplast) J Biol Chem **275:** 28455-28465

Ye GN, Hajdukiewicz PT, Broyles D, Rodriguez D, Xu CW, Nehra N, Staub JM (2001) Plastid-expressed 5-enolpyruvylshikimate-3-phosphate synthase genes provide high level glyphosate tolerance in tobacco. Plant J **25:** 261-270

Yukawa M, Tsudzuki T, Sugiura M (2005) The 2005 version of the chloroplast DNA sequence from tobacco (*Nicotiana tabacum*). Plant Mol Biol Rep **23:** 359-365

Zarivach R, Ben-Zeev E, Wu N, Auerbach T, Bashan A, Jakes K, Dickman K, Kosmidis A, Schluenzen F, Yonath A, Eisenstein M, Shoham M (2002) On the interaction of colicin E3 with the ribosome. Biochimie **84:** 447-454

Zerges W, Girard-Bascou J, Rochaix JD (1997) Translation of the chloroplast *psbC* mRNA is controlled by interactions between its 5' leader and the nuclear loci TBC1 and TBC3 in *Chlamydomonas reinhardtii*. Mol Cell Biol **17:** 3440-3448

Zhou F, Badillo-Corona JA, Karcher D, Gonzalez-Rabade N, Piepenburg K, Borchers A-MI, Maloney AP, Kavanagh TA, Grey JC, Bock R (2008) High-level expression of human immunodeficiency virus antigens from the tobacco and tomato plastid genomes. Plant Biotechnol J ***in press***

Zhou F, Karcher D, Bock R (2007) Identification of a plastid intercistronic expression element (IEE) facilitating the expression of stable translatable monocistronic mRNAs from operons. Plant J **52:** 961-972

Zoschke R, Liere K, Boerner T (2007) From seedling to mature plant: *Arabidopsis* plastidial genome copy number, RNA accumulation and transcription are differentially regulated during leaf development. Plant J **50:** 710-722

Zuker M (2003) Mfold web server for nucleic acid folding and hybridization prediction. Nucleic Acids Res **31:** 3406-3415

6.2 Internet sources

Center for Disease Control and Prevention (CDC) (http://www.cdc.gov)

National Academy Press (http://www.nap.edu)

National Institute of Allergy and Infectious Diseases (http://www3.niaid.nih.gov)

New England Journal of Medicine (http://content.nejm.org)

New York Times (http://www.nytimes.com)

NCBI (http://www.ncbi.nlm.nih.gov/genomes/static/euk_o.html)

Robert Koch Institute (RKI) (http://www.rki.de)

Union of Concerned Scientists (http://www.ucsusa.org)

7 Appendix

7.1 DNA sequences

7.1.1 Probes used for Southern or Northern blotting

psaB probe:

5’ACATAAAGTCCCAGGGTATGGAATCCCAGAAAGAGGCTGGCCCAACTTAAAT
GAGATATGATAGCTTCTTTATGCTCTAACATTCTTGCCAATACATTATCTTCATT
TTGCTCCGGATTGTAATCTCTAATGAAAAATATAGCTCCATGAGCAAAAGCTCC
TGTCATGATGAATCCTGCGATATATTGGTGGTGGGTATATAATGCAGCTTGAGT
AGTAAAGTCTTGTGCTATGAATGCATAAGCAGGTAAAGAGTACATGTGTTGAGC
TACCAAAGAAGTAATAACCCCTAAAGAAGCTAGAGCAAGGCCTAATTGAAAAT
GAAGCGAATTATTGATTGTGTCATAAAGACCCTTATGTCCACGCCCCAATCGTC
CCCCCGGGGGAATATGTGCATCTAAAAGGTCTTTCATACTGTGCCCAATCCCGA
AATTGGTTCTATACATATGACCAGCAACGAGAAAAATAAATGCAATAGCTAAA
TGGTGATGGGCAATATCAGTCAGCCATAAACTTTGCGTTTGTGGATGGAATCCC
CCG 3’

aadA probe:

5’GTGGACAAATTCTTCCAACTGATCTGCGCGCGAGGCCAAGCGATCTTCTTCTT
GTCCAAGATAAGCCTGTCTAGCTTCAAGTATGACGGGCTGATACTGGGCCGGCA
GGCGCTCCATTGCCCAGTCGGCAGCGACATCCTTCGGCGCGATTTTGCCGGTTA
CTGCGCTGTACCAAATGCGGGACAACGTAAGCACTACATTTCGCTCATCGCCAG
CCCAGTCGGGCGGCGAGTTCCATAGCGTTAAGGTTTCATTTAGCGCCTCAAATA
GATCCTGTTCAAGAACCGGATCAAAGAGTTCCTCCGCCGCTGGACCTACCAAGG
CAACGCTATGTTCTCTTGCTTTTGTCAGCAAGATAGCCAGATCAATGTCGATCGT
GGCTGGCTCGAAGATACCTGCAAGAATGTCATTGCGCTGCCATTCTCCAAATTG
CAGTTCGCGCTTAGCTGGATAACGCCACGGAATGATGTCGTCGTGCACAACAAT
GGTGACTTCTACAGCGCGGAGAATCTCGCTCTCTCCAGGGGAAGCCGAAGTTTC
CAAAAGGTCGTTGATCAAAGCTCGCCGCGTTGTTTCATCAAGCCTTACGGTCAC
CGTAACCAGCAAATCAATATCACTGT 3’

rbcL probe:

5’GGTACATGCGAAGAAATGATCAAAAGAGCTGTATTTGCTAGAGAATTGGGCG
TTCCGATCGTAATGCATGACTACTTAACGGGGGGATTCACCGCAAATACTAGCT
TGGCTCATTATTGCCGAGATAATGGTCTACTTCTTCACATCCACCGTGCAATGCA
TGCGGTTATTGATAGACAGAAGAATCATGGTATCCACTTCCGGGTATTAGCAAA
AGCGTTACGTATGTCTGGTGGAGATCATATTCACTCTGGTACCGTAGTAGGTAA
ACTTGAAGGTGAAAGAGACATAACTTTGGGCTTTGTTGATTTACTGCGTGATGA
TTTTGTTGAACAAGATCGAAGTCGCGGTATTTATTTCACTCAAGATTGGGTCTCT
TTACCAGGTGTTCTACCCGTGGCTTCAGGAGGTATTCACGTTTGGCATATGCCTG
CTCTGACCGAGATCTTTGGGGATGATTCCGTACTACAGTTCGGTGGAGGAACTT
TAGGACATCCTTGGGGTAATGCGCCAGGTGCCGTAGCTAATCGAGTAGCTCTAG
AAGCATGTGTAAAAGCTCGTAATGAAGGACGTGATCTTGCTCAGGAAGGTAAT

GAAATTATTCGCGAGGCTTGCAAATGGAGCCCGGAACTAGCTGCTGCTTGTGAA
GTATGGAAAGAGATCGTATTTAATTTTGCAGCAGTGGACGTTTTGGATAAGTAA
AAACAGTAGACATTAGCAGATAAATTAGCAGGAAATAAAGAAGGATAAGGAG
AAAGAACTCAAGTAATTATCCTTCGTTCTCTTAATTGAATTGCAATTAAACTCG
GCCCAATCTTTTACTAAAAGGATTGAGCCGAATACAACAAAGATTCTATTGCAT
ATATTTTGACTAAGTATATACTTACCTAGATATACAAGATTTGAAATACAAAAT
CTAGAAAACTAAATCAAAATCTAAGACTCAAATCTTTCTATTGTTGTCTTGG 3'

7.1.2 Promoter sequence and 3' UTR of pTox

5'TTTGAGCTC**GCTCCCCCGCCGTCGTTCAATGAGAATGGATAAGAGGCTCG**
TGGGATTGACGTGAGGGGGCAGGGATGGCTATATTTCTGGGAGCGAACTCC
GGGCGAATACGAAGCGCTTGGATACAGTTGATAACTTCGTATAATGTATGCTAT
ACGAAGTTATTAG*GGAGG*GATTCATG 3'

Prrn: promoter of rRNA operon
G: transcription initiation site
loxP site
SD: Shine- Dalgarno sequence
ATG: translation start

7.1.3 Synthesized E. coli terminator from pTox - schematic map and sequence

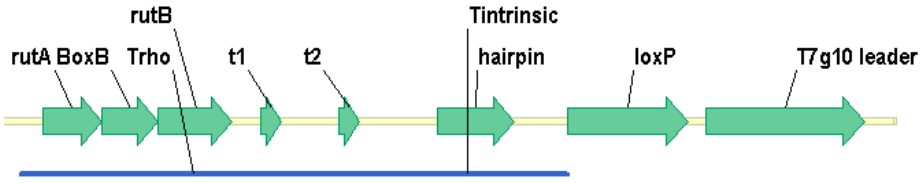

Fig. 55 Schematic map of the synthetic *E. coli* transcription block in the pTox vector.

Sequence of the synthetic *E. coli* transcription block:

5'**ATAACC[CCGCTCTTACACATTCC][AGCCCTGAAAAAGGGC][ATCAAATTA**
AACCACACCTAT]GGTGTATGCATTTATTTGCATACATTCAATCAATTGTTA
GCTTTCAAATAAAACGAAA[GGCTCAGTCGAAAGACTGGGCC]TTTCGTTTTAAT
CTG*ATAACTTCGTATAATGTATGCTATACGAAGTTAT*GGATCCTAGAAATAATTTTGT
TTAACTTTAAGAAGGAGATATACCCATGGAAATCTAGA3'

Trho: rho-dependent terminator from *E.coli* (λtR1)
[rutA]: rho utilizing site A
[rutB]: rho utilizing site B
[boxB]: hairpin structure that clamps rutA and rutB
[t1], [t2]: uridine rich regions that serve as termination sites
Tintrinsic: intrinsic terminator from *E.coli* (*rrn*B T1)

[hairpin]: stem-loop structure
loxP site
T7g10: leader sequence of T7 phage gene 10

7.2 Protein information and sequences

7.2.1 Rubisco large subunit (RbcL)

Analysis	Entire Protein
Length	477 aa
Molecular Weight	52894.37
1 microgram =	18.906 pMoles
Molar Extinction coefficient	69640
1 A[280] corr. to	0.76 mg/ml
A[280] of 1 mg/ml	1.32 AU
Isoelectric Point	6.43
Charge at pH 7	-3.03

Amino Acid(s)	Number count	% by weight	% by frequency
Charged (RKHYCDE)	155	38.56	32.49
Acidic (DE)	59	13.51	12.37
Basic (KR)	55	14.45	11.53
Polar (NCQSTY)	101	21.92	21.17
Hydrophobic (AILFWV)	173	35.10	36.27
A Ala	45	6.52	9.43
C Cys	9	1.77	1.89
D Asp	27	5.85	5.66
E Glu	32	7.66	6.71
F Phe	21	5.64	4.40
G Gly	46	5.62	9.64
H His	14	3.53	2.94
I Ile	21	4.48	4.40
K Lys	25	5.95	5.24
L Leu	41	8.75	8.60
M Met	8	1.94	1.68
N Asn	15	3.22	3.14
P Pro	21	3.93	4.40
Q Gln	13	3.09	2.73
R Arg	30	8.50	6.29
S Ser	17	2.91	3.56
T Thr	29	5.62	6.08
V Val	37	7.05	7.76
W Trp	8	2.66	1.68
Y Tyr	18	5.30	3.77
B Asx	42	9.07	8.81
Z Glx	45	10.75	9.43
X Xxx	0	0.00	0.00

Protein sequence:

```
  1  MSPQTETKAS  VGFKAGVKEY  KLTYYTPEYQ  TKDTDILAAF  RVTPQPGVPP
 51  EEAGAAVAAE  SSTGTWTTVW  TDGLTSLDRY  KGRCYRIERV  VGEKDQYIAY
101  VAYPLDLFEE  GSVTNMFTSI  VGNVFGFKAL  RALRLEDLRI  PPAYVKTFQG
151  PPHGIQVERD  KLNKYGRPLL  GCTIKPKLGL  SAKNYGRAVY  ECLRGGLDFT
```

201	KDDENVNSQP	FMRWRDRFLF	CAEALYKAQA	ETGEIKGHYL	NATAGTCEEM
251	IKRAVFAREL	GVPIVMHDYL	TGGFTANTSL	AHYCRDNGLL	LHIHRAMHAV
301	IDRQKNHGIH	FRVLAKALRM	SGGDHIHSGT	VVGKLEGERD	ITLGFVDLLR
351	DDFVEQDRSR	GIYFTQDWVS	LPGVLPVASG	GIHVWHMPAL	TEIFGDDSVL
401	QFGGGTLGHP	WGNAPGAVAN	RVALEACVKA	RNEGRDLAQE	GNEIIREACK
451	WSPELAAACE	VWKEIVFNFA	AVDVLDK*		

7.2.2 PlyGBS

Analysis	Entire Protein
Length	447 aa
Molecular Weight	49993.82
1 microgram =	20.002 pMoles
Molar Extinction coefficient	102180
1 A[280] corr. to	0.49 mg/ml
A[280] of 1 mg/ml	2.04 AU
Isoelectric Point	4.93
Charge at pH 7	-13.73

Amino Acid(s)	Number count	% by weight	% by frequency
Charged (RKHYCDE)	135	35.88	30.20
Acidic (DE)	52	12.36	11.63
Basic (KR)	38	10.15	8.50
Polar (NCQSTY)	145	34.25	32.44
Hydrophobic (AILFWV)	148	32.02	33.11
A Ala	42	6.45	9.40
C Cys	4	0.84	0.89
D Asp	34	7.80	7.61
E Glu	18	4.56	4.03
F Phe	18	5.12	4.03
G Gly	33	4.27	7.38
H His	6	1.60	1.34
I Ile	27	6.10	6.04
K Lys	26	6.55	5.82
L Leu	22	4.97	4.92
M Met	6	1.54	1.34
N Asn	27	6.15	6.04
P Pro	18	3.57	4.03
Q Gln	20	5.04	4.47
R Arg	12	3.60	2.68
S Ser	33	5.98	7.38
T Thr	26	5.34	5.82
V Val	29	5.85	6.49
W Trp	10	3.52	2.24
Y Tyr	35	10.92	7.83
B Asx	61	13.95	13.65
Z Glx	38	9.60	8.50
X Xxx	1	0.22	0.22

Protein sequence:

1	HMASATYQEY	KSRSNGNAYD	IDGSFGAQCW	DGYADYCKYL	GLPYANCTNT
51	GYARDIWEQR	HENGILNYFD	EVEVMQAGDV	AIFMVVDGVT	PYSHVAIFDS
101	DAGGGYGWFL	GQNQGGANGA	YNIVKIPYSA	TYPTAFRPKV	FKNAVTVTGN
151	IGLNKGDYFI	DVSAYQQADL	TTTCQQAGTT	KTIIKVSESI	AWLSDRHQQQ
201	ANTSDPIGYY	HFGRFGGDSA	LAQREADLFL	SNLPSKKVSY	LVIDYEDSAS
251	ADKQANTNAV	IAFMDKIASA	GYKPIYYSYK	PFTLNNIDYQ	KIIAKYPNSI
301	WIAGYPDYEV	RTEPLWEFFP	SMDGVRWWQF	TSVGVAGGLD	KNIVLLADDS

```
351  SKMDIPKVDK    PQELTFYQKL    ATNTKLDNSN    VPYYEATLST    DYYVESKPNA
401  SSADKEFIKA    GTRVRVYEKV    NGWSRINHPE    SAQWVEDSYL    VNATDI*
```

7.2.3 Pal

Analysis	Entire Protein
Length	300 aa
Molecular Weight	34855.00
1 microgram =	28.690 pMoles
Molar Extinction coefficient	134210
1 A[280] corr. to	0.26 mg/ml
A[280] of 1 mg/ml	3.85 AU
Isoelectric Point	5.02
Charge at pH 7	-10.72

Amino Acid(s)	Number count	% by weight	% by frequency
Charged (RKHYCDE)	109	42.19	36.33
Acidic (DE)	41	14.05	13.67
Basic (KR)	30	11.87	10.00
Polar (NCQSTY)	84	29.60	28.00
Hydrophobic (AILFWV)	91	30.44	30.33
A Ala	28	6.20	9.33
C Cys	3	0.90	1.00
D Asp	27	8.93	9.00
E Glu	14	5.12	4.67
F Phe	11	4.52	3.67
G Gly	29	5.41	9.67
H His	6	2.31	2.00
I Ile	14	4.56	4.67
K Lys	16	5.81	5.33
L Leu	12	3.91	4.00
M Met	10	3.71	3.33
N Asn	16	5.25	5.33
P Pro	8	2.29	2.67
Q Gln	6	2.18	2.00
R Arg	14	6.06	4.67
S Ser	19	4.96	6.33
T Thr	11	3.26	3.67
V Val	9	2.62	3.00
W Trp	17	8.63	5.67
Y Tyr	29	13.05	9.67
B Asx	43	14.18	14.33
Z Glx	20	7.30	6.67
X Xxx	1	0.32	0.33

Protein sequence:

```
  1  HMASGVDIEK    GVAWMQARKG    RVSYSMDFRD    GPDSYDCSSS    MYYALRSAGA
 51  SSAGWAVNTE    YMHAWLIENG    YELISENAPW    DAKRGDIFIW    GRKGASAGAG
101  GHTGMFIDSD    NIIHCNYAYD    GISVNDHDER    WYYAGQPYYY    VYRLTNANAQ
151  PAEKKLGWQK    DATGFWYARA    NGTYPKDEFE    YIEENKSWFY    FDDQGYMLAE
201  KWLKHTDGNW    YWFDRDGYMA    TSWKRIGESW    YYFNRDGSMV    TGWIKYYDNW
251  YYCDATNGDM    KSNAFIRYND    GWYLLLPDGR    LADKPQFTVE    PDGLITAKV*
```

7.2.4 Cpl-1

Analysis	Entire Protein
Length	343 aa
Molecular Weight	39619.90
1 microgram =	25.240 pMoles
Molar Extinction coefficient	117710
1 A[280] corr. to	0.34 mg/ml
A[280] of 1 mg/ml	2.97 AU
Isoelectric Point	4.66
Charge at pH 7	-15.89

Amino Acid(s)	Number count	% by weight	% by frequency
Charged (RKHYCDE)	106	35.36	30.90
Acidic (DE)	45	13.63	13.12
Basic (KR)	29	9.69	8.45
Polar (NCQSTY)	107	32.04	31.20
Hydrophobic (AILFWV)	104	31.23	30.32
A Ala	19	3.70	5.54
C Cys	3	0.79	0.87
D Asp	27	7.85	7.87
E Glu	18	5.78	5.25
F Phe	18	6.49	5.25
G Gly	28	4.59	8.16
H His	4	1.36	1.17
I Ile	15	4.30	4.37
K Lys	22	7.02	6.41
L Leu	19	5.44	5.54
M Met	12	3.91	3.50
N Asn	27	7.79	7.87
P Pro	13	3.27	3.79
Q Gln	12	3.83	3.50
R Arg	7	2.66	2.04
S Ser	22	5.05	6.41
T Thr	18	4.68	5.25
V Val	18	4.61	5.25
W Trp	15	6.69	4.37
Y Tyr	25	9.89	7.29
B Asx	54	15.64	15.74
Z Glx	30	9.62	8.75
X Xxx	1	0.28	0.29

Protein sequence:

```
  1 HMASVKKNDL FVDVSSHNGY DITGILEQMG TTNTIIKISE STTYLNPCLS
 51 AQVEQSNPIG FYHFARFGGD VAEAEREAQF FLDNVPMQVK YLVLDYEDDP
101 SGDAQANTNA CLRFMQMIAD AGYKPIYYSY KPFTHDNVDY QQILAQFPNS
151 LWIAGYGLND GTANFEYFPS MDGIRWWQYS SNPFDKNIVL LDDEEDDKPK
201 TAGTWKQDSK GWWFRRNNGS FPYNKWEKIG GVWYYFDSKG YCLTSEWLKD
251 NEKWYYLKDN GAMATGWVLV GSEWYYMDDS GAMVTGWVKY KNNWYYMTNE
301 RGNMVSNEFI KSGKGWYFMN TNGELADNPS FTKEPDGLIT VV*
```

7.3 Vector maps

7.3.1 pHK20

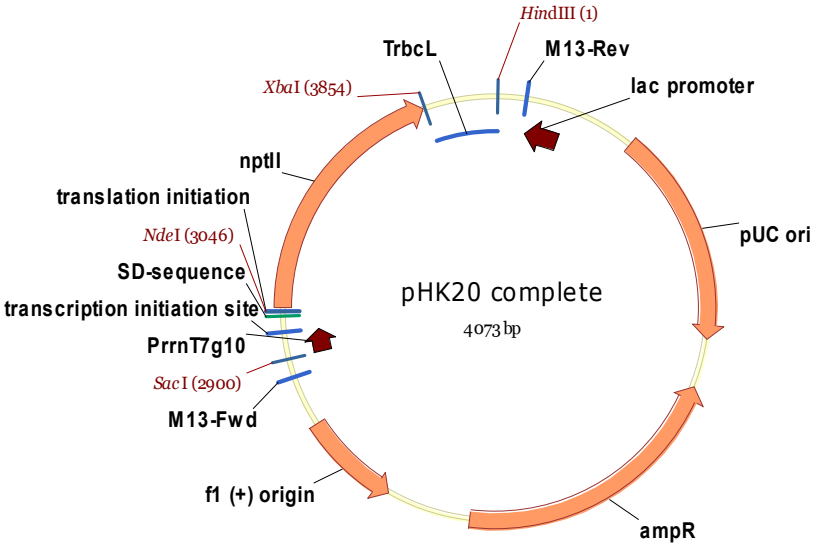

7.3.2 pKP9

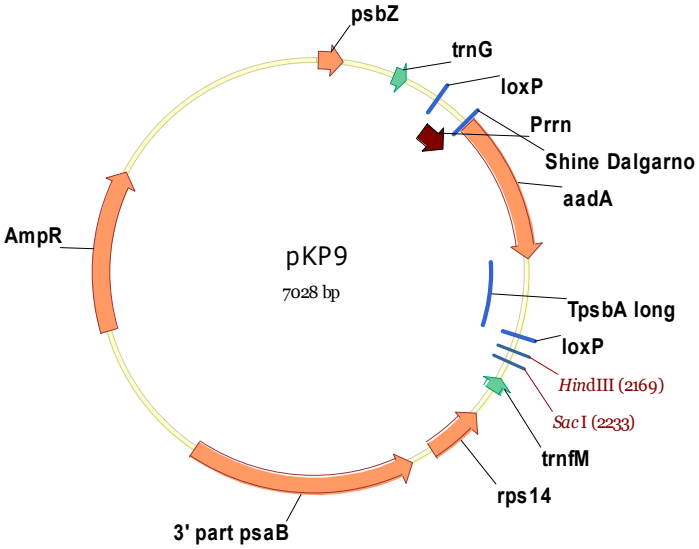

7.3.3 pMO16

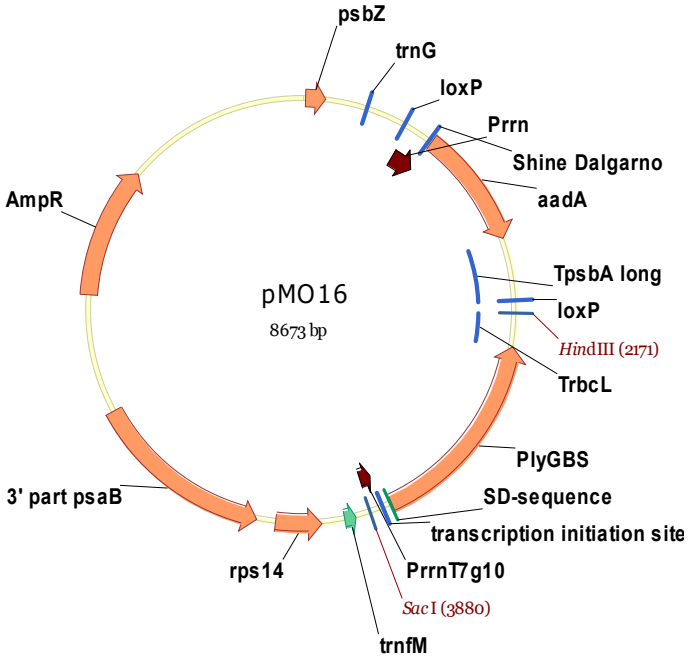

7.3.4 pOD1

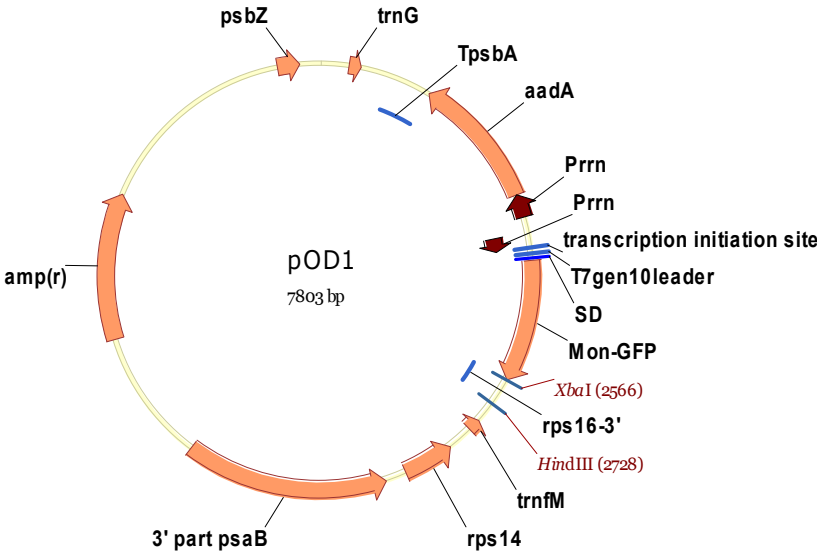

7.3.5 pMO24

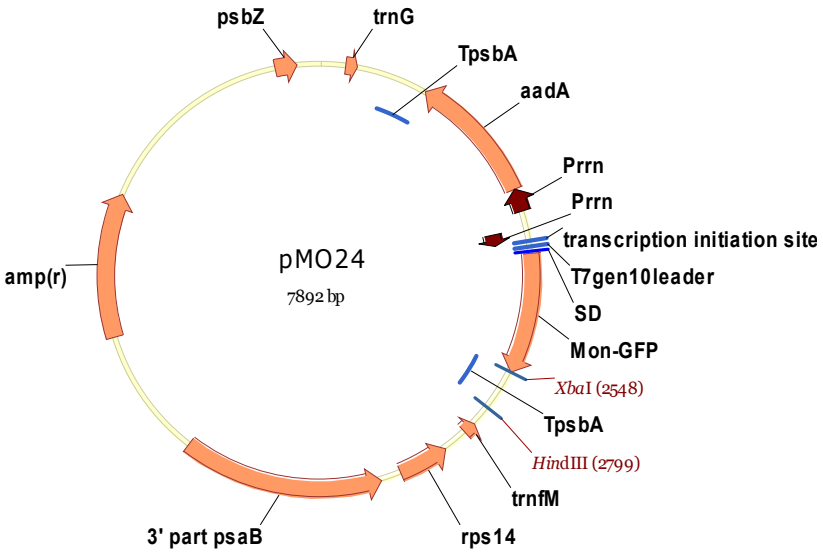

7.3.6 pKP6

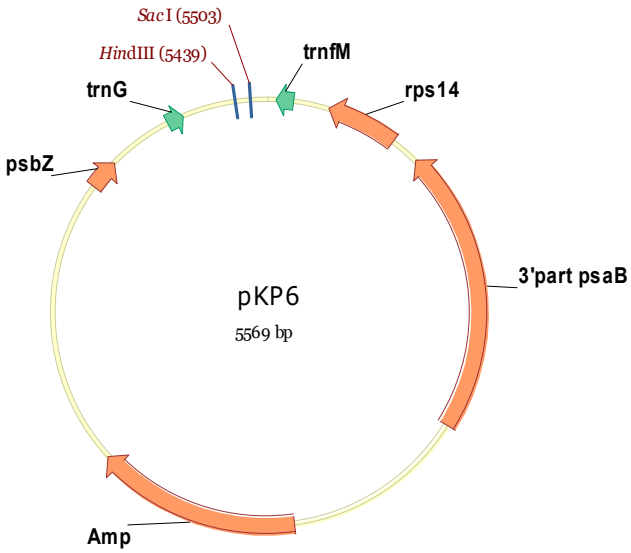

7.3.7 pTox

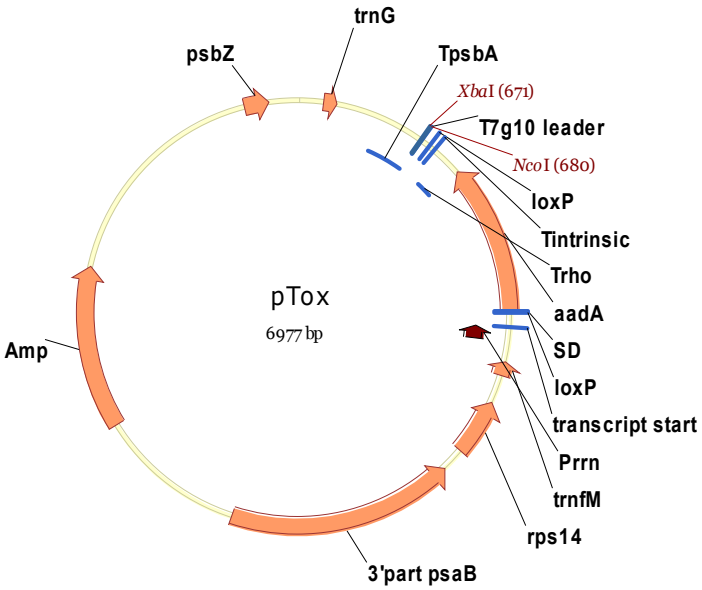

7.3.8 pToxCpl-1

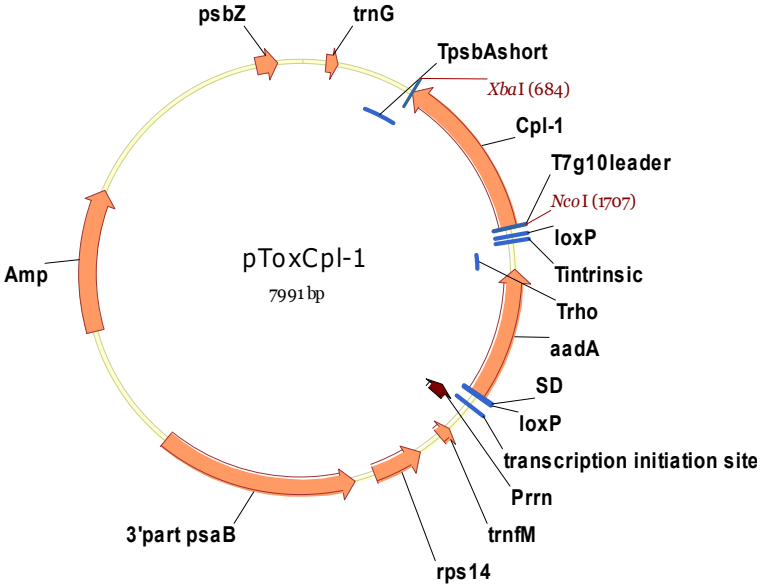

7.3.9 pToxPal

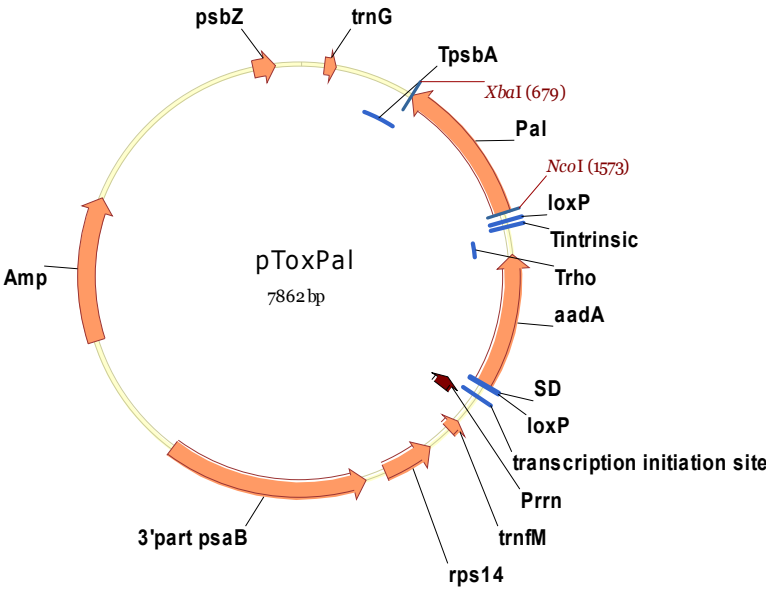

7.3.10 pToxGFP

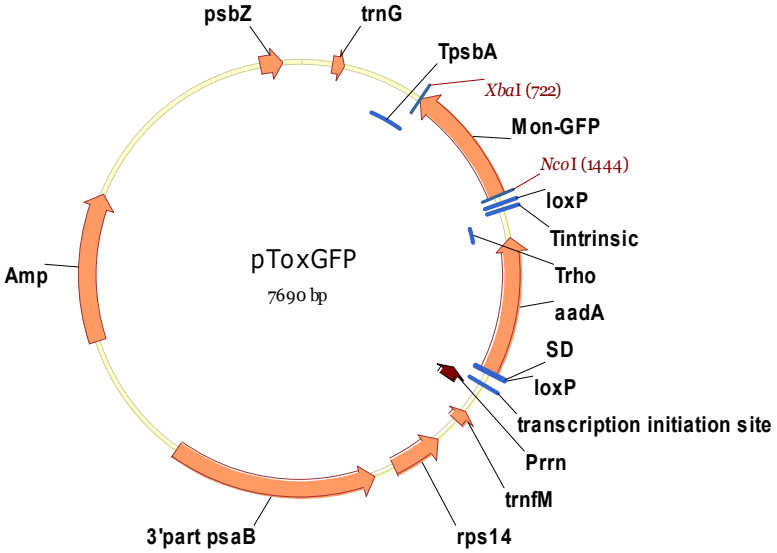

8 Acknowledgements

First of all I would like to thank Prof. Dr. Ralph Bock for giving me the opportunity to work in his group, for his supervision, encouragement and patience. – *Many, many thanks for all!*

I would like to thank Prof. Dr. Dirk Prüfer, Prof. Dr. Heribert Warzecha and Prof. Dr. Udo Johanningmeier for being reviewers of my thesis. – *I hope you enjoy the work!*

Further I would like to express my gratitude to Dr. Marc Lohse who helped me with his advice during the development of this work. – *You have been always patient to help me, thanks a lot.*

I would like to thank Dr. Stephanie Ruf, Yvonne Weber, Stefanie Seeger, Annett Kaßner and Claudia Hasse for all their help regarding transformation and plant cultivation. – *Thank you very much for taking care of my plants. You did a great job!*

Special thanks go to Dr. Lars Scharf, Dr. Jens Rupprecht, Dr. Yinhong Lu and Dr. Katharine "Kate" Howell for very helpful discussions and critical proof-reading of my thesis. – *Thanks a lot for you help!*

Further thanks go to all my cooperation partners Dr. Bernd Kreikemeyer, Dr. Waltraud Schulze, Dr. Stefanie Wienkoop, Cordula Lembke, Thomas Köller and Kerstin Standar for their help in preparing the nice results we could finally publish. – *It was great to work with you!*

I have to express my gratitude to my evaluation committee Dr. Dirk Hincha, Prof. Dr. Lothar Willmitzer and Dr. Karin Köhl. – *It was nice to present and discuss my results with you.*

Sincere thanks to all service teams in the house, specially to Dr. Karin Köhl and Britta Hausmann for taking care of my plants, the IT team for working computers and the media kitchen team for preparing cultivation media. – *Without you, probably nothing would work here!*

Many thanks go to the whole Ag Bock for the nice atmosphere. – *It was nice working with you all.*

Especially I would like to thank my parents who always supported me in my studies. – *Thanks a lot, without you, I wouldn't be here!*

Last but not least I would like to thank all people who have helped me and are not listed here. – *I'll think of you.*